ANALYSIS OF GENE EXPRESSION IN MOUSE FIBROBLAST CELLS DURING INFECTION WITH MINUTE VIRUS OF MICE

by

WARREN PERRY WILLIAMS

B.Sc., The University College of the Cariboo, 1996

A THESIS SUBMITTED IN PARTIAL FULFILMENT OF
THE REQUIREMENTS FOR THE DEGREE OF

DOCTOR OF PHILOSOPHY

in

THE FACULTY OF GRADUATE STUDIES

(Department of Biochemistry and Molecular Biology)

We accept this thesis as conforming
to the required standard

THE UNVERSITY OF BRITISH COLUMBIA

March 2003

In presenting this thesis in partial fulfilment of the requirements for an advanced degree at the University of British Columbia, I agree that the Library shall make it freely available for reference and study. I further agree that permission for extensive copying of this thesis for scholarly purposes may be granted by the head of my department or by his or her representatives. It is understood that copying or publication of this thesis for financial gain shall not be allowed without my written permission.

Department of Biochemistry & Molecular Biology

The University of British Columbia
Vancouver, Canada

Date July 6/03

Abstract

Minute Virus of Mice (MVM), a mouse parvovirus, has served as a model for understanding parvovirus infection. To further understand how parvoviruses replicate within the cell and cause disease, the effect of MVM infection on host cell gene expression in mouse fibroblast cells (LA9 cells) was studied. This was accomplished through three techniques: Differential display, Clontech macroarrays, and Affymetrix microarray analysis.

The RT/PCR technique differential display was used to studied altered gene expression in unsynchronized infected mouse fibroblast LA9 cells at 12, 24 and 36 hours post-infection. Twenty-four primer pair combinations were used, representing ~ 15% of actively transcribed RNA. Surprisingly, few genes were found to change, although the technique did detect MVM NS1 transcript. In addition, the rodent retroelements, B1 & B2 SINEs and the L1 LINE were all found to be increased as a result of MVMp infection.

Further gene expression studies on synchronized MVM infected LA9 cells at 12 and 24 hours post-block were undertaken with Clontechs macroarrays (~1000 genes per array). Overall, the signal from these arrays were low and there were problems with background. Again, very few transcripts appeared to change as a result of infection, with only 3 genes being altered at the 12 hour time point, and another 7 reproducibly (by independent arrays) at the 24 hour time point. These included the murine B2 SINE (2.8 fold increase, confirming the differential display results), RNA exchange factor binding protein 1 (two fold increase) and three cyclins.

A preliminary study was also done with the superior Affymetrix oligonucleotide microarrays (12,000 different genes, 16 oligonucleotides/gene). Of the 5347 genes and ESTs that were detected in the screen, 74 were found to be altered in unsynchronized

LA9 cells infected with MVMp. These included genes involved in promoting cell growth (epiregulin, 13.9 fold increase), genes that inhibited growth (nuclear protein p8, 3.3 fold decrease), immune/inflammatory genes, specifically targeting transforming growth factor β (2.5 fold decrease), a number of transcription factors (C/EBP, 2.5 fold decrease) and genes involved in cholesterol synthesis and transport (farnesyl diphosphate sythetase, 2 fold decrease) as well as a number of unknown ESTs.

The SINE response to MVM infection was further investigated. Primer extension assays confirmed that the murine B1 and B2 SINEs are up-regulated in LA9 cells throughout MVM infection. These studies also demonstrated that the SINE response was due to RNA polymerase III transcription and not contaminating DNA or RNA polymerase II transcription. Furthermore, expression of MVM NS1 in LA9 cells by transient transfection also leads to an increase in both murine SINEs. This is the first time that the B1 and B2 SINEs have been shown to be altered by viral infection. The increase in the SINE transcripts does not appear to be due to an increase in either of the basal transcription factors TFIIIC110 or 220, as these proteins do not increase during MVMp infection. However, nuclear run-on experiments to determine if increased SINE expression was due to increased SINE RNA transcription were inconclusive.

Protein levels of some 75 different protein kinases were also investigated in synchronized, MVMp infected LA9 cells. Very few changes were observed.

Table of Contents

List of Tables

List of Figures

Abbreviations

BLOTTO	PBS-T with 5% Powdered skim milk
DEPC	Diethyl Pyrocarbonate
DTT	Dithiothreitol
EDTA	Ethylene-diaminetetra-acetic acid
FBS	Fetal Bovine Serum
HEPES	N-[2-Hydroxyethyl]piperazine-N'-[ethanesulfonic acid]
MMLV	Moloney Murine Leukemia Virus
MOI	Multiplicity of infection
MOPS	3-[N-morpholino]propanesulfonic acid
MVM	Minute Virus of Mice
PB	Post Block
PBS	Phosphate buffered Saline
PBS-T	Phosphate buffered Saline with 0.05% Tween 20
PCR	Polymerase Chain Reaction
PI	Post Infection
PMSF	Phenylmethylsulfonyl fluoride
PVDF	Polyvinylidene Fluoride
RT	Reverse Transcription
SDS	Sodium Dodecyl Sulfate
SSC (20X)	Sodium Chloride (3M) and Sodium Citrate (0.3M, pH 7)
TAE buffer	40mM Tris-acetate, 1mM EDTA, pH 8.0
TBE buffer	90mM Tris-borate, 0.1 mM EDTA, pH 8.3
TES	N-Tris(hydroxymethyl)methyl-2-aminoethanesulfonic acid
TNE buffer	50 mM Tris·Cl pH 8.7, 150 mM NaCl, and 0.5mM EDTA
Tris	Tris(hydrixymethyl)aminomethane
X-gal	5-bromo-4-chloro-3-indolyl-beta-D-galactopyranoside

Acknowledgements

Completing a Ph.D. is no easy task. Luckily for me, there were many people who helped along the way. First and foremost, I would like to thank my supervisor, Dr. Caroline Astell for providing this project, all the helpful advice, and patience. I would also like to acknowledge all the past members of the Astell lab for all their input and help. Specifically, two people deserve to be singled out for further thanks: Dr. Janet St. Amand, who always had time to help a young "wet behind the ears" graduate student and who got me out of the lab and into the mountains, and Lilian Tamburic, whose exceptional trouble-shooting skills were exploited mercilessly and who introduced me to Kurosawa, Kusturica, and scotch. These three women taught me how to do good science and opened my eyes to new ideas and new horizons.

My family (Joanne, Perry, Angie and Bradley) played a crucial role in the completion of this thesis with countless phone calls of encouragement, support and love. Thanks also go out to Emily Crowe, Cameron Mackereth, and Tye Teames for providing the a pitcher of beer or a bottle of wine for those experiments that did not quite make it into this work.

Finally and most importantly, I would like to thank my partner Adam Lorch. Without him, this thesis would not be possible.

Introduction

The Parvoviridae

The family Parvoviridae includes extremely small non-enveloped icosohedral viral particles containing a single stranded DNA genome of approximately five to seven kilobases. It is divided into two separate sub-families based on the viral host. The Densovirinae are a group of autonomously replicating viruses that infect arthropods while the Parvovirinae are a group of both autonomously and helper-dependent viruses that replicate in vertebrates. The Densovirinae consist of three genera, the Densoviruses, the Iteraviruses and the Brevidensoviruses based on genome length, presence or absence of inverted terminal repeats (ITR's), and genome organization (monosense vs ambisense) [1]. The Parvovirinae can also be further divided into three genera: the Erythroviruses, the Dependoviruses and the Parvoviruses. The Erythroviruses are autonomously replicating viruses that replicate in erythroid progenitor cells. Examples include the human pathogen B19 and simian parvovirus (SPV), which infects Cynomolgus monkeys. Dependoviruses are characterized by the requirement, though not absolute, of a helper virus for viral replication. Examples are the human adeno-associated viruses (AAV), serotypes one to five. Finally the Parvovirinae are a group of autonomously replicating viruses that replicate in a wide variety of cells. This is a diverse group of viruses with examples including minute virus of mice (MVM), Rat H-1 parvovirus, Hamster parvovius (HPV), canine parvovirus (CPV), feline panleukopenia virus (FPV), Aleutine mink disease parvovirus (ADV), and Porcine parvovirus (PPV) [2]. Table 1 shows the classification scheme of the Parvoviridae with representative viruses of each genus.

Family Parvoviridae:

Sub-family Denosovirinae

- Athropod hosts

Genus Densovirus

- Large genome 5.5 -6 kb
- Large ITRs
- Ambisense genomic organization

Examples

Galleria mellonella densovirus (*Gm*DNV)
Acheta domesticus densovirus (*Ad*DNV)
Culex pipiens denosovirus (*Cp*DNV)

Genus Iteravirus

- Genome size of 5 kb
- ITRs of about 250 nt
- Monosense genomic organization

Example

Bombyx mori densovirus (*Bm*DNV)

Genus Brevidensovirus

- Genome size of 4 kb
- No ITRs but terminal hairpins
- Monosense genomic organization

Example

Aedes aegypti densovirus (*Aae*DNV)

Sub-family Parvovirinae

- Vertebrate hosts

Genus Erythrovirus

- Replicates in erythroid progenitor cells

Examples

Human B19 Parvovirus
Simian Parvovirus (SPV)

Genus Dependovirus

- Requires helper virus for optimal replication

Examples

Adeno-associated viruses (AAV) 1-5

Genus Parvovirus

- Autonomously replicating viruses that do not replicate in erythroid progenitor cells

Examples

Minute virus of Mice (MVM), Feline panleukopenia virus (FPV)
Rat H1 parvovirus, Aleutian mink disease parvovirus (ADV)
Porcine Parvovirus (PPV), Canine parvovirus (CPV)

Table 1: Parvovirus classification.

Biological significance and applications of the Parvoviridae

The purpose of this section is to give a very broad overview of parvoviruses and their uses as reviewed in Contributions to Microbiology Vol. 4: Parvoviruses from Molecular Biology to Pathology and Therapeutic Uses, edited by S. Faisst and J. Rommelaere. A thorough review of these topics is beyond the scope of this thesis. Wherever possible, I have cited relevant review articles.

The Parvoviridae are of interest for many reasons. Their most predominant features are their ability to cause disease in both humans and animals (of important economic value) and their increasing use as gene transfer vectors. However, there is also considerable interest in using them for pest control and in studying basic cell functions.

The human pathogen B19 parvovirus causes hematological disease due to its tropism for replication in erythroid progenitor cells with the disease outcome depending on the age and state of the human host. The virus is extremely common in the population; 50% of children over the age of 5 have been infected and this increases to 90% in the elderly. An acute B19 infection in otherwise healthy children and adults results in fifth disease/Erythema Infectisosum. B19 infection is initially characterized by fever, chills, headache, myalgia and also by a decrease in reticulocytes due to viral replication in the progenitor cells. As the host develops antibodies and the virus is cleared from the system, the infection enters the second phase. This is characterized by the development of a rash and arthralgia and in some cases transient arthritis. These symptoms resolve in about two to six days. B19 infection is of more concern in immunodeficient/immunocompromised hosts and patients with increased erythropoesis

(due to hemolysis or hemorrhage) where persistent anemia (due to the inability to clear the virus) or transient aplastic crisis, respectively, can result. Pregnant women are also at risk, as a B19 infection during the second trimester of pregnancy can lead to Hydrops fetalis (a form of spontaneous abortion as a result of B19 infection of the fetus) or chronic anemia, possibly due to immunotolerance of the B19 virus [3]. Individuals with a genetic based hemolytic anemia can also undergo transient aplastic crisis as a result of B19 infection [4].

Parvoviruses also cause disease in animals of interest, with the outcome depending on the age and state of the host, with the fetus and newborn being most at risk. As parvoviruses generally require specific host cell replication factors, they infect tissues with rapidly developing cells, such as the gut epithelium, immune cells, or bone marrow, as well as many different tissues in the fetus [5]. Feline panleukopenia virus (FPV), canine parvovirus (CPV, closely related to FPV) and porcine parvovirus (PPV) cause pathological infection in cats, dogs, and pigs, respectively. In all three viruses, the fetus and newborn are most susceptible to infection, with a high risk of spontaneous abortion or re-adsorption of the fetus. Vaccines are available for FPV, CPV, and PPV [5, 6]. Infection of adult mink with Aleutian mink disease parvovirus, ADV, leads to either death or chronic infection. As there is no successful vaccine for ADV, the only treatment is the destruction of the infected animals [5, 7]. Finally, infection with *Bm*DNV leads to the death of *Bombyx mori* (silk worm) larva. This caused significant economic hardship among silk growers until *Bm*DNV resistant strains were developed [8, 9].

With the emergence of gene therapy came the interest in using parvoviruses as gene transfer vectors. The most well studied and successfully used parvovirus transfer

vectors are the adeno-associated viruses and there are many review articles on this subject [10, 11]. AAV is not known to cause disease in humans and, in the absence of helper virus, becomes latent, integrating into the host genome. The only major limitation with this viral vector is that only genes of less than approximately four kilobases can be used. A literature search reveals that a large number of AAV gene therapy trials are ongoing, including studies for treatment of cystic fibrosis [12] and Hemophila B [13]. Efforts are also underway to determine the potential of using B19/AAV hybrids as a viral vector to target the erythroid progenitor cells [14]. Likewise, MVM is also being studied as a possible vector where the death of the infected cell is desired or inconsequential such as in oncolytic treatment or vaccination [15]. Finally, the densoviruses JcDNV, GmDNV (greater wax moth virus), and AaeDNV (mosquito virus) are being pursued as gene transfer vectors [16].

The densoviruses are being examined as potential agents for arthropod pest control. Densoviruses are suited for this work as they are usually lethal in the host's larval stage, and are not known to infect humans or mammals. SfDNV and CeDNV have been used to control outbreaks of *S. fusca* and *C. extranea* (oil palm leaf eaters) infections [17, 18]. AaeDNV has also been used to control *Aedes aegypti* mosquito larvae in the former Soviet Union and a commercial formulation has been developed [19, 20]. The development of densovirus gene transfer vectors will further aid in this area.

Finally, the high dependence of parvoviruses on the host cell for viral replication presents an opportunity to study host cell-virus interactions. Parvoviruses are currently being used to study apoptosis and other forms of cell death [21-23], anti-neoplastic activity [24], cell cycle [25, 26], and DNA replication [27, 28].

Minute Virus of Mice (MVM)

The parvovirus minute virus of mice (MVM) has served as a prototype for the vertebrate parvoviruses. The genome has been completely sequenced [29], the viral transcripts and viral proteins identified [30-33], and the genome replication cycle worked out [27, 28, 34], although some details of the replication mechanism remain to be elucidated. MVM can be cultured *in vitro* (causing an acute infection in a mouse fibroblast cell line) and grown to high titre [33]. It has extremely stable capsids [35], and importantly, infectious clones are available [36]. Furthermore, MVM is usually non-pathogenic for its murine host [37], (although some strains of inbred neonatal mice are susceptible [38, 39]) and so can be handled with limited biosafety precautions. Finally, a variant, MVM_i, [40] displays a tropism for murine lymphocytes [41] and, unlike MVMp, does not infect mouse fibroblasts providing a useful comparison between the two strains. MVM has been successfully used to model parvovirus genome replication and to characterize the functions of the major non-structural protein.

MVM Structure:

MVM consists of ~26 nm non-enveloped icosohedral viral particles, with each particle containing one copy of a single-stranded (negative sense) DNA genome. These particles are stable up to 56°C and through a pH range of 3 to 9 and can survive treatment with alcohol or ethers but are susceptible to bleach [27, 35]. The structure of MVMi determined to 3.5 Å [42] resolution by x-ray diffraction of crystals is shown in Figure 1a. The capsid has a T=1 symmetry and is made up 60 viral capsid proteins (VP1, VP2, & VP3) with VP2 being the dominant capsid protein.

A

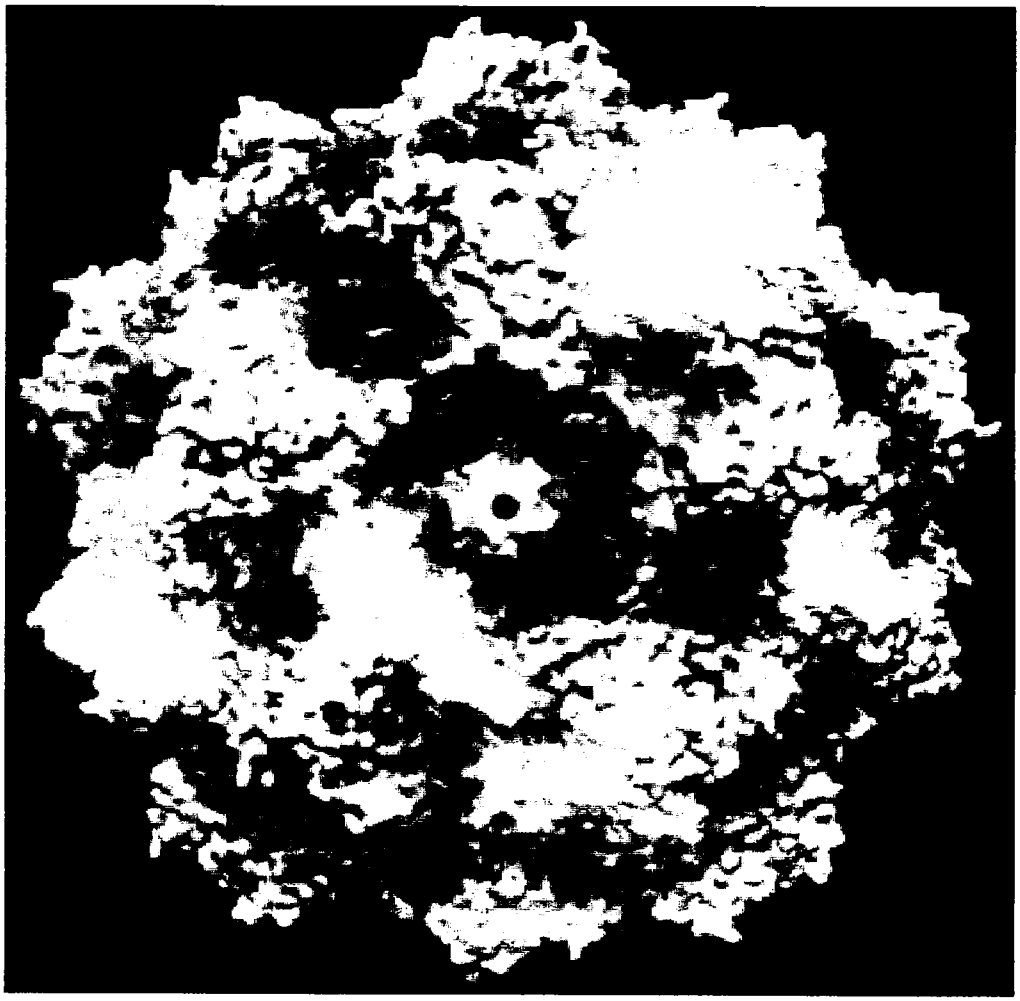

B

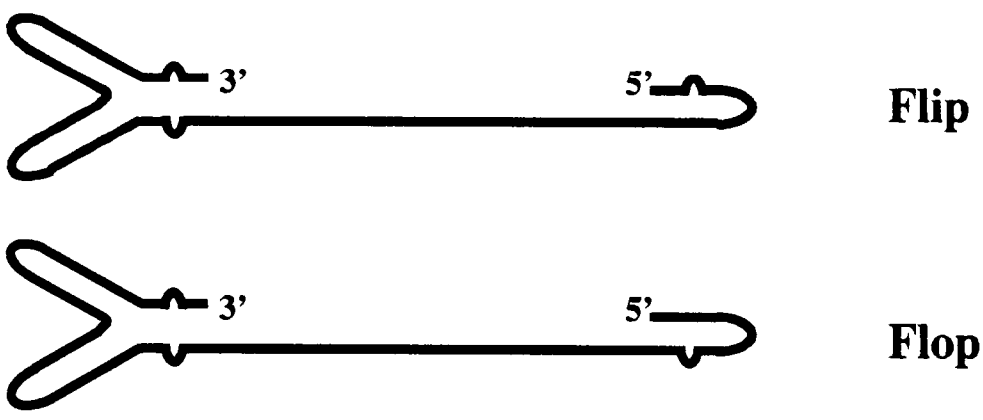

Figure 1: MVM Structure. **A.** 3D crystal structure of MVM as viewed from the 5-fold axis of symmetry. Taken from Agbandje-McKenna et al., 1998. **B.** MVM genome structure showing the 3' and 5' hairpins, unpaired bubbles and flip and flop designations.

MVM Genome structure and replication:

The MVM genome is a single-stranded linear DNA molecule of 5149 nucleotides in length [29]. It is packaged predominantly in the negative form (i.e. complementary to the transcripts) and contains hairpins at both the 3' and 5' ends (Figure 1b). The 3' hairpin is "y" shaped with only one small sequence in the hairpin stem that is unpaired. The 5' hairpin sequence exists in two forms, "flip" and "flop", which differ only at three nucleotides within the hairpin turn itself and in a small unpaired sequence bubble within the stem. The unpaired sequences found in the 5' hairpin of flip are the inverted complement of those found in flop and both flip and flop are packaged equally into the capsid. Both the 3' and 5' hairpins are essential for MVM replication [43]. A molecule of the major non-structural viral protein NS1 can be found covalently linked to the 5' end of the genome, and extends outside the virus particle once the genome is encapsulated [44, 45]. This protein can be removed without affecting viral replication.

Replication of the MVM genome is a complicated and not completely understood process. The virus has two origins of replication, located at the left and right hairpins, respectively [43, 46]. These two origins differ in size, primary sequence and secondary structure. The virus does not encode any polymerases and so is dependent on a series of host cell factors for replication to occur. These include DNA polymerase δ, PCNA [47], parvovirus initiation factor (PIF) [48], the high-mobility group 1/2 proteins (HMG1/2) [49], replication protein A (RPA) and Replicative factor C [34]. Presumably, as a result of these requirements, the virus requires the host cell to be in S phase in order to replicate [50]. Furthermore, MVM cannot induce cells to enter S phase and so must wait until the cell enters S phase naturally. However, once S phase is reached, the virus causes the host

cell to arrest permanently in S/G2 and thus allow extensive replication of the virus. The viral non-structural protein NS1 is also required for a number of functions in replication. Replication is thought to occur through a modified form of rolling circle DNA replication [28, 51] using a single continuous DNA strand containing multiple copies of the viral genome. The processing of this molecule into viral progeny is not completely understood; however NS1, with its nickase, helicase, and DNA binding functions, is required. MVM genome replication occurs in specific bodies within the nucleus of the cell [52].

MVM Transcription

MVM contains two promoters: P4 located at the left hand end of the genome, at 4 map units, and P38 located in the middle of the genome, at 38 map units [29]. A poly-adenylation signal is located on the extreme right hand end of the genome [53]. Transcription runs from left to right with the coding information being present in the complementary strand to the original viral genome. There are three major open reading frames in MVM, one in each of the three reading frames [32] (Figure 2).

The P4 promoter controls transcription on the left hand side of the genome and generates the R1 and R2 transcripts, which encode the non-structural proteins NS1 and NS2, respectively [31, 54]. The R2 transcript is an alternatively spliced form of the R1 transcript where ~1.5 kb of sequence is removed and the reading frame is shifted [55]. The resulting translation product, NS2, thus shares its N terminal sequence with NS1 but has its own unique C terminal sequence. There is also a second smaller splice site located near the center of the genome that contains multiple splice donor and acceptor

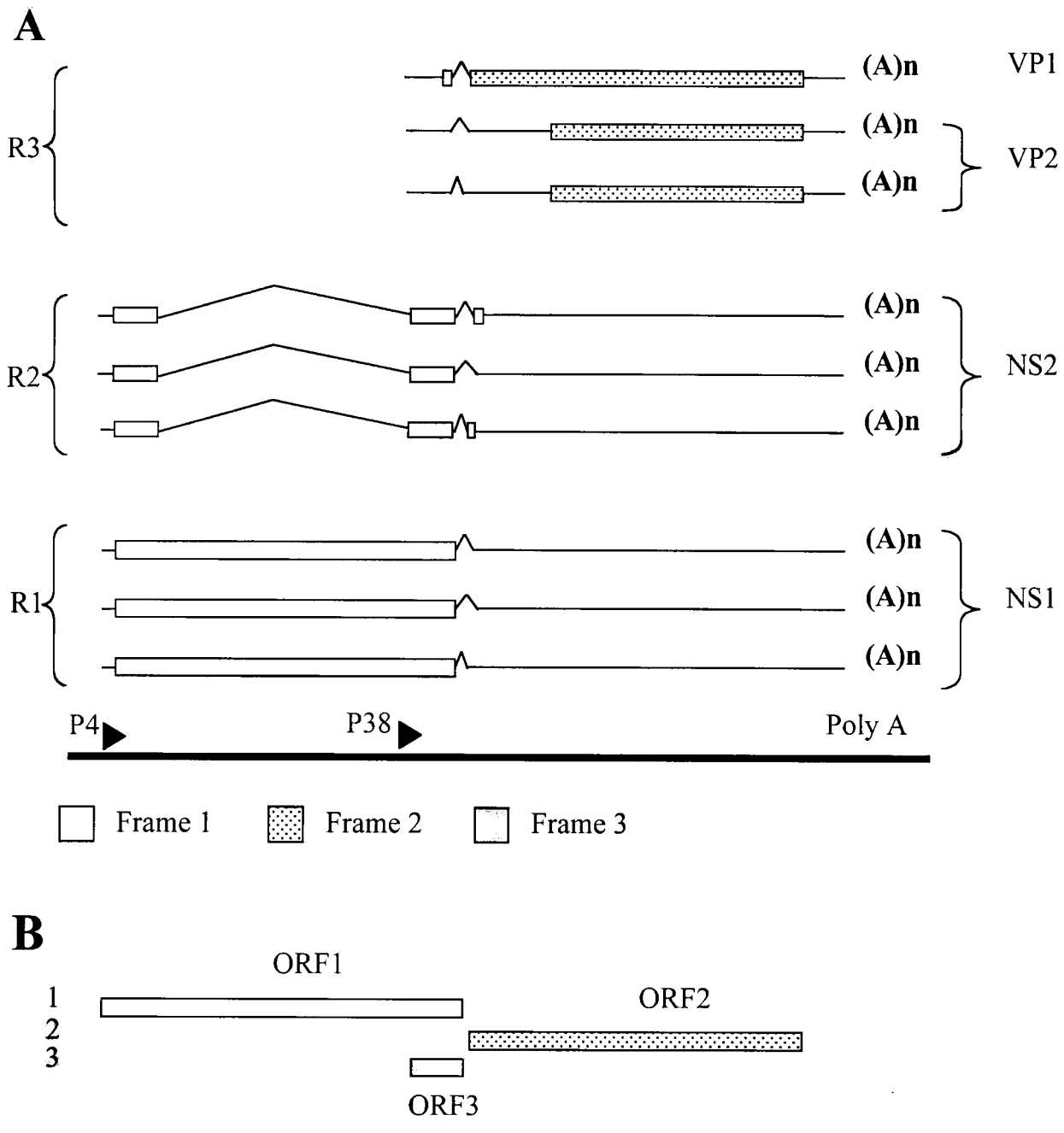

Figure 2: MVM Transcription. **A.** The three major MVM transcripts (R1, R2, and R3), splicing patterns and their products. The shading in the box indicates reading frame. For example, translation of the top R2 transcript starts in frame one and then changes (as a result of splicing) to frame three, and then switches back (again due to splicing) to frame one. **B.** The three major open reading frames in MVM.

sites [56]. As a result of further alternate splicing at this site, the R2 transcripts are actually a group of three slightly different transcripts. Each of these R2 transcripts encodes a NS2 protein whose protein sequence differs at its C terminal end (between 6 to 11 amino acids [57]). The significance of this heterogeneity is not known. The R1 transcript also contains the small splice site, but as the NS1 coding sequence terminates before the splice donor sites, all three R1 transcripts will produce the same protein (Figure 2).

The P38 promoter controls transcription on the right hand of the genome and generates the R3 transcripts, which encodes the structural proteins VP1 and VP2 [58]. As in the R1 and R2 transcripts, the R3 transcript exists in three forms, again due to the presence of the small splice site. In one transcript, a translation start site is preserved upstream of the splice donor site and the VP1 protein is generated. In the other two transcripts, the same translation start site is removed, and translation does not start until much further along the mRNA, yielding the VP2 protein (Figure 2).

There are several transcription factors involved in control of MVM transcription. NS1 has the ability to both bind and transactivate both promoters. It first enhances transcription at the P4 promoter (although it is not required for efficient transcription [59]), and then later as the infection progresses, it transactivates the P38 promoter (where it is essential, [60]). This ensures that the non-structural proteins are predominantly expressed early in infection and the capsid proteins later in infection. The transcription factor E2F is also needed for P4 activation [61, 62] along with the basal RNA polymerase II machinery. The P38 promoter seems to require Sp1 [63] and CREB binding protein (CBP, [64]) interactions with NS1 in order for transcription to occur.

MVM Proteins

There are five viral proteins encoded by MVM. These include the non-structural proteins NS1 and NS2 and the structural capsid proteins VP1, VP2, and VP3 (derived from VP2; see below) (Figure 3a).

The NS1 protein has a number of functions. It is a multi-domain protein of 672 amino acids with an apparent molecular weight of 83 kDa [54]. It is heavily phosphorylated by at least two kinases, casein kinase II and protein kinase C λ (PKC λ). Phosphorylation of NS1 by PKC λ controls a number of NS1 functions [65-68]. NS1 is predominantly nuclear (NS1 has a nuclear localization signal) and is present in specific MVM replication bodies within the nucleus [47, 69]. As mentioned above, NS1 contains nicking [70], helicase [71], DNA binding [72] and ATP binding/hydrolysis domains [73] that are essential for replication. NS1 is also required for transactivation of the P4 and P38 promoters [74], cell cycle arrest [25], and is cytotoxic to the host cell. It forms dimers and oligomers through its oligomerization domain [75]. Figure 3b shows the various domains present in NS1. Finally NS1 has been found to interact with a large number of different proteins, including: Survival of Motor Neuron (Immunopreciptation, BIAcore biosensor) [77], TATA Binding Protein (TBP) (GST-NS1 capture assay), Transcription Factor II A (TFIIA) (GST-NS1 capture assay), Sp1 (GST-NS1 capture assay) [63], and NS1 associated protein/HnRNP-Q (NSAP1) (yeast two hybrid) [78]. NS1 also interacts with Parvovirus Initiation Factor (PIF) [76] although no evidence of binding has been shown.

The function(s) of NS2 protein is much less understood. As mentioned above, it consists of three proteins that vary in their C-terminal sequence. They have apparent

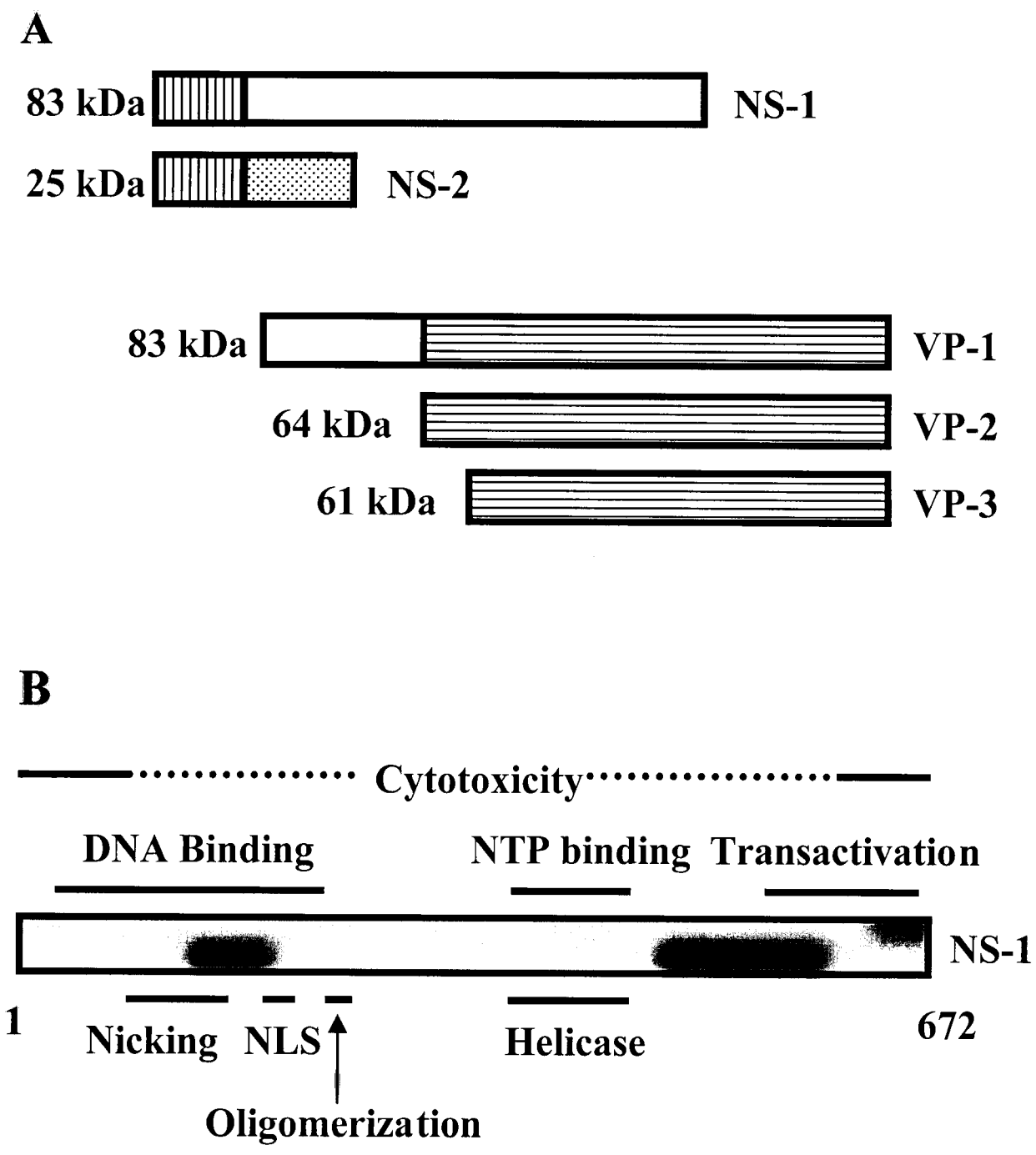

Figure 3: The MVM proteins. A: The MVM proteins and their apparent molecular weights. Common areas indicate sequence of shared amino acid sequence. B: NS1 and its associated domains (taken from Corbau et al., 2000).

molecular weights of 25 kDa and lengths of 188 or 197 amino acids. The NS2 proteins exist in both phosphorylated and unphosphorylated forms with the unphosphorylated forms found both in the nucleus and cytoplasm and the phosphorylated form found exclusively in the cytoplasm [79]. The NS2 proteins are needed for efficient viral replication [80, 81], and viral protein translation [82] in the murine cells. Furthermore, they are important for capsid assembly [83]. NS2 proteins bind to Crm1 (exportin-1) [79, 84] and, through a nuclear export signal (NES) present in NS2, are exported to the cytoplasm. Mutation of the NS2 NES leads to retardation of viral egress from the nucleus and a decrease in the production of viral progeny ssDNA [85, 86]. Finally they have been found to associate with SMN [87], and the 14-3-3 proteins [88].

VP1, which is present as 15% of the capsid, is a multifunctional protein with an apparent molecular weight of 83 kDa and a length of 718 amino acids. It contains a unique N terminal sequence and shares its C terminal sequence with VP2 and VP3 [89]. The shared C terminal sequence of VP1 forms part of the full viral capsid, analogous to that of VP2, while the unique N terminal sequence is tucked inside the capsid. Details on the structural role of VP1 and VP2 are reported in Agbandje-McKenna et al., 1998 [42]. The unique N terminal sequence of VP1 is not required for capsid assembly but is found to be essential for viral infectivity and has a role in viral entry at some stage past the point of capsid binding [90]. More recently, it was found that this region contains a functional phospholipase A_2 (PLA_2) active site that is needed for infection and is conserved among many different parvoviruses [90]. The role of this viral PLA_2 is not known.

VP2 is the major capsid protein, forming the majority of the capsid. It has an apparent molecular weight of 64 kDa and a length of 584 amino acids. The protein

adopts an eight-strand β-barrel conformation and can spontaneously form empty capsids [42].

VP3 is a cleavage product of VP2 [89]. The first approximately twenty amino acids are lost from the N-terminus, yielding a protein with an apparent molecular mass of 63 kDa and a length of 564 amino acids. This cleavage event appears to have no effect on the stability of the virus capsid.

MVM-host cell interactions

Viruses interact with their host cells in a number of different ways. They can alter replication, transcription and translation, RNA and protein trafficking, the cell cycle, apoptosis, the stress response, intracellular and extracellular signaling, and the immune response. This next section will examine some of these interactions observed with MVM.

MVM, the cell cycle, and apoptosis

MVM can arrest transformed cells in S/G_2. This is accompanied by an increase in p53 and $p21^{cip}$ (a cyclin dependent kinase inhibitor that acts downstream of p53) proteins with p53 required for the block in S and both p53 and $P21^{cip}$ required for the block in G_2 [25]. Initially, the block in cell cycle was thought to be due to NS-1 [91] as expression of NS-1 led to cell cycle arrest in $G_1/S/G_2$. However, NS1-expressing cells only showed an increase in $p21^{cip}$ and not p53. This is an interesting result as NS1 can induce nicks in host cell DNA [91] and DNA damage is a potent activator of p53. It is now hypothesized that MVM-induced cell cycle arrest is a combination of NS1 expression and the sudden increase in linear single stranded viral DNA, which could lead to p53 activation. Another

interesting observation is the accumulation of cyclin A, and not cyclin E or cdk2, in the MVM replication bodies [52]. Cyclin A is responsible for the transition from S to G_2 and so sequestering cyclin A could also contribute to cell cycle arrest.

Many parvoviruses can induce apoptosis in their host cells with examples including B19 [21, 22] and Rat H1 parvovirus [23]. Given that MVM activates p53 and NS1 causes nicking in host cell DNA, it would be expected that MVM infection would induce apoptosis in the host cell. So far, this remains unproven. DNA "ladders" characteristic of apoptosis have been observed in a mouse fibroblast cell line; however, effector caspases were not activated and the classic apoptotic morphology was not seen (L. Tamburic and C. Astell, unpublished results). It has been reported recently that NS1 and NS2 interact with SMN [77, 87]. SMN has been shown to protect primary neuronal cells from virus-induced apoptosis [92]; however, what role SMN plays in MVM infection remains undefined.

MVM and host transcription/RNA processing/RNA transport

MVM's effect on host transcription has not been well characterized. There has been a report that MVM infection of Ehrlich ascities cells modifies host cell transcription and alters *c-fos* expression [93]. NS1 has also been shown to have a transinhibiting effect on the Rous sarcoma virus long terminal repeat promoter [74] and the CMV promoter [94] as visualized by reporter constructs. Interestingly, if a NS-1/lexA fusion was tested on the same Rous sarcoma promoter with a LexA binding site, NS1 exhibited a transactivating effect [95]. NS1 has also been shown to exert a transactivating effect on the *c-erbA1* promoter, again by a reporter gene assay, and MVM infected cells showed increased amounts of the *c-erbA1* transcripts in ras-transformed FREJ4 rat fibroblasts

[96]. Furthermore, NS1 was found to bind to FRE (a sequence that interacts with transcription factors belonging to the FTZ-F1/SF sub-group of nuclear hormone receptors) in the *c-erbA1* promoter [97]. The *c-erbA1* gene encodes thyroid hormone (T3) receptor α, which is involved in cell differentiation and proliferation, among other functions [98, 99]. There has been no further characterization of the interaction between MVM/NS1 and thyroid hormone (T3) receptor α. Finally, it has been suggested recently that NS1 oligomerization is needed for its transactivating/transrepressing functions [94].

There are no definititive studies to indicate that MVM alters host RNA processing, but there is increasing evidence that MVM proteins interact with the splicing machinery. The recently found NS1 binding protein NSAP1/hnRNP Q, [78] was identified as a component of the spliceosome [100]. Furthermore, NSAP1/hnRNP Q interacts with SMN [100] and, as already stated, SMN interacts with NS1/NS2 [77, 87]. The roles of these NS1 interactions are not understood.

There have been no reports in the literature that MVM affects host cell RNA transport. The initial discovery of the NS2/Crm1 interaction did suggest a possible role in RNA transport as interactions of other viral proteins like HIV Rev [101] or Adenovirus E1B 55 [102] with Crm1 affect host or viral RNA transport. However, disrupting the NS2/Crm1 interaction did not affect viral protein synthesis [85] and there are no reports of changes in global protein expression during MVM infection.

MVM and host cell translation/protein trafficking

There are no known reports of MVM altering global host cell protein translation and trafficking. Total cellular protein levels do not change upon MVM infection until

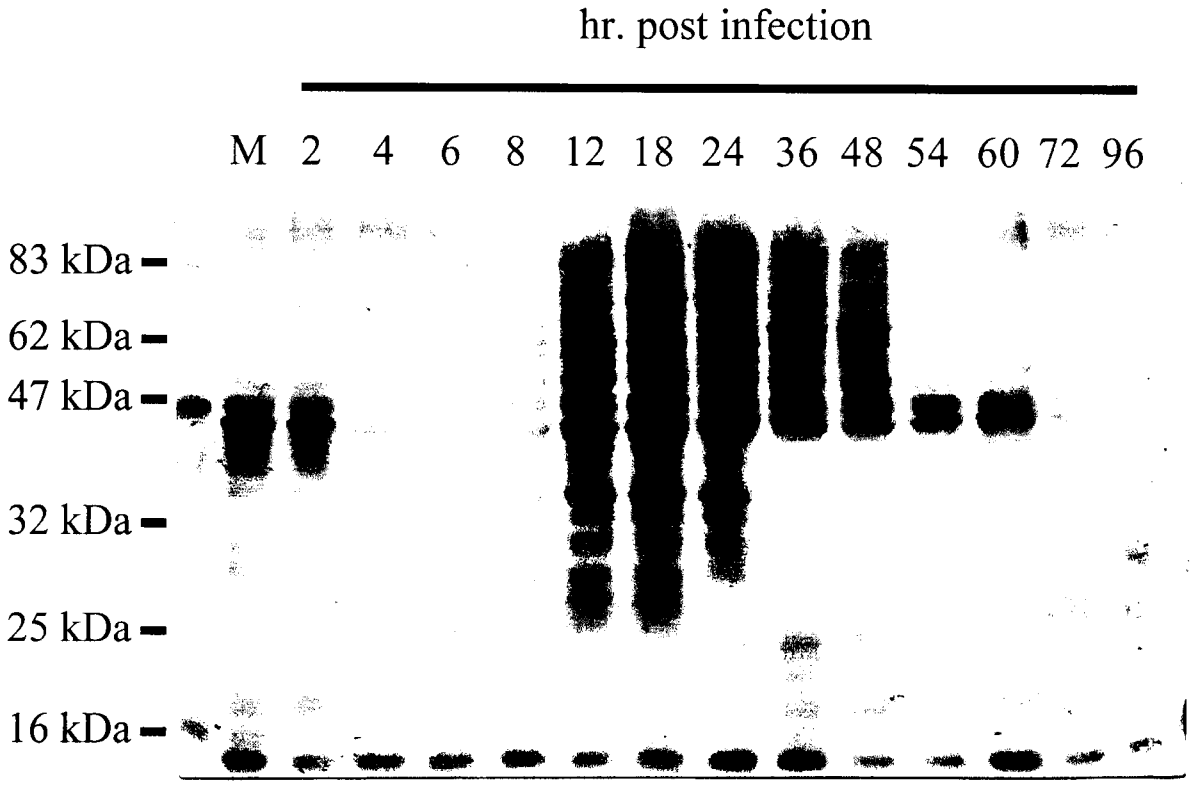

Figure 4: Total LA9 protein levels do not change during MVMp infection until late in infection. PVDF membrane of LA9 fibroblast total cell protein stained with Coomassie blue. M: mock infected cells. Each lane represents 5 µl of total protein extract from one dish of infected LA9 cells. The decrease seen at late time points is presumably due to increased cell death caused by the virus. Membrane provided by Dr. Cynthia Shippam-Brett.

late time points, presumably due to cell lysis (Figure 4; C. Shippam-Brett & C. Astell, unpublished results). The MVM NS2 protein is needed for efficient translation of the viral proteins [82], although how this is accomplished is not known.

MVM and host intracellular/extracellular signaling

Several signaling pathways have been implicated in MVM infection but have not been well characterized with respect to the virus or host. As already reported, MVM infection leads to increased transcription of *c-erbA1* and this could alter the thyroid hormone induction pathway. MVM protein VP1 contains an active phospholipase A_2 domain (PLA_2). Besides being used for lipid turnover, PLA_2 is associated with inflammatory, signal transduction, and various physiological and pathological processes [103, 104]. Finally, NS2 protein interacts with the 14-3-3 proteins [88]. The 14-3-3 proteins display a variety of functions in the cell including signal transduction, checkpoint control, and apoptotic and nutrient sensing pathways. It is thought to accomplish these functions by altering the sub-cellular localization of partners [105]. The exact role of the NS2/14-3-3 interaction is not known.

MVM induced cytotoxicity

MVMp is cytopathic for many types of transformed cells [106, 107] including the mouse fibroblast cell line LA9 (Figure 5). This cytopathic effect is believed to be mediated by NS1, as expression of NS1 alone in transformed cells also leads to cell death [108, 109] although NS2 can enhance this process [110]. NS-1 cytotoxicity has been mapped to the C and N terminals of the protein [74]. How NS-1 is cytotoxic to cells is not known, although there are several theories. These include the ability of NS1 to

60 hours mock infected

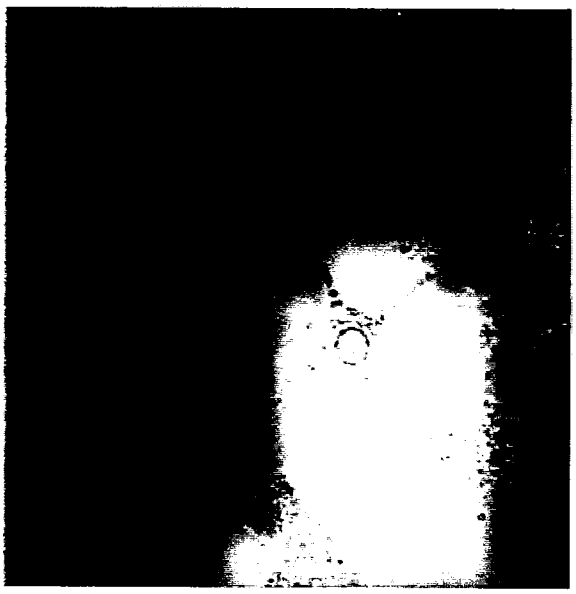

60 hours infected

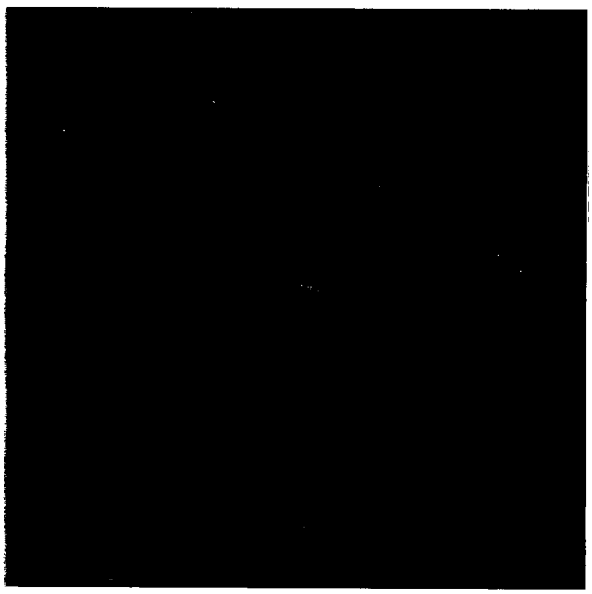

72 hours infected

Figure 5: Cytotoxic effects of MVM. Transformed mouse fibroblast LA9 cells infected or mock infected with MVMp at various times indicated. Photos taken by L. Tamburic.

transactivate or transinhibit other genes [74], to nick host cell DNA [91], to induce cell-cycle arrest [25] and to alter specific protein phosphorylation and synthesis [111].

Project Goals:

The purpose of my studies was to further characterize the host cell response to infection by a small DNA virus. Specifically, I have focused on changes in gene expression in the mouse fibroblast cell line LA9 during infection with MVMp. My studies included examining changes in mRNA expression using differential display analysis and commercially available macro and microarrays. I also used a commercially available service to detect changes in kinase levels following infection. This work is to be considered as a survey of gene expression changes and does not examine the entire mouse transcriptome.

SINEs and LINEs

Introduction

As this thesis examines Short INterspersed Elements (SINEs) and Long INterspersed Elements (LINEs) expression during MVM infection, a brief review is included to aid the reader. LINEs and SINEs are members of the retroelement family and are commonly referred to as retroposons (Figure 6a) [112]. Large numbers of retroposons are found in eukaryotic DNA, including plants, mollusks, chordates, and arthropods [113, 114]. In humans, there are approximately 860,000 copies of the various LINEs, composing approximately 21% of the genome, while SINEs comprise another 13% of the genome with over 1.5 million copies [115]. The numbers are similar in the mouse genome, with LINEs composing approximately 19% of the genome with 660,000

A

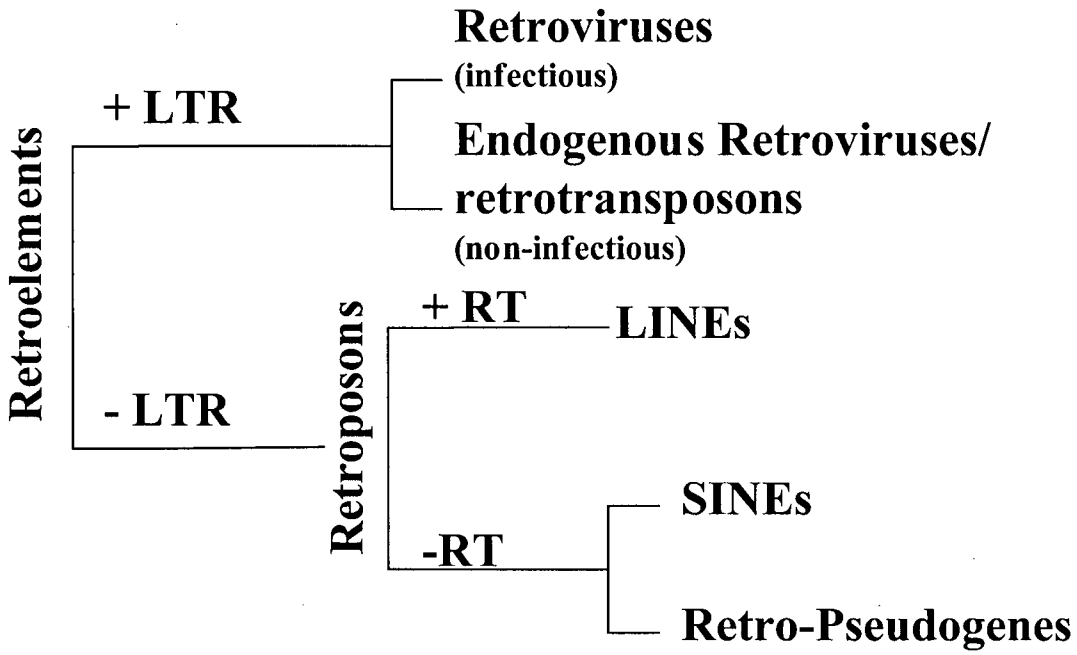

B

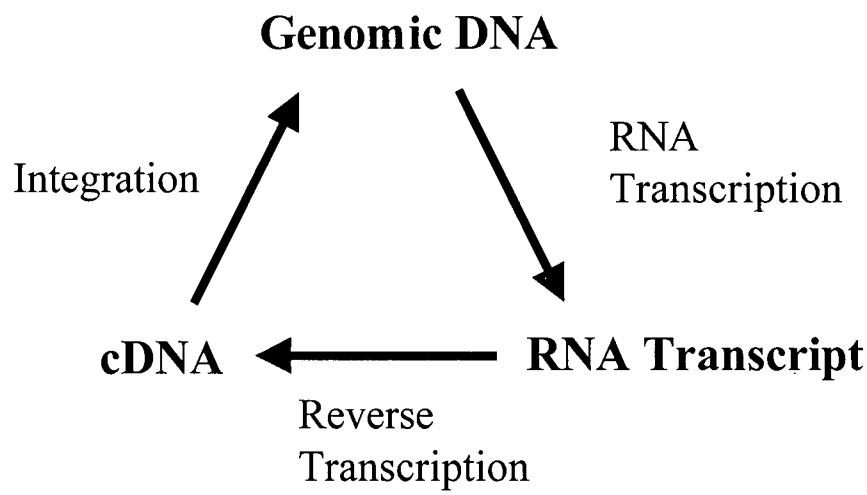

Figure 6: **A:** Retroelement classification. LTR: Long terminal repeat; RT: Encoding reverse transcriptase. **B:** Generalized retroposon replication.

copies and SINEs comprising another 8.3% of genome with over a million and a half copies [116]. Retroposons replicate via a RNA intermediate that is reverse transcribed prior to re-integration into the genome (Figure 6b). A brief review of SINE and LINE structure, SINE replication, and factors that affect SINE expression will be discussed below.

LINE and SINE Structure

LINEs average 6 kb in size and contain a internal RNA polymerase II promoter, one or two open reading frames (depending on the LINE), and a poly-adenylation signal at the extreme 3' end (Figure 7a). The first ORF, ORF 1, is only found in younger LINEs, for example L1 LINE, and its function is unknown. The second ORF, ORF2, encodes a protein with both reverse transcriptase and endonuclease domains. In younger LINEs this is an apurinic/apyrimidinic endonuclease, while in older LINEs it is a restriction-like endonuclease. The integrated LINE DNA is flanked by direct repeats, thought to be a result of the integration and DNA repair process [117]. Human and mice share L1, L2, and L3 LINEs and only the L1 LINE is considered to be active, i.e. replicating.

SINEs range in size from 50-500 nt in size and do not contain any coding sequence. They contain an internal RNA polymerase III promoter (AB box) and a poly A tract at the 3' end (Figure 7a). Like LINEs, they are flanked by direct repeats of 5-20 nt in size. Many SINEs are derived from tRNAs (for example the murine B2 SINE resembles Ala tRNA) or other small RNAs [118] and can also have a LINE like sequence at the 3' end (for example the MIR SINE and L2 LINE share some of the same sequence)

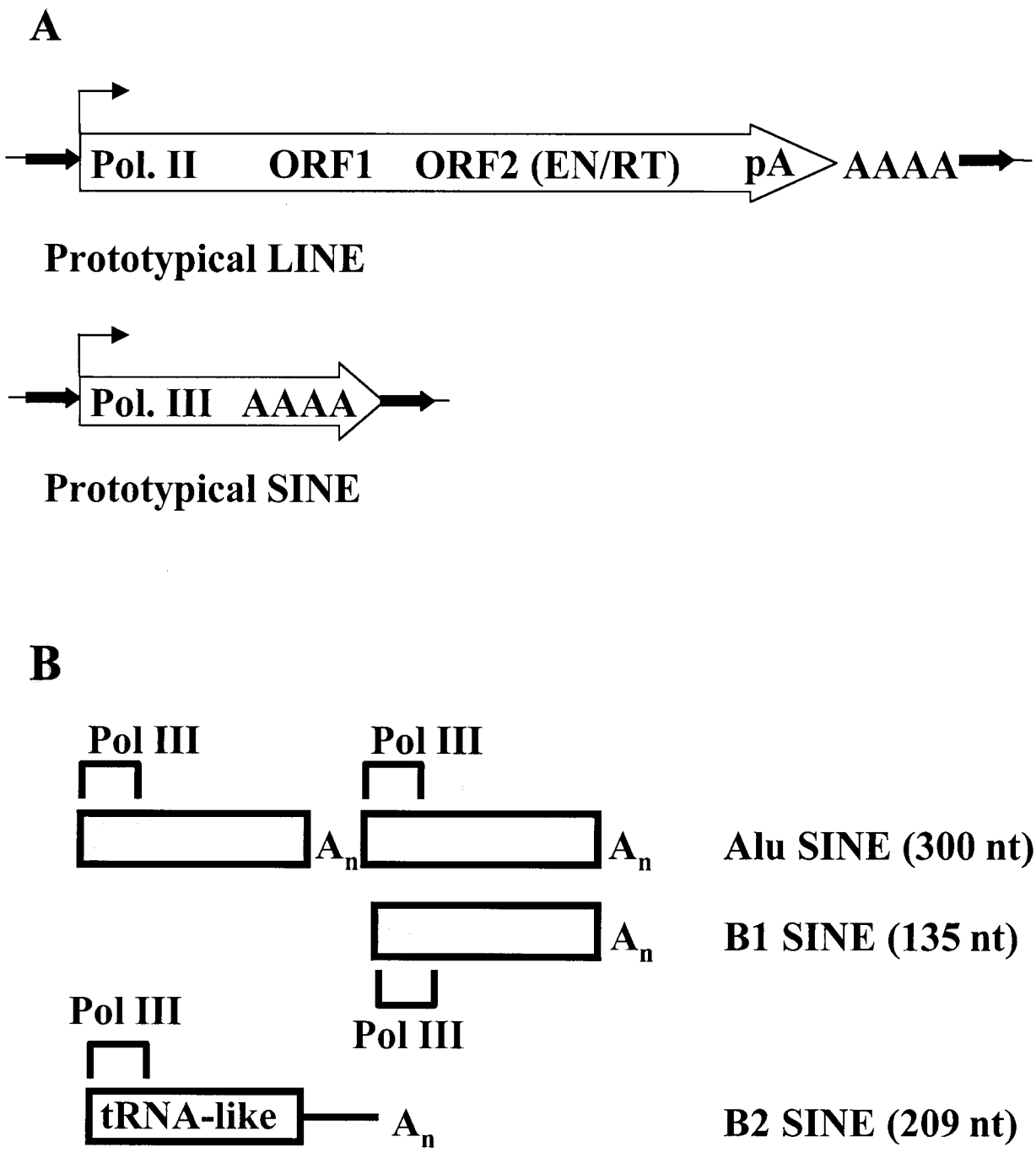

Figure 7: SINE and LINE structure. **A:** SINE and LINE prototypical structures. Note that older LINEs lack ORF1. Pol II & Pol III: RNA polymerase II & III promoters; EN: Endonuclease; RT: Reverse transcriptase; pA: Poly-adenylation signal; Solid arrow: Target site sequence duplication (adapted from Weiner et al., 2002). **B:** Alu, B1 & B2 SINEs. Pol III: RNA polymerase A-B box promoter; Shaded box: Shared sequence with 7SL. Size in brackets indicates the size of the core repetitive element.

[119]. The human Alu and the murine B1 SINE differ from the tRNA-like SINEs as they contain a sequence closely related to that of the signal recognition particle 7SL RNA (Figure 7b). Termination of RNA polymerase III transcription requires an oligothymidylate tract. SINEs lack this tract, and so transcription terminates at a random oligothymidylate tract downstream of the SINE, resulting in SINEs with variable 3' ends [117]. Humans and mice share the MIR/MIR3 SINEs and have similar 7SL derived SINEs, referred to as Alu SINEs in humans and B1 SINEs in mice. Mice also have three additional SINEs, the B2 SINE (which exists in low copy number in humans [120]), ID SINEs, and B4 SINEs (similar to a B1/ID SINE fusion). In humans, only the Alu SINE is considered to be active, whereas in mice, at least the B1, B2, and ID SINEs are active. The rest of this review will focus on SINEs, specifically the murine B1 and B2 SINEs.

SINE replication

SINE replication is not fully characterized. The current model starts with RNA polymerase III transcription of the DNA SINE. The SINE RNA is then transported to the cytoplasm where it binds to a LINE reverse transcriptase/endonuclease protein. This complex is then transported back to the nucleus, where the endonuclease induces a staggered double stranded cut. The free 3' OH is used to prime reverse transcription of the SINE RNA. Host cell DNA repair mechanisms and DNA ligase repair the nicks and fill in the missing sequence [117, 121]. The replication scheme for SINEs is illustrated in Figure 8.

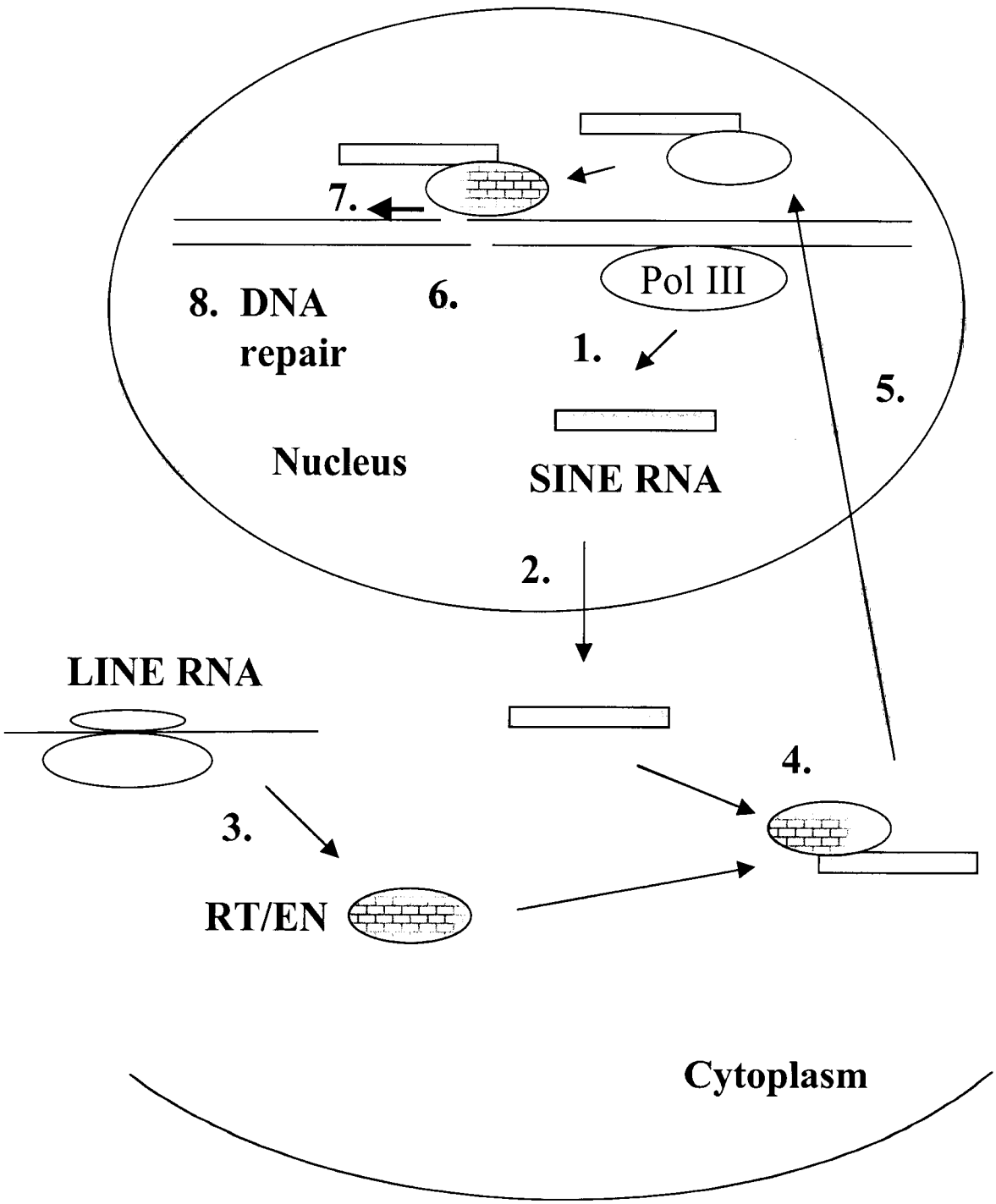

Figure 8: Current model of SINE replication. 1. SINE transcription. 2. SINE RNA transport to the cytoplasm. 3. Translation of LINE reverse transcriptase (RT) and endonuclease (EN). 4. SINE binds RT/EN. 5. SINE transport to nucleus. 6. Endonuclease induced staggered break. 7. 3' OH prime reverse transcription. 8. DNA repair. Pol III: RNA polymerse III.

SINE transcription

SINEs contain a type II A-B box promoter that is recognized by RNA polymerase III. Transcription of SINEs is, therefore, dependent on the presence of a host of basal RNA polymerase III transcription factors. The process of RNA polymerase III transcriptional initiation at type II promoters and subsequent elongation is complicated and still under investigation. This section will attempt to provide a basic view of what is currently understood based on several excellent reviews [122-124].

Initiation of RNA polymerase III transcription seems to occur in a stepwise dependent manner, at least *in vitro*. A protein complex termed TFIIIC2 first recognizes the type II promoter. This complex is comprised of five proteins: TFIIIC220, 110, 102, 90 and 63. Together, these proteins recognize the promoter A and B boxes and recruit a second complex called TFIIIB (another complex, TFIIIC1, is also recruited but it is not well characterized). TFIIIB is composed of three proteins: TBP (TATA binding protein), BRF1 (TFIIB related protein), and Bdp (B double prime protein). This second complex functions to open the helix and, with the help of TFIIIC2, recruit the RNA polymerase complex (Figure 9). Transcription then occurs without elongation factors and the TFIIIC and TFIIIB complexes remain associated with the promoter. Termination occurs when the polymerase reaches an oligothymidylate tract.

Controlling SINE expression

With the large number of SINEs present in a cell's genome, it becomes essential for the host to control SINE expression or risk serious alterations to its genome.

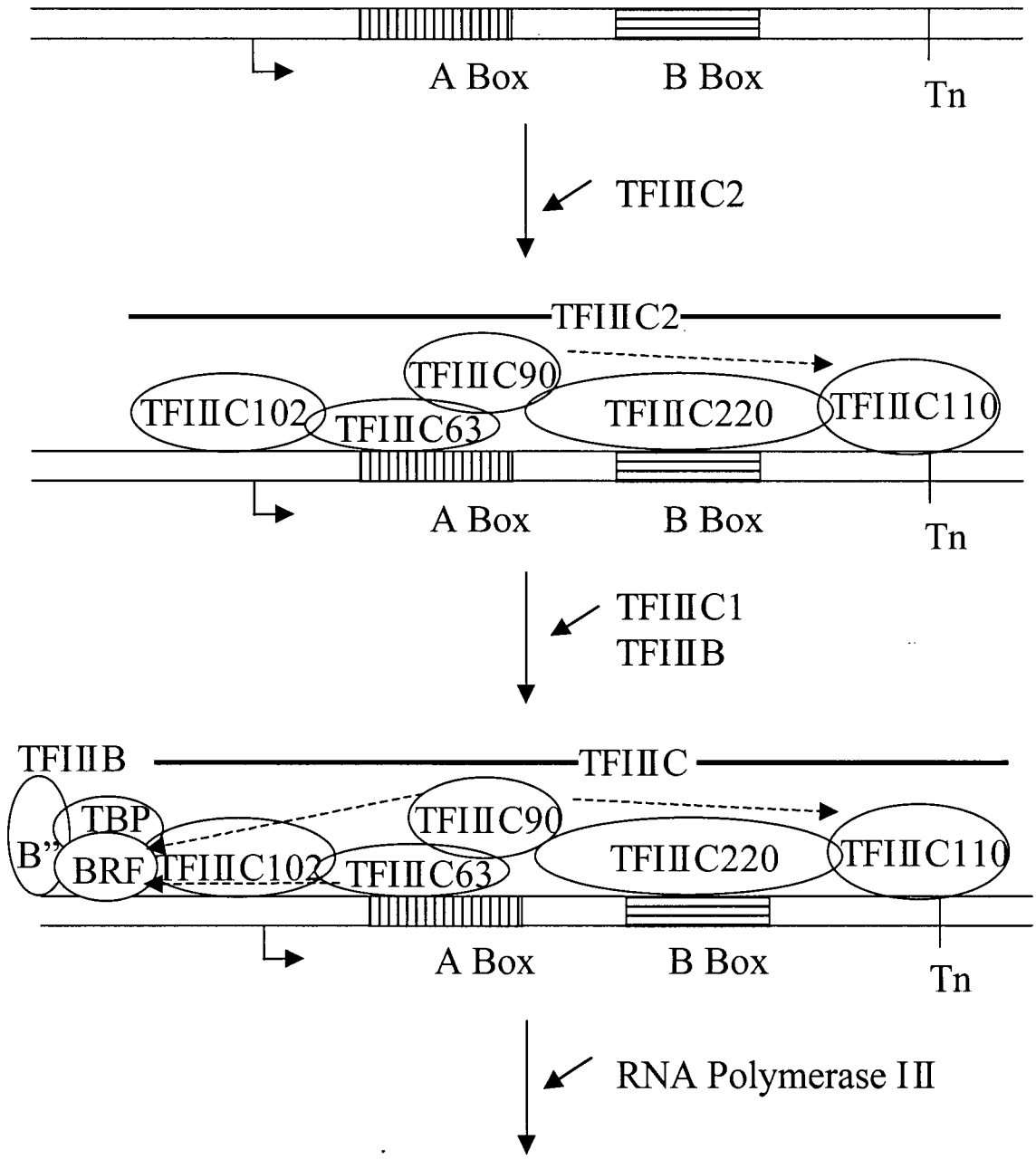

Figure 9: Stepwise assembly of RNA polymerase III transcription factors. TFIIIC2 recognizes the type II promoter and recruits TFIIIB. TFIIIB recruits RNA polymerase and opens the helix. B": B double prime protein; TBP: TATA binding protein; BRF: TFIIB related factor; The A and B boxes are components of the RNA polymerase III type II promoter. Dashed arrows indicate additional protein-protein interactions.

Currently there are several theories on how the cell accomplishes this. One possibility is that the SINE DNA becomes methylated, leading to re-arrangement of the chromatin environment and suppression of transcription [125-127]. However, not all SINEs contain large numbers of methylation sites and some of the methylation repression (of transcription) machinery doesn't seem to repress SINE transcription [128]. Another possibility is RNA interference, by which transcribed SINE RNA can be identified and destroyed before it integrates back into the genome [129]. Finally, at the individual SINE level, the presence of cis elements, chromatin context and individual promoter sequences will all affect transcription [126].

Materials and Methods

1. LA9 cell culture

Adherent LA9 mouse fibroblasts [130] were cultured in low glucose DMEM (Gibco BRL) supplemented with 5% fetal bovine serum (Gibco BRL) and 25 mM HEPES (Sigma) on Falcon #3003 100mm plates at 37°C, 5% CO_2 in a humid environment.

Cells were routinely passaged by the removal of spent media, washed twice with 5ml PBS followed by addition of 1ml trypsin-EDTA (Gibco BRL) for 2 minutes at 37°C. The cells were resuspended in fresh media and routinely diluted 1:10 with DMEM containing 5% FBS and 25 mM HEPES. Cells were counted using an hemocytometer.

2. MVM production

MVMp was cultured following a modified protocol of Tattersall et al., 1976 [33]. LA9 cells were grown in suspension in high glucose DMEM enriched with nucleotides (Gibco BRL), 5% FBS, 25mM HEPES in an environment of 5%CO_2, 37°C to a concentration between ~ 1 x 10^5 to 5 x 10^5 cells/ml, diluting as necessary. Cells were infected at low MOI (typically 0.01 to 0.001 pfu/cell) and monitored for cytopathic effects and cessation of growth. Cells were pelleted, washed with TNE buffer, taken up in low salt buffer (50 mM Tris-Cl pH 8.7, 0.5mM EDTA, 0.1 MPMSF) and lysed by homogenization (VirTis 45") and sonication (Branson Sonifier 250). Cellular debris was pelleted and discarded. Virus particles were precipitated from the supernatant with 25 mM $CaCl_2$ and resuspended in viral uptake buffer (50 mM Tris-Cl pH 8.7, 20 mM EDTA) with gentle sonication. The virus preparation was purified by centrifugation in a

CsCl gradient (SW-41, 28,000 rpm for 20 hr.) and full virus particles (ρ = 1.41 g/ml) were collected through the side of the tube using a syringe and subsequently dialyzed against TE pH 8.7. Host cell genomic DNA was removed from the virus preparation by addition of micrococcal nuclease (Pharmacia) to 20 μg (800 U)/ml and $CaCl_2$ (to 5 mM), and full virus particles were repurified through another round of CsCl gradient centrifugation and dialysis. Virus preparations were titred as described below.

3. Virus titration

MVM virus stock was titred using a plaque assay [131]. LA9 cells were seeded at 5 x 10^4 – 1 x 10^5 cells in 60 mm plates and infected with serially diluted viral stock in viral uptake buffer (50 mM Tris-Cl pH 8.7, 20 mM EDTA). After one hour to allow attachment of the virus to cells, the virus was removed by suction and cells covered with a mixture of 7 ml of 0.75 % low melting point agarose (Gibco-BRL) / DMEM / 1% Tryptose Phosphate (Gibco-BRL) / 5% FBS/ 20 μg/ml gentamicin (Gibco-BRL). After the agarose solidified at room temperature, the cells were grown for 5 days at 37°C, 5% CO_2 at which point they were fixed by addition of 10% formaldehyde on top of the agarose layer for 30 minutes. The agarose/formaldehyde was removed and the cells stained with 0.3%methylene blue in 10% formaldehyde stain for 30 minutes. Excess dye was washed off, and the plates were allowed to dry. Plaques were then scored and the virus titre calculated.

4. MVM infection

100 mm plates containing unsynchronized LA9 cells were typically infected at a MOI of 5-10 pfu/cell in 1 ml DMEM, 0.1% FBS, 10 mM HEPES at 37°C, 5% CO_2 for 1 hour, rocking every 30 minutes. Virus containing media was then replaced with 10 ml of regular media. Serum starved synchronized cells were infected by direct addition of virus to the low serum media, followed by rocking to mix the virus and an overnight incubation at 37°C, 5% CO_2.

5. Cell synchronization

LA9 cells were synchronized by serum starvation [47]. 100 mm plates containing 1 x 10^5 cells were washed 3 times with MEM (no serum), overlayed with MEM/0.5% FBS/25 mM HEPES, and incubated at 37°C/5% CO_2 for 4.5 days. If cells were to be infected, virus was added directly to media 12 hours before release. Cells were released from the cell cycle block by replacing the media with DMEM/20% FBS/25 mM HEPES.

Cell synchrony was assessed by flow cytometry. LA9 cells were pelleted, washed with PBS, fixed with ice cold 70% ethanol for 30 minutes and then suspended in Vindelov's stain [5 mM Tris-Cl pH 8.0, 5 mM NaCl, 5 μg/ml RNase A, 0.05 mg/ml Propidium iodide (Molecular Probes, Inc), and 0.05% NP-40] at 4°C for 30 minutes. Cells were sorted on a BD FACScan instrument and analyzed using ModFitLT 2.0 software.

6. Transfection of LA9 cells

60mm dishes of LA9 cells (1.5 x 10^6 cells) were transfected with various plasmids using lipofectamine plus (Invitrogen) following the manufacturer's instructions, using a solution of 8 μg plasmid DNA, 80 μl Plus reagent, and 20 μl of lipofectamine in DMEM lacking FBS. After 3 hours, medium with FBS was added back to the cells and the cells were harvested at the various times indicated.

7. Differential Display RT/PCR

LA9 cells were infected at an MOI of 5 as described above and harvested at 12, 24, & 36 hr. P.I. As a control, LA9 cells were harvested at 24 h after mock infection (same infection procedure except no virus). Cells were directly lysed on the plate by the addition of 1ml TRIzol reagent (Gibco/BRL) per 100 mm dish. RNA was isolated according to the TRIzol procedure. RNA concentration was measured by absorbance at 260 nm in a Pharmacia Ultrospec 3000 spectrophotometer. To remove any residual DNA, RNA samples were further treated with DNase I (GenHunter) and purified by Phenol/Chloroform extraction. Differential Display RT/PCR was carried out as described in the GenHunter's RNAimage kit. Briefly, first strand DNA synthesis was carried out using 2 μg RNA (or water to control for DNA contamination), MMLV and either H-T_{11}A, H-T_{11}C or H-T_{11}G primers. Second strand synthesis and subsequent PCR amplification was carried out using the above reverse transcribed RNA, Taq DNA polymerase (Perkin Elmer), 25 μM dNTPs, one of the three H-T_{11}N primers, one of the 8 arbitrary primers (H-AP1 to H-AP8, see Appendix 2) and 2 μCi α-^{33}P dATP. This was repeated twice for every possible H-T_{11}/H-AP primer combination for a total of 24 primer

combinations. DNA products were amplified in a Perkin Elmer 2400 Thermocycler through 40 cycles of 94°C for 30 seconds, 40°C for 2 minutes and 72°C for 30 seconds followed by one last elongation step at 72°C for 5 minutes. The resulting PCR products were separated in a 6% denaturing polyacrylamide sequencing gel for approximately 2 hours at 32 watts in TBE buffer and visualized by exposure to Kodak Biomax X-ray film. Only bands that showed a reproducible change in two or more of the infected samples as compared to the control sample were analyzed further. These bands were cut out from the gel and the DNA eluted. This was accomplished by soaking the gel slice in water for five minutes, pelleting the debris by centrifugation, and precipitating any DNA present in the supernatant by addition of sodium acetate and 95% ethanol along with 50 μg glycogen (Boehringer Mannheim) as a carrier. The DNA present in the slice was re-amplified by another round of PCR using the same primer set. The PCR conditions were the same except that the radiolabel was omitted and the dNTP concentration was increased to 250 μM. The resulting DNA was separated on a 1.5% agarose gel and imaged by ethidium bromide staining. The correct size DNA product was cut out of the gel and purified using the MERmaid low molecular weight DNA purification kit (Bio-101) as per the manufacturer's instructions. The resulting DNA was cloned into the plasmid TOPO-TA pCR2.1 (Invitrogen), transformed into TOP10 *E. coli* cells, plated on LB ampicillin (75 μg/ml), and the resultant clones were screened for blue/white colony production following the manufacturers instructions. Plasmid DNA was isolated using the mini-prep protocol as described below and digested with EcoRI (Gibco-BRL) to confirm the presence and size of the insert. To compare clones, T ladder sequencing (described below) was conducted on inserts of the correct size using M13R-24 and

M13F-20 primers. To confirm the differential display results, northern blot analysis was conducted on total RNA isolated from a second infection using probes generated from the most abundant clones isolated. Clones that were confirmed to show altered expression patterns were sequenced completely. Sequence data was used to search the NCBI databases using BLAST [132].

8. Plasmid DNA preparation

Small scale plasmid preparation from bacteria grown in LB medium was carried out by either the alkaline lysis or boiler lysis method [133]. Plasmid DNAs to be machine sequenced (PE ABI prism 310 genetic analyzer) were further purified by Qiagen miniprep columns. Large-scale plasmid preparations were carried out by alkaline lysis/polyethylene glycol precipitation [133]. Plasmids to be used in transfection experiments were further purified using a Qiagen plasmid maxi kit. A list of plasmids used in this thesis can be found in Appendix 1.

9. Transformations/bacterial growth

Competent DH10b *E. coli* were transformed by the heat shock method [134] and plated on to LB agar plates containing 75 μg/ml ampicillin and incubated overnight at 37°C.

10. Sequence determination

Plasmids were routinely sequenced by either manual sequencing using a T7 Sequenase 2.0 kit (Amersham) using ^{32}P label (as per the manufacturer's instructions) or

by automated sequencing using an ABI prism 310 sequencer. Sequence data were analyzed in EditView 1.0.1 (ABI Biosystems) and stored in DNA Strider 1.1. A list of primers used in sequencing can be found in Appendix 2.

11. Probe generation

DNA probes used in Northern analysis were either labeled by the random primer method or by PCR.

Random primed labeling was done using a method similar to that described in the USB random primed labeling kit. 25 ng of purified DNA was added to a solution containing 25 μM each dCTP/dGTP/dTTP, 0.0175 A_{260} units random hexamers, 1.7mM $MgCl_2$, 200 mM HEPES pH 6.6, 0.5 mM 2-mercaptoethanol, 10 μM EDTA, 400 μg/ml BSA, 16.6 mM Tris-Cl pH 8.0, 50 μCi α ^{32}P dATP and 2 units of DNA polymerase, Klenow fragment. The reaction was incubated at 37°C for thirty minutes and terminated by heating at 65°C for 10 minutes.

PCR amplification labeling was used to label various DNA fragments identified by differential display. A PCR cocktail was prepared as described for the differential display reaction except that the dNTP concentration was adjusted to 20 μM, α–^{32}P dATP was added to a concentration of 1 μM (60μCi), and the concentration of template DNA was set at 5 pg/μl. A set of duplicate reactions containing either water instead of template (negative control) or unlabelled dATP instead of α–^{32}P dATP (positive control to confirm amplification) was also carried out.

All probes were purified using Sephadex G-50 spin columns [133], counted using a Beckman coulter LS6000IC scintillation counter and stored at –20°C until needed.

12. RNA isolation

Unless otherwise stated, total RNA was routinely isolated using an RNeasy mini kit (Qiagen) as per the manufacturer's instructions. An on-column treatment with DNase I (Qiagen) was also performed to remove any residual DNA. The resulting RNA was collected from the column in two 30 µl washes. RNA concentration was determined by measuring the A_{260} of samples, diluted in water, in an Ultraspec 3000 spectrophotometer (Pharmacia). If needed, RNA was precipitated using ethanol and taken up in a small volume of water. RNA samples were aliquoted and stored at –80°C until needed.

13. DNA dot blot analysis

Plasmid DNA preparation and blotting was done according to Bio-Rad's Bio-Dot microfiltration apparatus instructions. 200 µg of each plasmid DNA was linearized by restriction digestion, extracted with phenol/chloroform, precipitated with 3 M sodium acetate/ethanol, dissolved in 100 µl water, and quantified by A_{260}. Linearized plasmids were diluted to 62.5 ng/µl, denatured by addition of 2 M NaOH/50 mM EDTA (to 0.4 M NaOH/10 mM EDTA) followed by a 10 minute incubation at 95°C, and neutralized by addition of ice cold 2 M ammonium acetate (to 1 M). Blotting onto nitrocellose (Bio-Rad) was accomplished using Bio-Rad's Bio-Dot microfiltration (96 well) apparatus. A 9 x 12 cm nitrocellose membrane was soaked briefly in 6X SSC, assembled into the blotting apparatus and rehydrated once with 100 µl 2X SSC per well using vacuum to pull the fluid through the membrane. Plasmids, 5 µg (200 µl) per well, were blotted onto the membrane and washed once with 25 ml 2X SSC. The membrane was dried overnight

at room temperature, baked at 80°C for 2 hours, and finally cut into strips for use in hybridization with the nuclear run-on probes.

14. Northern blot hybridization

RNA blotting and hybridization was done by a modified protocol from Molecular Cloning: A Laboratory Manual [133]. 15 μg of total RNA per sample was mixed with formamide loading buffer to a final concentration of 26 mM MOPS, 0.6 mM EDTA, 6.5 mM sodium acetate, 64% formamide, 14% formaldehyde and bromophenol blue and xylene cyanol dyes. Samples were heated at 65°C for 10 minutes, and separated on a 5.5" by 4.25" 1.25% agarose/6% formaldehyde gel in MOPS running buffer at 70V. To check the integrity of the RNA, ethidium bromide was also added to the gel to visualize rRNAs. The gel was washed 5 times with DEPC-treated water and once in 10X SSC for 30 minutes. The RNA was transferred to a Hybond N+ positively charged nylon membrane (Amersham Pharmacia) in 10X SSC via the capillary transfer method over a period of 3 days. Subsequently, the membrane was washed in 2X SSC and exposed to UV light (Biorad GS Gene Linker,150 mJ setting) to cross-link the RNA to the membrane. Blots were dried at 80°C, briefly examined under UV to examine the efficiency of transfer and stored at 4°C until needed.

Membranes were soaked briefly in 2X SSC and then pre-hybridized with 5-10 ml ExpressHyb (Clontech) solution and 100 μg denatured salmon sperm DNA for 1 h at 68°C. Radiolabeled probe (see section 11) (denatured at 95°C for 10 minutes) was mixed with an additional 5 ml ExpressHyb solution and then added to the pre-hybridization/membrane mix. Blots were hybridized with probe at 68°C for one hour and

then washed 2 times with 2XSSC/0.05% SDS at room temperature for 15 minutes each. Washing efficiency was assessed by a brief exposure to a storage phosphor screen and examined in a phosphorimager. If warranted, blots were washed a further 2 times with 0.1X SSC/0.1% SDS at 50°C for 20 minutes. Blots were then visualized using a phosphorimager with various exposure times.

15. Autoradiography and band quantification

All band quantification and most autoradiography was done using a phosphorimager. The gel or membrane was exposed to a phosphorimager plate for varying amounts of time, depending on signal strength. Initially, the plates were scanned on a Molecular Dynamics phosphorimager SI and the acquired data was analyzed with IP lab gel 1.5. Later, a Molecular Dynamics Typhoon 8600 phosphorimager was used with Typhoon scanner control 1.0 to acquire the data. Data was analyzed using ImageQuant 5.2 and Microsoft Excel.

16. Protein isolation

LA9 cells were collected using a cell scraper and transferred with medium to a 15 ml conical tube. Cells were pelleted and washed twice with ice cold PBS. Cell pellets were then lysed with protein sample buffer (10% glycerol, 1.5% SDS, 62.5 mM Tris-Cl pH 6.2, 2.5% 2-mercaptoethanol, and bromophenol blue) and boiled for 5 minutes. Samples were stored at –20°C until needed.

17. Western blot hybridization

Protein samples were separated by electrophoresis on a SDS-polyacrylamide (6-15%) gel (8.9 cm by 10.2 cm) at 80-120V. Protein samples were then transferred to PVDF membrane (Pall) by semi-dry transfer using a Biorad trans-blot SD apparatus. Transfer was accomplished in transfer buffer (39mM glycine, 48 mM Tris-Cl, 0.037% SDS and 20% methanol) for approximately 20-30 minutes at 10-12 volts. When transferring proteins larger than 150 kDa, transfer buffer without methanol was used and the transfer time was increased to 45-60 minutes. Blots were dried at room temperature.

Antibody binding was as follows: PVDF membranes were soaked briefly in methanol, washed with PBS/0.05% Tween 20 (PBS-T), blocked for 1 hour with BLOTTO (5% powdered milk, weight by volume, in PBS-T) at room temperature, followed by several washes with PBS-T. The primary antibody (either a rabbit or a mouse antibody) was diluted in BLOTTO and incubated with the membrane with shaking at room temperature for an hour followed by several more washes with PBS-T. Either peroxidase-conjugated donkey anti-rabbit IgG secondary antibody at a dilution of 1:50,000 or peroxidase-conjugated goat anti-mouse IgG secondary antibody at a dilution of 1:5,000 was diluted in Blotto and incubated with the membrane for one hour at room temperature, followed by another several washes of PBS-T. The secondary antibody was visualized by chemiluminescence with either ECL or ECL Plus kits (Amersham-Pharmacia) according to the manufacturer's instructions. This signal was detected either with Hyperfilm ECL film (Amersham-Pharmacia) or using a FluroS max scanner (Biorad) with a clear filter, 50 mm lens f/1.4 and no excitation (courtesy of the Steve Pelech lab). Multiple exposure times were collected for each method. Films were developed using a M35 XOMAT processor (Kodak). Data from the FluorS max scanner

was processed, analyzed, and quantified using Quantity one software (Biorad). A list of antibodies used in this thesis can be found in Appendix 3.

18. Primer extension analysis

Primers WPW25, 26 and 27 (Appendix 2) were 5' end-labeled with γ-^{32}P ATP using T4 polynucleotide kinase and the DNA precipitated by addition of 95% ethanol, ammonium acetate (to 150 mM) with glycogen as a carrier. Radiolabeled primers were hybridized to 1 μg of total RNA at 60°C for 5 minutes and chilled on ice. First strand synthesis was accomplished by the addition of MMLV (Gibco BRL), dNTPs, DTT and buffer, followed by incubation at 37°C for 45 minutes. The resulting RNA/DNA hybrids were then denatured by heating at 95°C for five minutes and then separated on a 5% urea polyacrylamide mini-gel (Triezenberg, 1992). Gels were dried (Biorad model 583 gel drier) and bands imaged and quantified using a phosphorimager. To accurately determine the size of the primer extension products, some of the labeled DNA was loaded onto a 6% urea polyacrylamide sequencing gel alongside a pUC19 sequencing ladder.

19. Clontech array analysis

Total RNA was isolated from synchronized or unsynchronized infected or mock-infected cells and reverse transcribed in the presence of ^{32}P label using the Atlas Pure total RNA labeling system (Clontech). To check for genomic DNA contamination, PCR was used to amplify the β-actin gene. RT/PCR was also used to detect the mRNA for NS-1 to confirm infection. Radiolabeled RNA hybridized to Clontech's Atlas mouse 1.2 arrays (a cDNA array), as per the manufacturer's instructions. Arrays were washed four

times with 2X SSC/1% SDS at 68°C, once in 0.1X SSC/0.5% SDS at 68°C and once in 2X SSC at room temperature. Arrays were wrapped in saran wrap and visualized using a phosphorimager. The images were saved as tiff files and analyzed using AtlasImage 1.01a software, which can be used to locate, identify and calculate signals for each cDNA spot. Background was determined by averaging the signal in the background regions of the array. Background was subtracted from each signal. Initially, the arrays were normalized to a series of housekeeping genes, specifically cytoplasmic β-actin and 40S ribosomal protein S29. However, subsequent re-analysis of the data suggested that this method was biased. Hence, the arrays were normalized by the following method: First, spots with signals less than 500 counts were discarded from the data set. The infected/mock-infected ratio was calculated for the remaining spots and these data were plotted versus gene identity. It is expected that the majority of spots should have a ratio of approximately one, so a single normalization factor was estimated for the control array from the above plot such that the majority of the spots fell into this range (Figure 10). All control signals were then multiplied by this factor and the ratios recalculated.

20. Affymetrix microarray analysis

Total RNA was isolated as above (section 12) from mock infected and MVMp infected LA9 cells (unsynchronized) at 36 hours post infection. 5 μg of RNA was shipped on dry ice to the Genome Sciences Center at the British Columbia Cancer

A

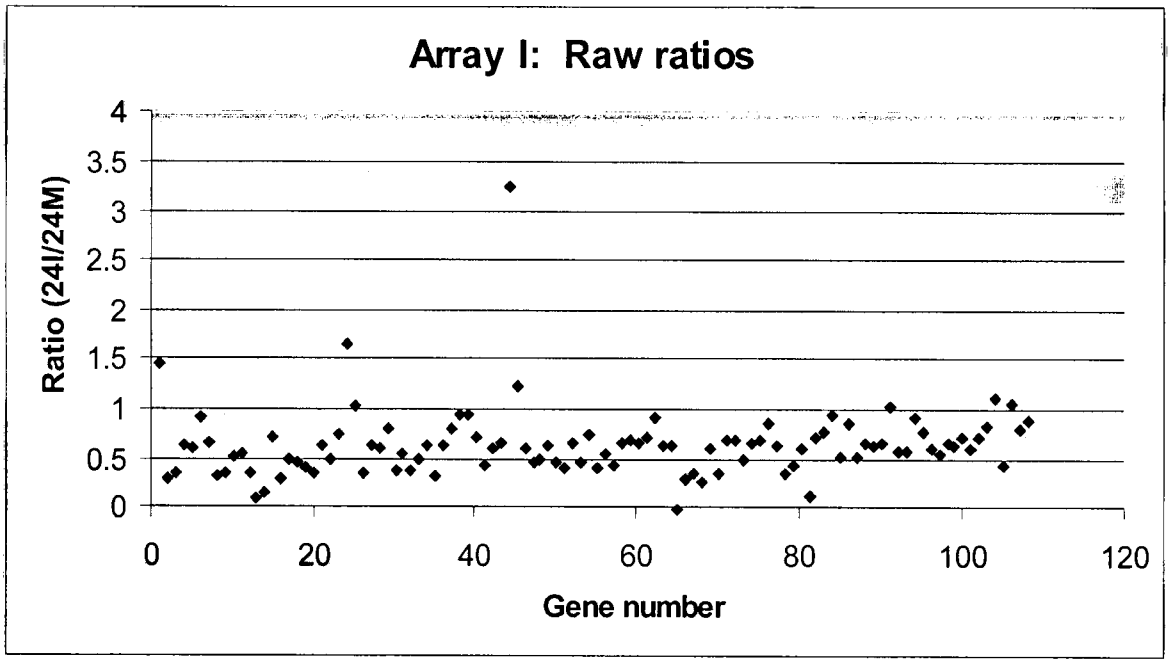

B

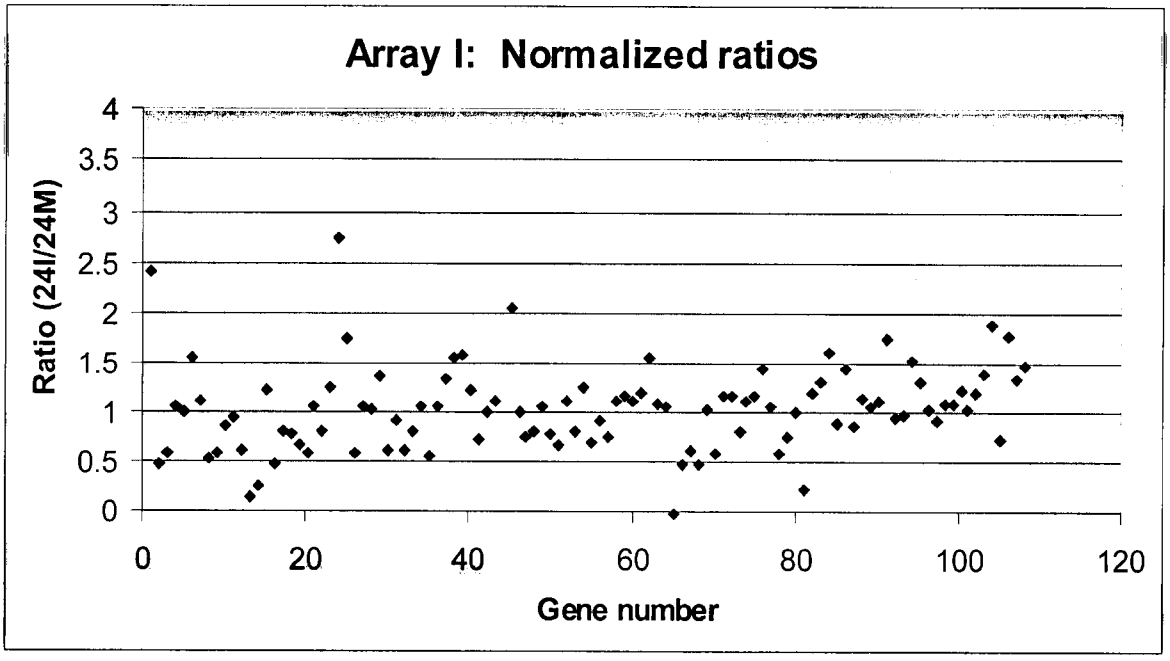

Figure 10: Normalizing the array data: **A:** Array I (24 hr post block synchronized mock vs infected) ratios versus gene number. **B:** Normalized array I ratios versus gene number. The two arrays were normalized by multiplying all mock-infected signals by 0.6.

Agency where the lab staff prepared the probes for hybridization with Affymetrix microarrays using Affymetrix's instructions. Briefly, the sample was reverse transcribed into DNA, used to generate biotinylated complementary RNA, fragmented, and then hybridized an Affymetrix microarray chip. Two types of arrays were hybridized with the above-prepared samples. First, an Affymetrix Test 3 microarray was used. This array contains multiple housekeeping genes and is used to determine if the RNA sample is suitable for array hybridization. The remaining prepared RNA sample was hybridized to Affymetrix's U74Av2 microarray. This consists of the approximately 6000 genes found in the mouse UniGene database that have been characterized and an additional 6000 expressed sequence tags (ESTs) for a total of 12,000 genes per array. As the Affymetrix system uses a one-fluor system, each sample was hybridized to a separate array. After staining with streptavidin phycoerythrin and washing, the chip was scanned and the data analyzed in Microarray Suite 5.0. Data analysis and manipulation will be discussed further in the results section.

21. Preparation of nuclei for nuclear run-on assays

Nuclei were isolated from LA9 cells using a modified detergent lysis method. LA9 cells were grown in suspension, pelleted, washed twice with PBS and then re-suspended in NP-40 lysis buffer (0.5% NP-40, 10 mM Tris-Cl pH 7.5, 10 mM NaCl, and 3 mM $MgCl_2$) with gentle vortexing. Cells were allowed to lyse on ice for 5 minutes and were then pelleted by centrifugation at 4°C. These steps were repeated two more times. The nuclei were examined under a phase contrast microscope to make sure that the cells lysed and that the nuclei remained intact. The resulting nuclei were taken up in nuclei storage

buffer (40% glycerol, 50 mM Tris-Cl pH 8.3, 5 mM $MgCl_2$ and 0.1 mM EDTA) and stored in liquid nitrogen until needed.

22. Nuclear Run-on assays

Nuclear run-on assays were done using a significantly modified protocol from that described in Current Protocols in Molecular Biology [135]. An aliquot of ~ 2 x 10^7 to 2.5 x 10^7 nuclei in 100 µl glycerol storage buffer was mixed with 100 µl of 2X reaction buffer (10 mM Tris-Cl, 5 mM $MgCl_2$, and 300 mM KCl) containing 100 µM each ATP, GTP, CTP and 5 mM DTT and 250 µCi α-^{32}P UTP in a 15ml conical tube. Samples were incubated in a 30°C shaking water bath for 30 minutes. Nuclei were lysed by addition of 4 ml QRL1 (Qiagen) with 2-mercaptoethanol (Sigma) and total RNA isolated using Qiagen's RNA/DNA maxi kit using the manufacturer's instructions with the following modifications: DNA in the QRL1 lysed nuclei mixture was sheared by pipetting through a 18 gage needle 10 times and the mixture transferred to a 50 ml Sarstedt conical centrifuge tube. 4 ml of QRV1 was added and the entire mixture centrifuged at 8,000 RPM for 35 minutes in a JA-12 rotor. The supernatant was transferred to a silanized (Sigmacote, Sigma) 30 ml glass corex tube, mixed with 6.4 ml of ice cold isopropanol, centrifuged at 11,000 rpm in a JA-20 rotor for 30 minutes, and the pellet collected and washed with 4 ml 70% ethanol (11,000 rpm, JA-20, 15 minutes). The pellet was resuspended in QRL1 solution (with heating and vortexing) and loaded onto a Qiagen maxi kit column. The column was washed with 30 ml of QRW solution and followed by addition of 14 ml of QRU at 45°C to elute the RNA into another silanized 30ml corex tube. The RNA was precipitated with 14 ml isopropanol,

centrifuged and washed as above. The RNA pellet was dissolved in 2 ml of water. 5 µl of this mixture was counted in a scintillation counter to normalize the mock and infected samples. The remaining sample was mixed with 2 ml 2X TES solution with NaCl (20 mM TES pH 7.4, 20 mM EDTA, 0.4% SDS, 0.6 M NaCl), heated to 65°C, and hybridized to nitrocellulose dot blots at 65°C for 36 hours. The blots were washed twice in 2X SSC at 65°C for an hour each, followed by an optional 30 minute incubation with 10 ml 2X SSC with 10 µg/ml RNase A at 37°C, and a one hour wash at 37°C. Signal detection and quantification was achieved using a phosphorimager as described in 14 (above).

23. Kinexus protein kinase screen

Protein samples for the Kinexus protein kinase screen were prepared following instructions from Kinexus. Briefly, pellets of synchronized adherent infected or mock-infected LA9 cells were taken up in Kinexus lysis buffer (0.5% NP-40, 20 mM MOPS, 5 mM EGTA, 2 mM EDTA, 5 mM NaF, 40 mM β-glycerophosphate, 1 mM sodium orthovanadate, 1 mM PMSF, 3 mM benzamidine, 5µM pepstatin A, 10 µM leupeptin), sonicated at a low setting for two rounds of 15 seconds each (Branson Sonifier 250), and centrifuged at 55,000 rpm (100,000 x g) in a TLA 100.4 rotor (Beckman Optima TL untracentrifuge) for 30 minutes at 4°C to pellet the lipid membranes. The supernatant was collected and protein concentration was determined by the BCA method (Pierce's bicinchoninic acid assay) as per the manufacturer's instructions using bovine serum albumin as a standard. Samples were mixed with protein sample buffer, boiled for 5

minutes and adjusted to equal concentrations. Approximately 500 μg of each sample was sent to Kinexus for analysis.

From Kinexus, tiff images of the western blots and excel files containing the quantification data for each of the bands imaged were received. Initial analysis was done by visual inspection with the guidence of Dr. Steven Pelech (Kinexus). Infected sample data was normalized to control data by calculating a normalization factor based on the top ten expressed proteins in both control and infected samples.

24. Reverse transcription and PCR amplifications

To test for genomic DNA contamination of RNA samples, the RNA samples were screened for the presence β-actin DNA. 1 μg total RNA was added to a solution containing 1U Taq DNA polymerase and buffer (Perkin Elmer), 200 μM dNTPs, 3mM $MgCl_2$, and 0.5 μM PW10 (skeletal β-actin, nucleotides 987 to 1004) and PW11 (skeletal β-actin, nucleotides 461 to 478) primers. If detectable DNA contamination is present this PCR assay should yield a 546 bp product. Amplification was accomplished through an initial denaturation step of 94°C for 5 min., followed by 35 cycles of 30 sec. at 94°C, 30 sec. at 55°C and 30 sec. at 72°C, and then one final extension at 72°C for 7 min. The resulting products were separated on a 1.5% agarose gel. Control tubes contained water or 260, 26, or 2.6 ng of LA9 genomic DNA.

NS1 RT/PCR: 1 μg total RNA was reverse transcribed using MMLV Reverse transcriptase (Gibco BRL), 5 μM T_{18} primer, and 1mM dNTPs at 37°C for 50 minutes. An aliquot (4 μl) of the above cDNA mix was added to a solution of 200 μM dNTPs, 1U Vent DNA polymerase and buffer (New England Biolabs), 200 μg/ml BSA, and 0.17 μM

NS1-415 and NS1-265 primers. Amplification was accomplished using an initial denaturation step of 94°C for 5 min., followed by 35 cycles of 40 sec. at 92°C, 40 sec. at 55°C and 40 sec. at 75°C, and then one final extension at 75°C for 5 min. The resulting products were separated on a 1.5% agarose gel in 1X TAE buffer. As controls, water and pCMVNS1 [43], a plasmid containing the NS1 gene, were used. A list of primers used in this thesis can be found in Appendix 2.

Results

1. Differential Display

To begin to profiling changes in gene expression during a cytopathic infection of murine LA9 fibroblasts with MVM, differential display (DD), invented by Peng Liang [136], was used. This is an RT/PCR based technique that amplifies a set of semi-randomly chosen cDNAs (500-1000 per PCR reaction) based on primer selection. Differential display is based on semi-conservative PCR amplification. Therefore, transcripts expressed at low levels will have a corresponding lower number of PCR products whereas transcripts expressed at high levels will have a corresponding higher number of PCR products. By comparing the levels of these PCR products between uninfected and infected LA9 cells, genes that exhibit altered expression levels can be identified. As illustrated in Figure 11, in this technique RNA is first reverse transcribed to cDNA with an anchored poly T primer (VT_{11} where V = A, C, or G). This selects a specific subset of cDNAs to be examined in further reactions. This pool of cDNAs is then amplified through PCR using the above anchored primer and a second arbitrarily selected primer of 13 nucleotides (the arbitrary primer). Any arbitrary primer can be used provided there is no secondary structure. Using a low annealing temperature of 40°C, the arbitrary primer acts as an 8-9mer in the initial annealing step and binds to multiple cDNAs, resulting in the selection of a smaller, more manageable pool of transcripts containing approximately 50-100 products [136]. For the most part, this pool of DNA will represent the 3' ends of various cDNAs ranging in size from <100 nucleotides to ~500 nucleotides, due to the use of the anchored polyT primer and the

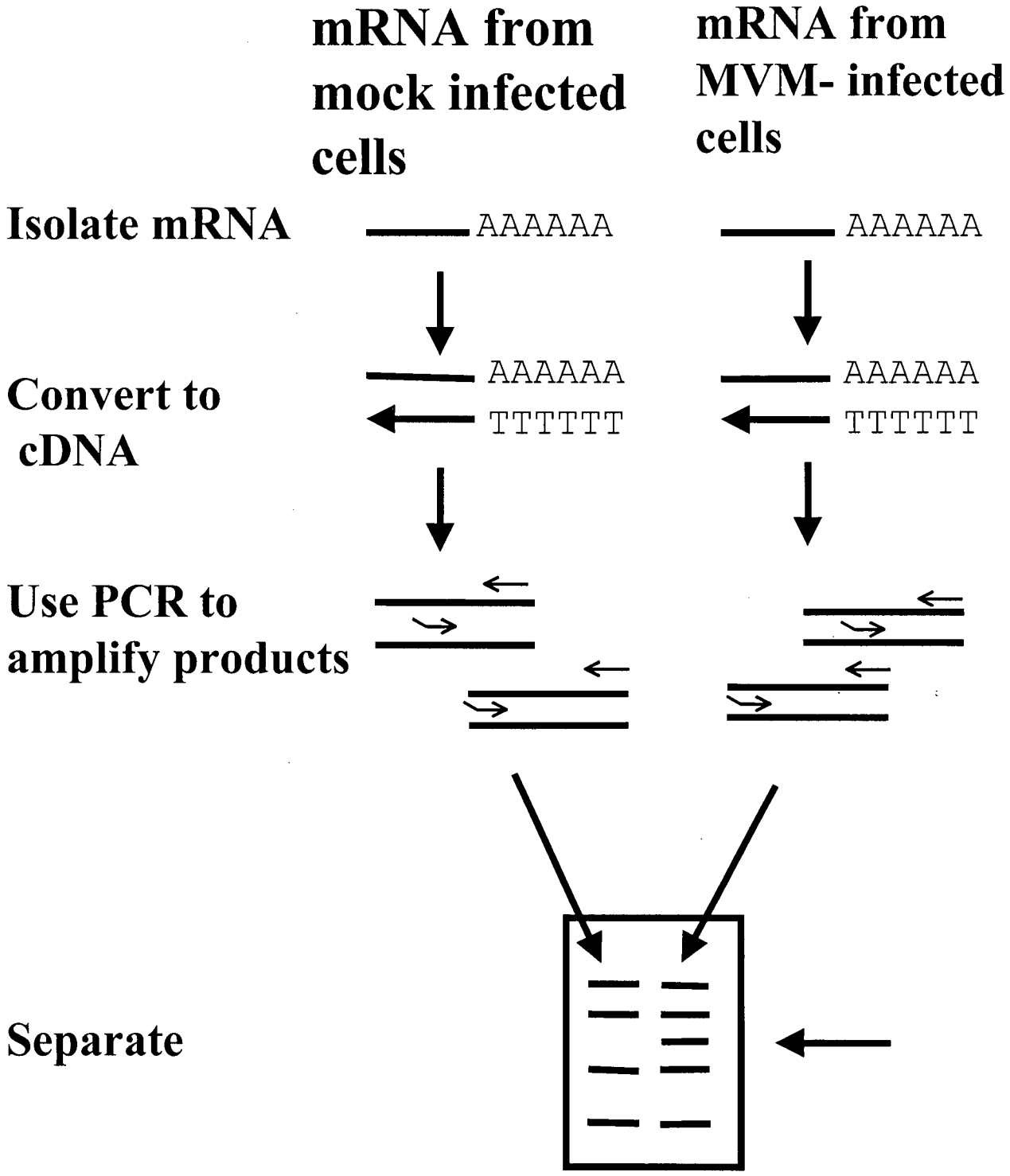

Figure 11: Differential Display. RNA is first reverse transcribed into cDNA through the use of reverse transcriptase and an anchored oligo dT primer. A smaller sub-set of this pool of cDNAs is amplified by PCR using an arbitrary selected 13 nt primer and a low annealing temperature in the presence of radioactive label. This set of cDNAs is then resolved on a polyacrylamide gel and quantified.

short elongation time. Amplified products can be separated on a denaturing polyacrylamide gel and quantified. Figure 12 shows a typical differential display gel.

Differential display PCR is not always 100% reproducible (see Figure 12a) due to pipetting errors, RNA quantification errors, and inherent errors in PCR amplification. To compensate for this, three different times post-infection were examined: 12, 24, and 36 h P.I. Only bands that showed distinct trends over the three time points were selected for further analysis. To further reduce the risk of false positives, two separate PCR reactions for each sample were done. Water was used as a negative control.

A total of 24 different primer pair combinations using 8 arbitrary and 3 anchored primers were screened. This detects approximately 15% of the estimated 15,000 actively transcribed genes within the cell [137]. Twenty-five bands were identified as being altered in expression level, with 10 of them being $\leq$ 150 bp (Table 2). The approximate size was determined by position on the differential display gel and by the size of the resulting PCR product. As recommended by Genhunter, bands with a size below 150 nt were not studied further for two reasons. First, the sequence in these bands would be predominately 3' untranslated sequence (3' UTR). At the time of these studies, the mouse genome had not been sequenced, and it would have been difficult to identify the mRNA species. Second, the 3' UTR sequence often can contain repetitive elements, which would also prevent identification.

Candidate bands were cut out of the gel from the lane giving the highest signal, re-amplified by another round of PCR (in some cases two), purified by agarose gel

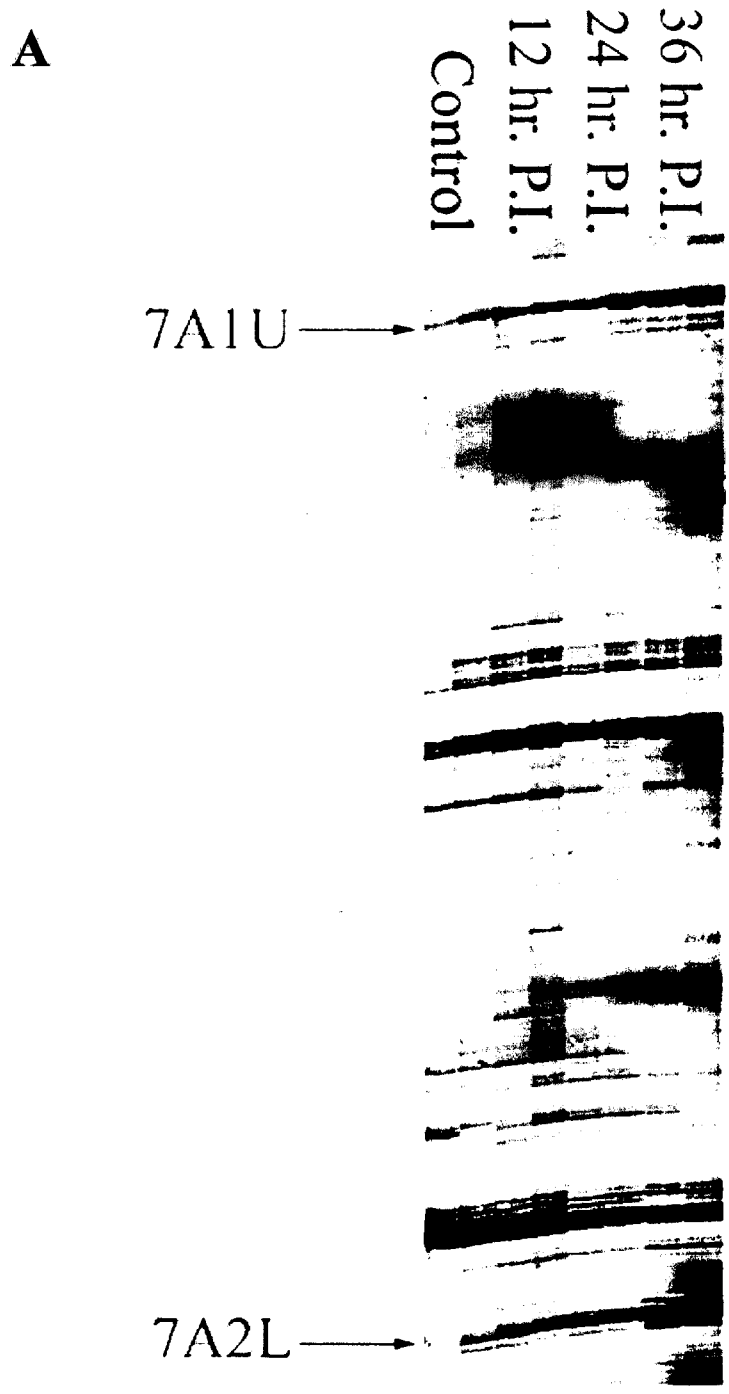

Figure 12: Legend on next page.

B

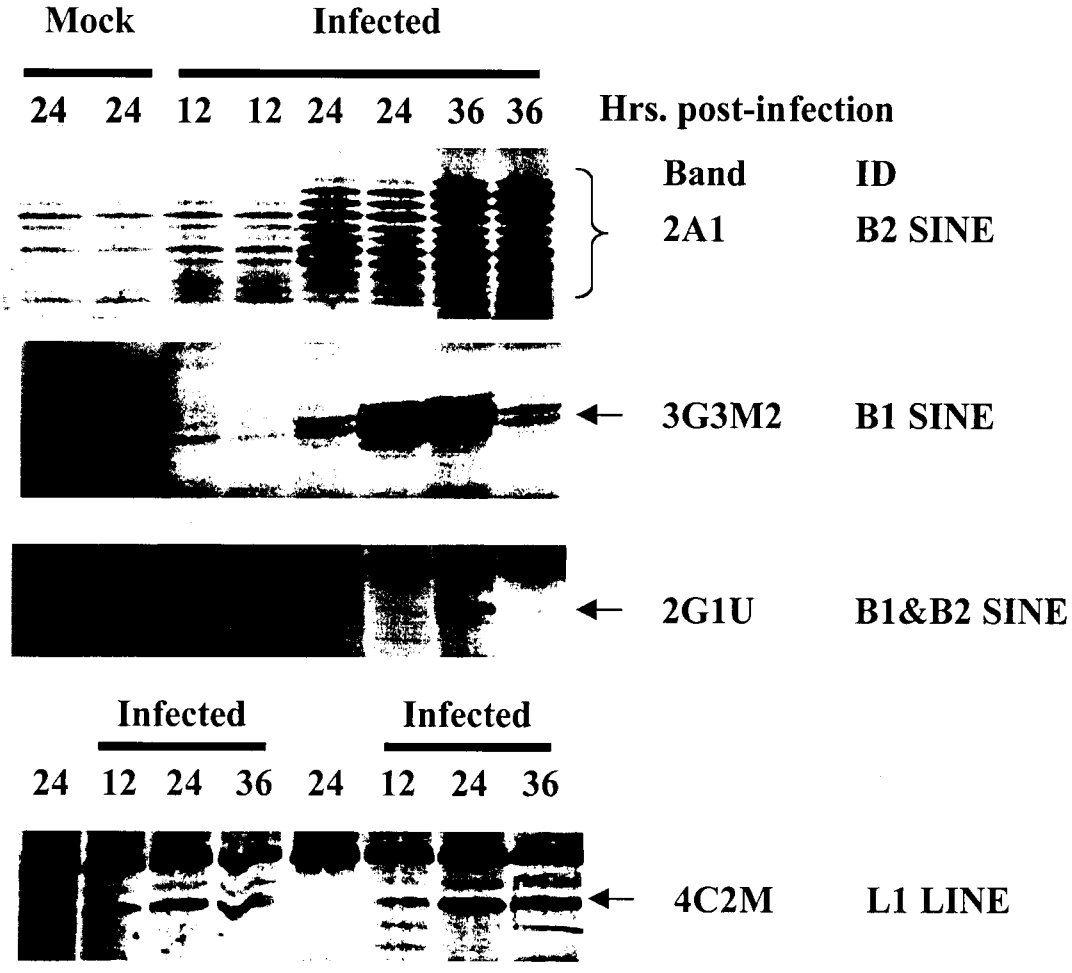

Figure 12: Differential display polyacrylamide gels. **A.** The PCR products from the H-AP-7 and H-AT_{11} primed reaction were separated on a 6% denaturing polyacrylamide sequencing gel. Templates were AT_{11} primed cDNAs as described. B. The differential display bands 2A1, 3G3M2, 2G1U, and 4C2M. Control: Mock infected LA9 cells harvested 24 hr after mock treatment., 12, 24, & 36 hr. P.I.: unsynchronized LA9 cells infected with MVMp and harvested at the times indicated. Each sample (two adjacent lanes) represents the results of two separate PCR reactions. This was repeated for each of the 24 different primer combinations. Bands that were further studied are indicated.

Band Id	Size (bp)	Relative Intensity	Amplified	Cloned	Reverse Northern	Northern	Change	Identity
C2B1	500	+/++	Can't amp	N/A	No	N A	N A	N/A
7A1U	500	++++	Yes	Yes	Yes	Yes	Yes	NS-1
4C1U	500	++	Can't amp	N/A	N/A	N A	N A	N/A
7C1U	500	+++	Yes	Yes	No	Yes	No	N/A
3G1U	500	++++	Yes	Yes	Yes	Yes	Yes	NS-1
4C2M	400	+++	Yes	Yes	Attempted	Yes	Yes	L1 Line
C2B2	350	+/++	Yes	Yes	No	Yes	not repro.	Mit. NAD depend. D/C
3G4M3	250	+++	Yes	Yes	No	Yes	not repro.	Unknown EST (sim to FGF receptor activating protein)
3G3M2	250	+++	Yes	Yes	No	Yes	Yes	B1 SINE
4C3M	250	+++	Yes	Yes	Attempted	Yes	No	N/A
3G2M1	250	+	No	No	No	No	?	?
2G1U	200	+++	Yes	Yes	No	Yes	Yes	B1/B2 SINE
5C2B1	200	+++	Yes	Yes	No	Yes	No	N/A
2A1	200	+++	Yes	Yes	No	Yes	Yes	B2 SINE
7A2L	200	+++	Yes	Yes	No	Yes	No Signal	?
1G1B	150	+++	-	-	-	_		-
5C1M	150	++	-	-	-	-	-	-
5C3B2	150	-	-	-	-	-		-
3A1U	150	-	-	-	-	-	-	-
3A2B	150	-	-	-	-	-		-
4C4L	100	-	-	-	Attempted	No	-	-
7G1U	100	-	-	-	-	-		-
7G2B	100	-	-	-	-	-	-	-
4A2B1	100	-	-	-	-	-		-
4A3B2	100	-	-	-	-	-	-	-

Table 2: Altered bands detected by differential display. This lists the altered bands detected by differential display and the progress in confirming and identifying them. Size is an estimate from the resulting PCR product, change indicates whether the northern or reverse northern confirmed the differential display results. All bands that were confirmed to change were found to be up-regulated. N/A: Not applicable. Can't amp: Band could not be amplified after two rounds of PCR amplification.

electrophoresis, and cloned into the pCR2.1-TOPO plasmid. Two bands could not be amplified by PCR. To confirm that the remaining cDNA fragments were altered in their expression levels, reverse northern blots were initially performed as explained in Figure 13. This technique has the advantage of being able to screen multiple clones at one time. This is crucial as a single band from the gel may contain multiple cDNA fragments of the same size and not all of them are necessarily altered in expression. Also, especially in the case of larger bands where there is less resolution between bands, there is always the risk of contamination from bands above or below the band of interest. This technique was successfully used to screen the 7A1U band, shown in Figure 14a. Sequencing analysis (both directions) identified the clone as a fragment of the MVM NS-1 transcript (viral nucleotides 439 to 899). Interestingly, this is in the 5' end of the transcript, spanning the shared sequence of NS1/NS2 and the alternatively spliced intron that is removed to generate NS2 (see Figure 2a). Further analysis of the data led to the conclusion that PCR amplification occurred with the anchored primer binding to an A-rich sequence (5'-TA_5GA_4TAA-3') present in this region of the transcript. This is illustrated in Figure 14b.

Although reverse northern blots were successful in identifying NS-1, they were less useful in confirming other bands. High background, low sensitivity and difficulty with relative changes in signal intensity led to a decision to use northern blots rather than reverse northern blots. To overcome the presence of multiple cDNA fragments present in one band, T ladder sequencing was used to characterize each clone. This is based on the Sanger sequencing method but only the ddTTP reaction is used, resulting in a fingerprint (T ladder) for each clone sequenced. The most abundant clone was then used to make a

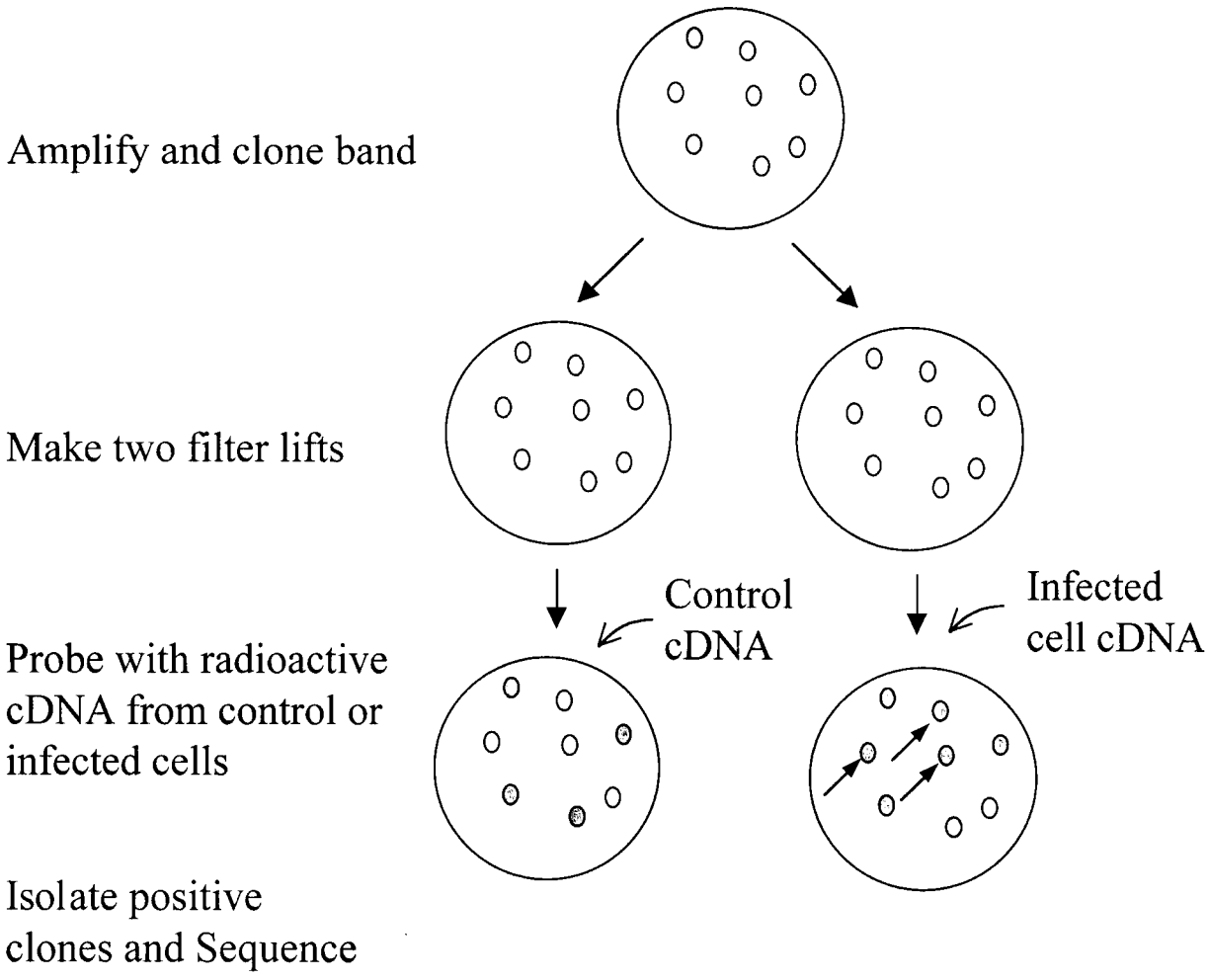

Figure 13: Reverse northern blots. Identical colony lifts containing a clone of the band of interest were probed with radioactively labeled cDNA from either mock or MVM infected LA9 cells. Colonies that showed altered expression were grown up and sequenced.

A

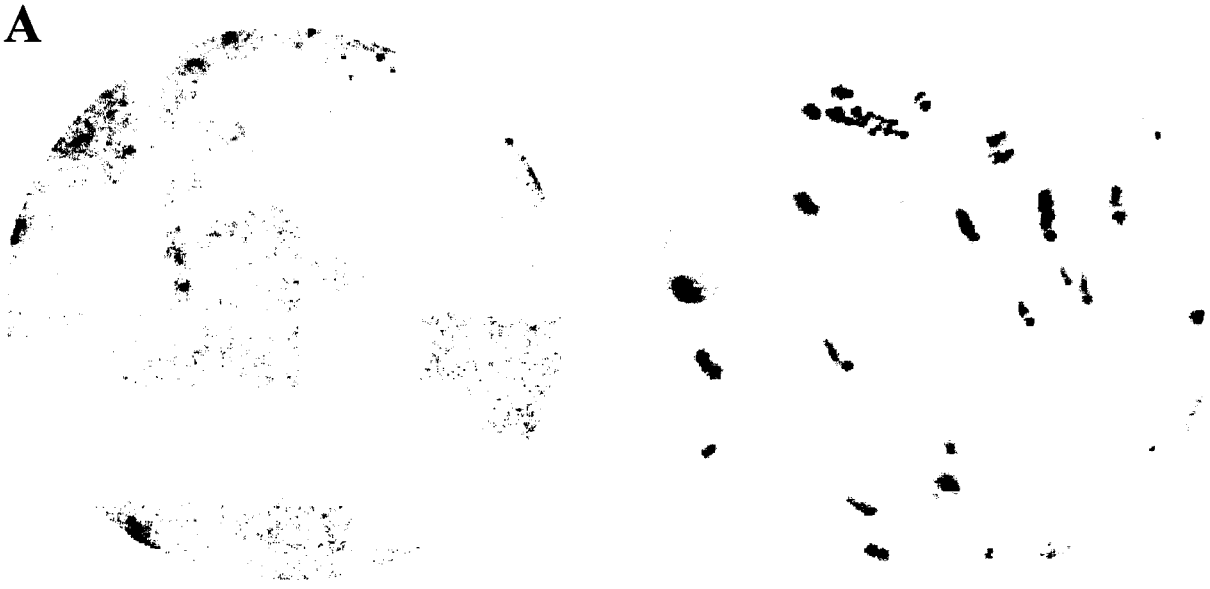

Probed with LA9 cDNA **Probed with MVM-infected LA9 cDNA**

B

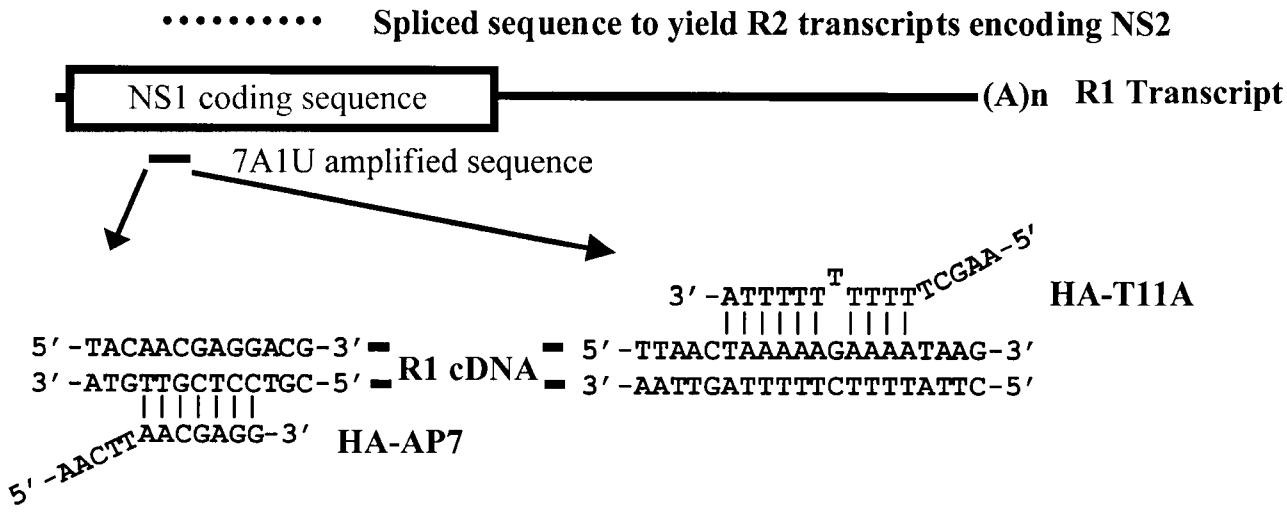

Figure 14: The 7A1U band results. **A:** Reverse northern of clones containing 7A1U (NS-1). **B:** Schematic identifying the R1 transcript sequence cloned from the 7A1U band. The sequence of the two primers used in the initial differential display amplification and the corresponding R1 cDNA sequence is also included.

probe for the northern blot. Using these techniques, three bands were found to give signals that did not change upon infection and one band that gave no signal.

Two more bands gave signals that appeared to show an approximately two-fold change but these changes were not always reproducible. These bands were sequenced and found to be "methylenetetrahydrofolate dehydrogenase (NAD dependent) methenyltetrahydrofolate cyclohydrolase" and an uncharacterized EST with similarity to the fibroblast growth factor receptor activating protein. Analysis of these clones was not pursued further. Northern blot analysis confirmed that the remaining bands were indeed altered upon infection. Band C2B2 (not shown) was found to contain another fragment of MVM NS-1 spanning viral nucleotides 1600 to 1660, which is a NS-1 specific sequence. Again, the anchored primer bound to an A rich sequence upstream of the poly-A tail. The remaining bands contained repetitive elements as detected by the CENSOR web server (Jurka et al., 1996). Band 3G3M2 (Figure 12b) contained a full-length copy of a B1 SINE (consensus sequence nucleotides 1 to 131) with the primer binding to the A rich region in the 3' end. Band 2A1 (Figure 12b) contained a fragment of a B2 SINE (consensus sequence nucleotides 32 to 174). Northern blots probed by 3G3M2 and 2A1 are shown in Figure 15. Band 2G1U (Figure 12b) contained a fragment containing both an entire B1 SINE (consensus sequence nucleotides 1 to 134) and part of a B2 SINE (consensus sequence nucleotides 19 to 174). Finally, band 4C2M (Figure 12b) contained a fragment of a L1 LINE (consensus sequence nucleotides 2520 to 2635).

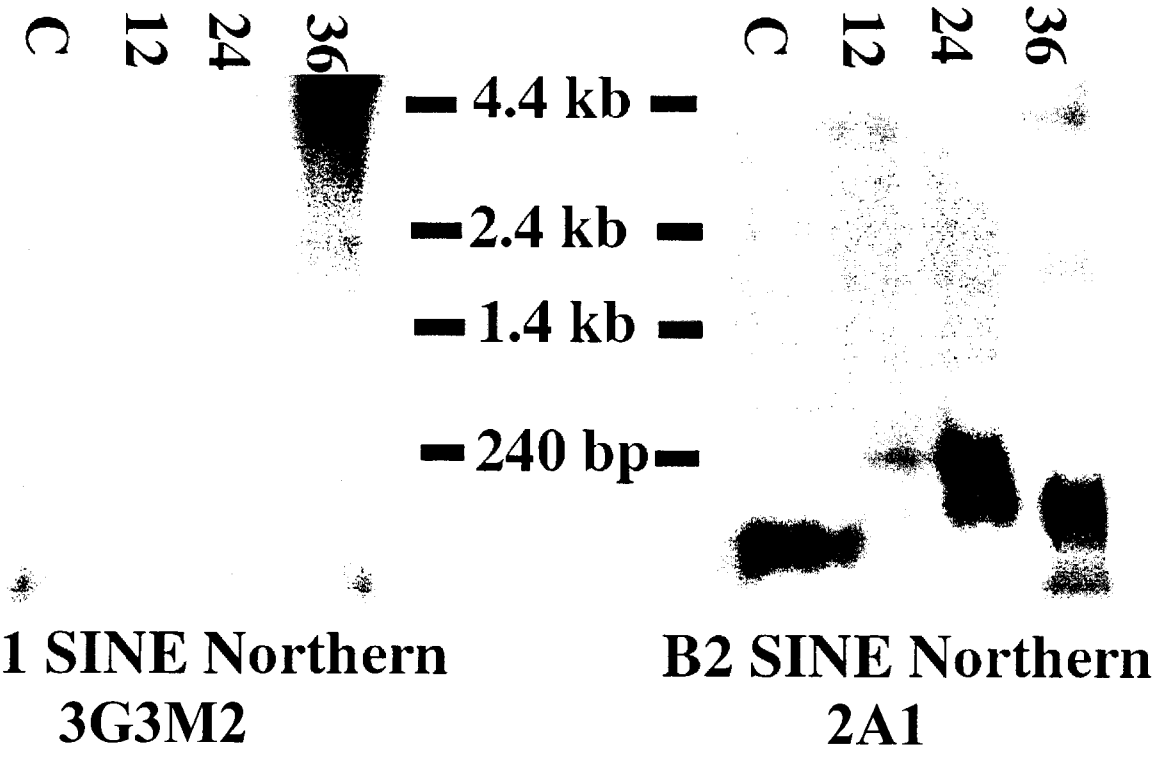

Figure 15: Altered expression of selected bands. Northern analysis of RNAs detectable by the most abundant clone from 3G3M2 (B1 SINE) and 2A1 (B2 SINE). Each lane contains 15 μg of total RNA Abbreviations are as follows: C: Mock infected LA9 cells at 24 hr after mock-infection. 12, 24, 36: LA9 cells 12, 24, & 36 hr after infection with MVMp. See Materials and Methods section 14.

2. Clontech Macroarray Analysis

The high numbers of false positives, the predilection to detect SINEs, the presence of multiple clones in a single band, and the large amount of effort needed for differential display prompted an investigation of alternative means of analyzing global gene expression. One attractive method was the then emerging technique of array analysis. Arrays have been successfully used to screen host gene expression during viral infection for many other viruses, including cytomegalovirus and HIV [138, 139]. Array analysis is advantageous as there is only one known sequence per spot (hence this avoids cloning), and it is rapid and easier to carry out than differential display. Arrays, however, are limited to studying expression of genes present on the array, they often exhibit lower sensitivity (as compared to differential display) and are much more expensive (at least 4-5 years ago when these studies were initiated).

Arrays are, in essence, a large series of reverse northern blots. The array itself is simply a support structure containing multiple spots of different sequence corresponding to many different genes of interest. It can be probed with labeled cDNA from either control or experimental (in my case mock or MVM infected LA9 cell cDNA). By comparing intensities of probes annealed to spots between two different arrays one can determine relative changes in gene expression for each of the genes on the array. At the time of these experiments, very few mouse arrays were available so our choices were extremely limited. We decided to use Clontech's Atlas mouse 1.2 arrays. This is a positively charged nylon macroscopic array containing 1176 different cDNA fragments (200 to 600 bp) in single spot format. These types of arrays are probed with radiolabeled cDNAs and require two separate arrays for each analysis.

As mentioned previously, MVM can only replicate when cells reach the S/G_2 phases [91]. Therefore, at any particular time during MVM infection, individual asynchronized LA9 cells will be at different stages of infection relative to each other. Since this could potentially mask changes in gene expression, it was decided to synchronize LA9 cells by serum starvation prior to infection [47]. To confirm that cells were synchronized, they were fixed and stained with propidium iodide and analyzed by FACS analysis (Figure 16). Propidium iodide stains DNA and is used to determine the relative amounts of DNA in cells and thus the stage of the cell cycle. The majority of LA9 cells are in G_o/G_1 immediately after block release and progress in an orderly fashion into S phase around 14 to 16 hours post block, and enter G_2 around 20 hours post block. I also confirmed that MVM arrests cells in S/G_2 by repeating the above experiment with MVM-infected cells. As can be seen in Figure 17, by 20 hours post block MVM-infected cells appear as a broad peak spanning the S/G_2 region with very few cells in G_o/G_1 as compared to uninfected cells that have a well defined G2 peak and are beginning to cycle back into G_o/G_1.

Array studies were conducted as described in the Materials and Methods section 20fs. Briefly, total RNA was isolated from cells, enriched for poly A RNAs (by using biotinylated oligo(dT) and streptavidin coated magnetic beads), and reverse transcribed in the presence of ^{32}P labeled dNTP using a primer set specific to the genes present on the array. As controls, I checked for RNA integrity by visualizing the major ribosomal RNAs, confirmed MVM infection by RT/PCR amplification of NS1 transcripts, and finally confirmed an absence of genomic DNA contamination by PCR amplification of actin DNA (Figure 18). The labeled cDNAs were then hybridized overnight to the

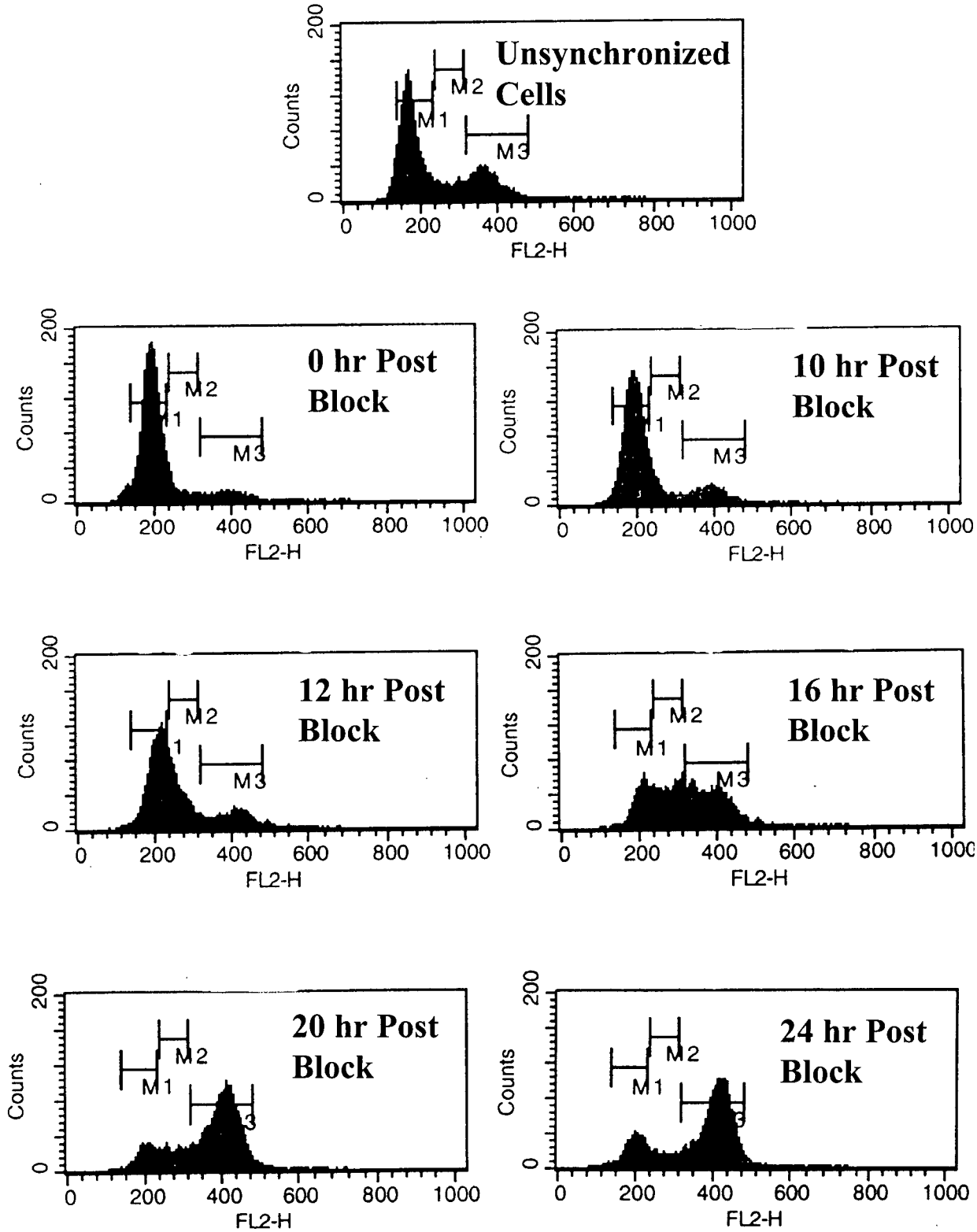

Figure 16: Synchronized LA9 cells by serum starvation. LA9 cells were stained with propidium iodide at various times post block and analyzed by FACS analysis (Materials and Methods Section 5). M1: cells in G_o/G_1, M2: cells in S, and M3: Cells in G_2 phase. FACS analysis of unsynchronized LA9 cells is provided for a comparison.

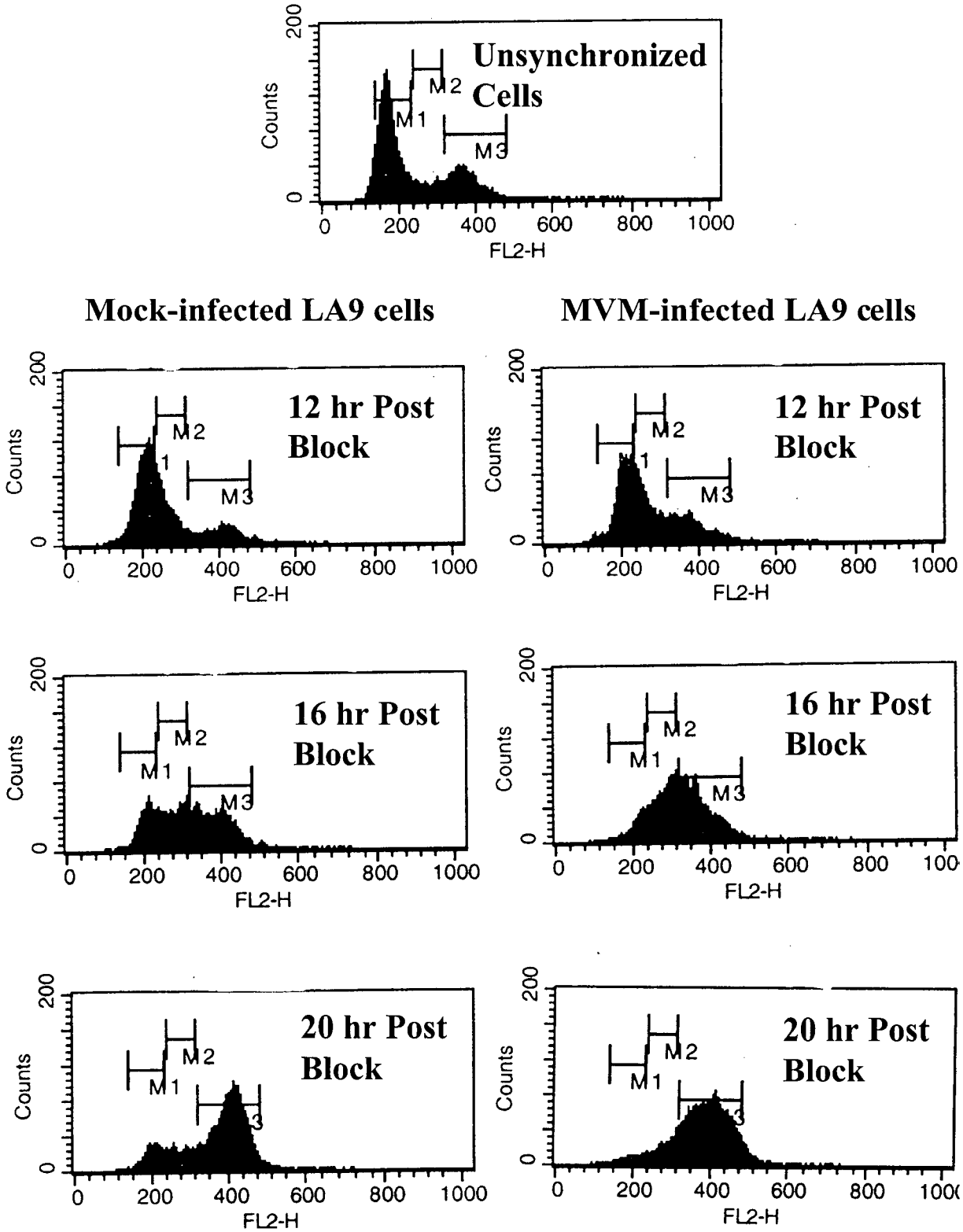

Figure 17: Arrest of MVM-infected LA9 cells in S/G_2. Synchronized LA9 cells were mock or MVM infected, stained with propidium iodide at various times post block and analyzed by FACS analysis (Materials and Methods section 5). M1: cells in G_0/G_1, M2: cells in S, and M3: Cells in G_2 phase. FACS analysis of unsynchronized LA9 cells is provided for a comparison.

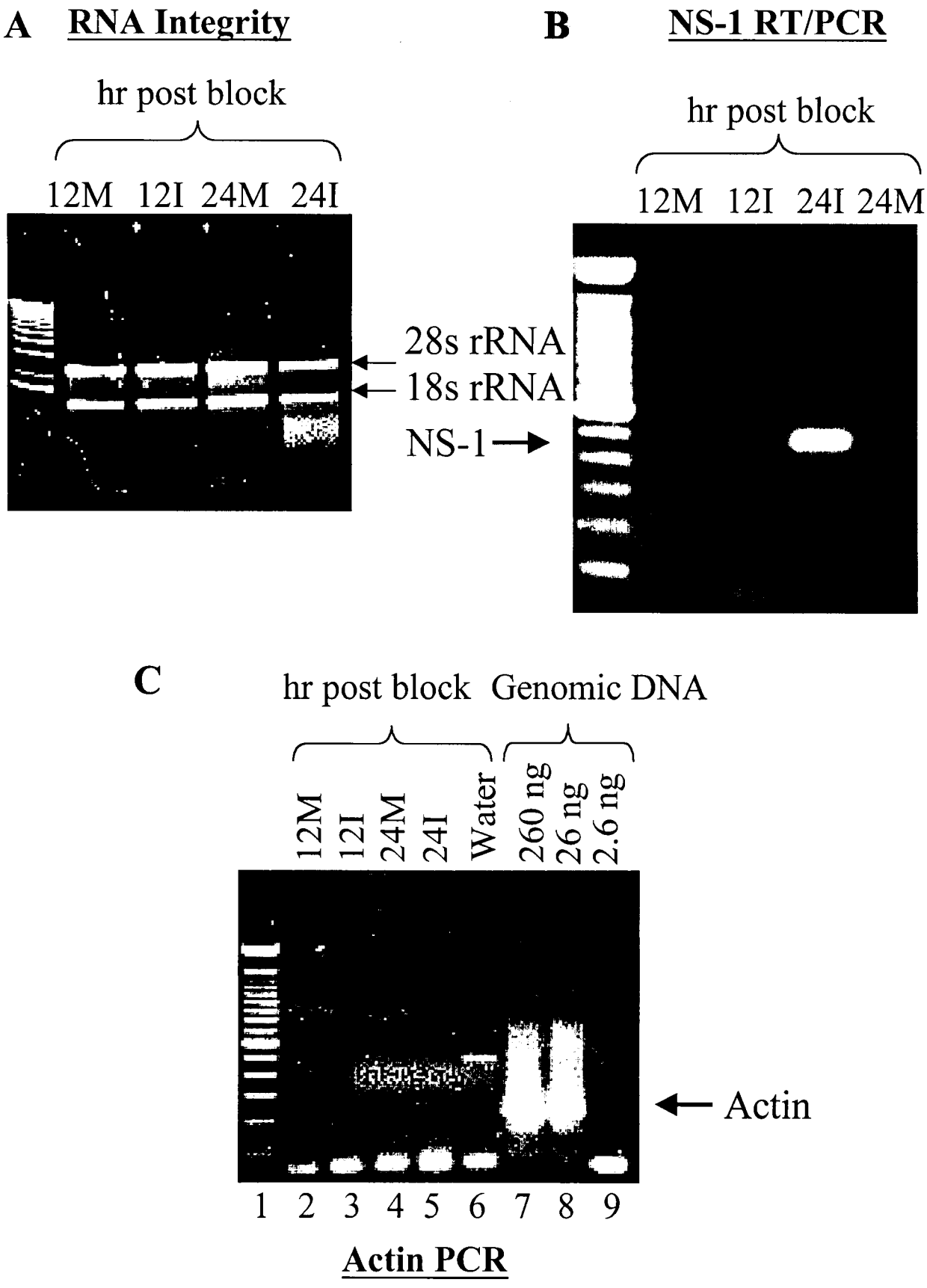

Figure 18: Legend on next page

Figure 18: Array RNA controls. **A:** RNA integrity analysis. Agarose gel showing the presence of the 28S and 18S rRNAs. **B:** Confirmation of MVM infection. RNA was reverse transcribed with an oligo T primer and a fragment of NS-1 transcript was amplified by PCR with NS1-265 & NS1-415 primers. **C:** Absence of genomic DNA in RNA preparation. PCR was used to detect the presence or absence of genomic DNA using actin-specific primers PW10 & 11 (lanes 2-5). Varying amounts of LA9 genomic DNA were used as a positive control (lanes 7-9).

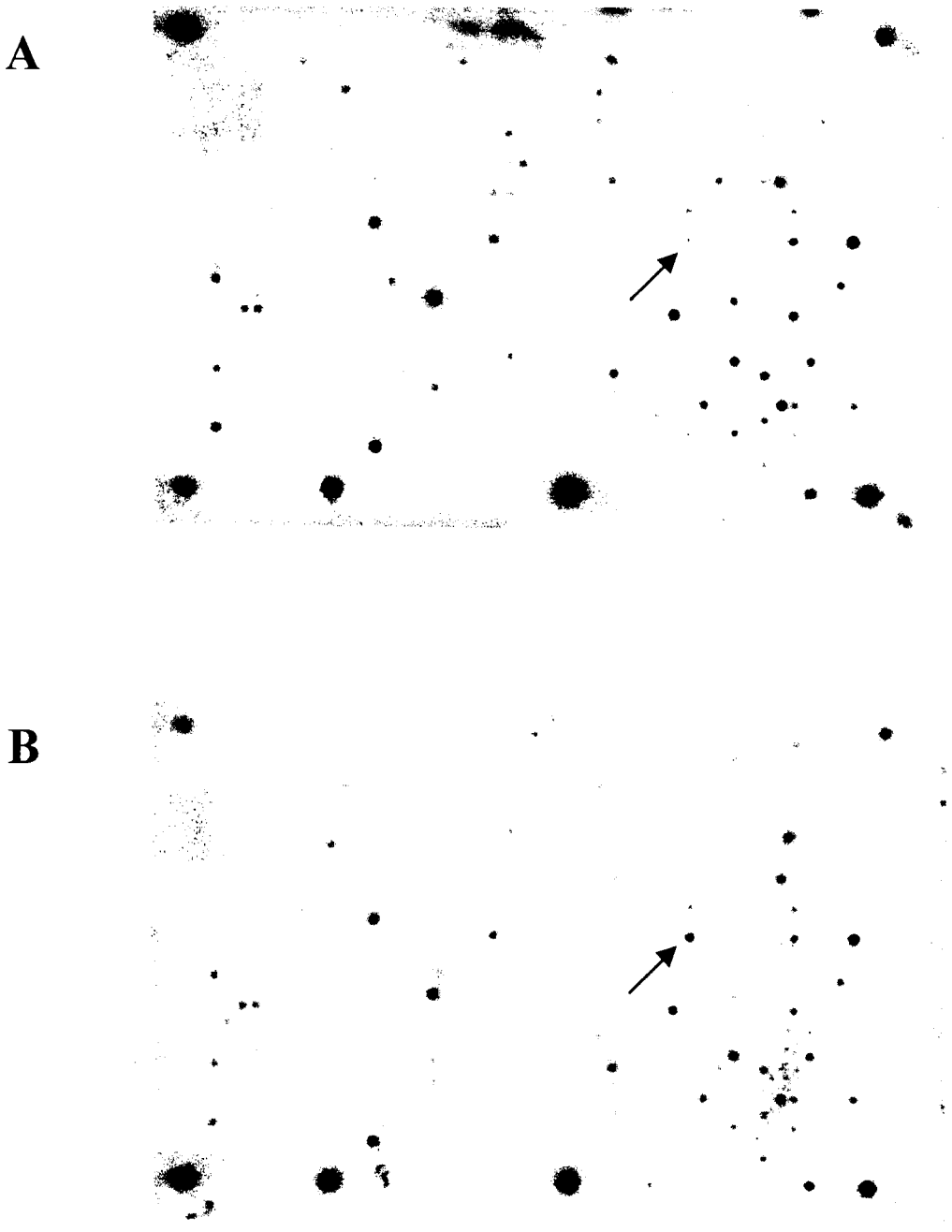

Figure 19: A typical Clontech Atlas mouse 1.2 array. **A:** Mock-infected, synchronized LA9 cells harvested at 24 hr P.B. **B:** MVM-infected, synchronized LA9 cells harvested at 24 hr P.B. The arrow indicates spot c02n (TTF, transcription termination factor/B2 SINE).

arrays, washed several times, and visualized using a phosphorimager. Figure 19 shows a typical array after hybridization.

Data analysis was a multi-step process. Phosphorimager data was analyzed using Clontech's Atlasimage 1.01a software, which can be used to locate, identify and calculate signals for each cDNA spot. Background was determined by averaging the signal in the background regions of the array and then was subtracted from each individual signal. Initially, I normalized the arrays to a series of housekeeping genes, specifically cytoplasmic β-actin and 40S ribosomal protein S29. However, subsequent re-analysis of the data suggested that this method was biased. Hence, the arrays were normalized by the following method. Spots with signals less than 500 counts (after background subtraction) were discarded from the data set, the infected/mock-infected ratio was calculated for the remaining spots and these data were plotted versus gene identity. It is expected that the majority of spots should have a ratio of approximately one, so a single normalization factor was estimated for the control array from the above plot such that the majority of the spots fell into this range (Figure 10, page 43). All control signals were then multiplied by this factor and the ratios recalculated.

I examined four different array sets: RNA was isolated for two array sets (arrays I and II) comparing mock (control) and infected LA9 cells at 24 hours post block (serum starvation. The results of one 24 h post block synchronized cells array set are shown in array I (Figure 20) and one set comparing cells at 12 hours post block synchronized cells in array III (Figure 21). An unsynchronized array set at 36 hours post infection was also examined (array IV, Figure 22) to compare differences in synchronized and unsynchronized cells. Genes that changed two-fold up or down were considered to be

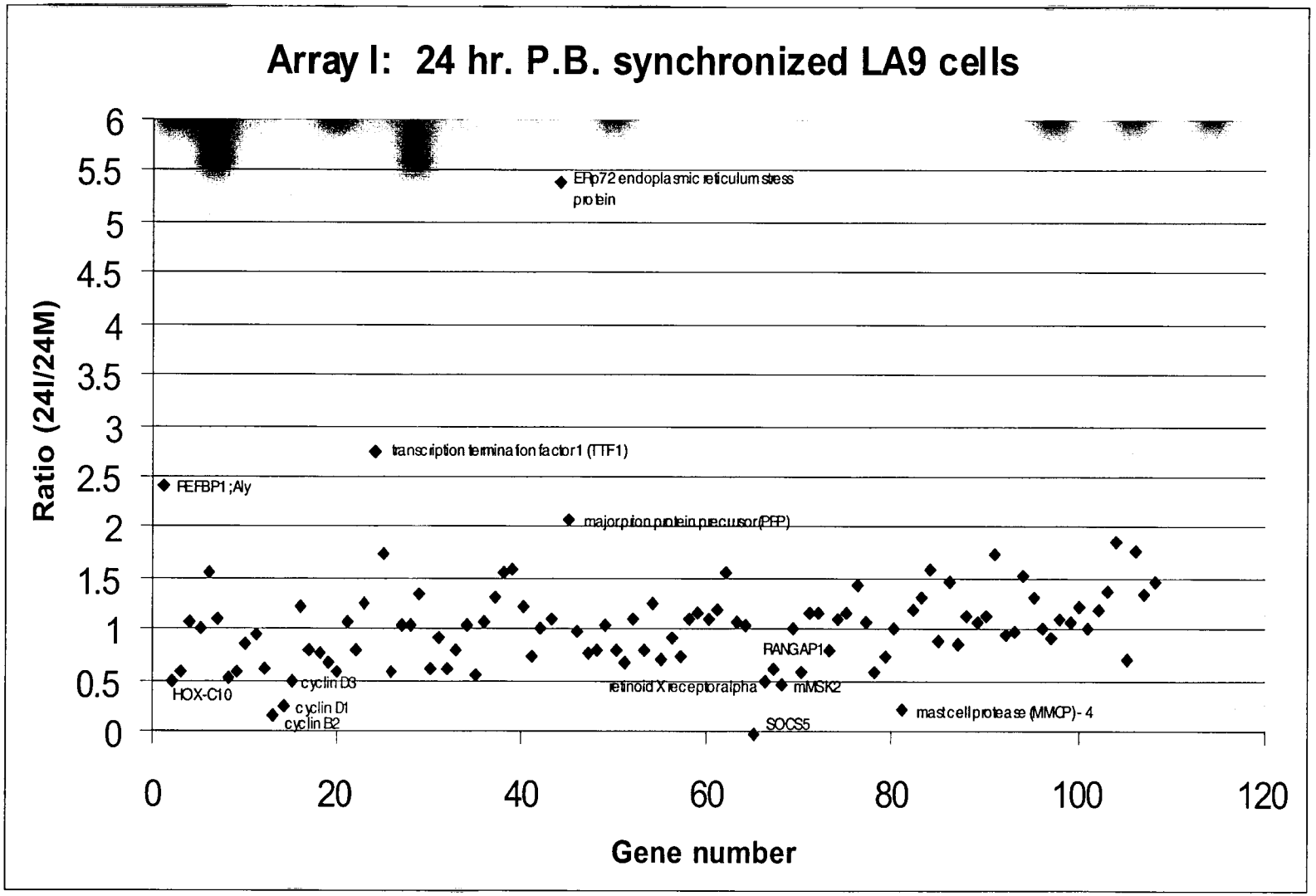

Figure 20: Gene ratios (24I/24M) with a signal >500 counts from synchronized LA9 cells 24 hours post block. Mock-infected array values were multiplied by 0.6 to normalize to infected array values. Ratios with a value >1 indicate an increase in abundance in the infected cells, ratios with a value <1 indicate a decrease in abundance. mMSK: Mitogen & Stress-activated Kinase 2; RANGAP: Ran GTPase Activating Protein 1; REFBP1: RNA and Export Factor interacting protein 1; SOCS5: Suppressor Of Cytokines Signaling protein 5.

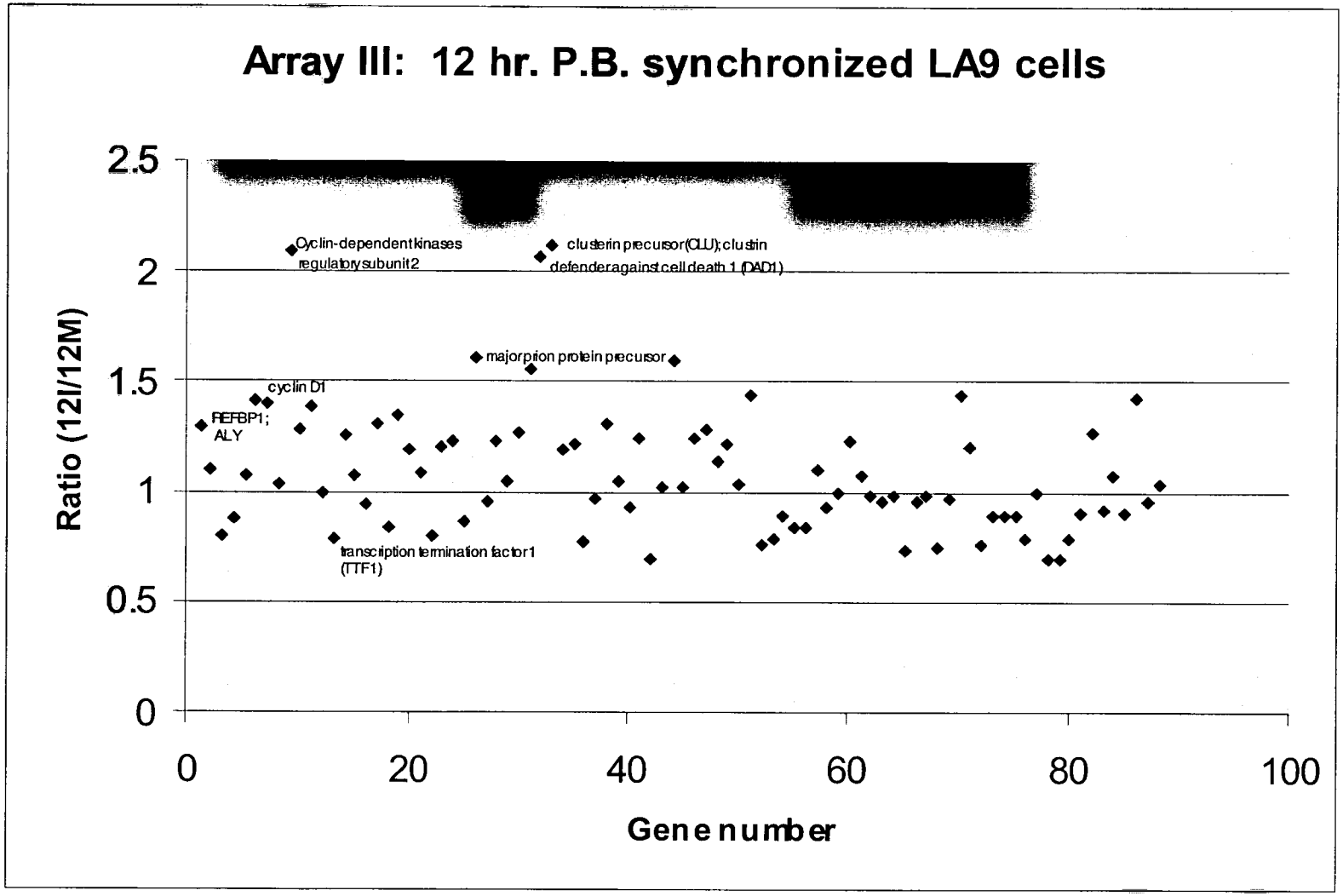

Figure 21: Gene ratios (12I/12M) with a signal >500 counts from synchronized LA9 cells 12 hours post block. A normalization factor was not needed. Ratios with a value >1 indicate an increase in abundance in the infected cells, ratios with a value <1 indicate a decrease in abundance. REFBP1: RNA and Export Factor interacting protein 1.

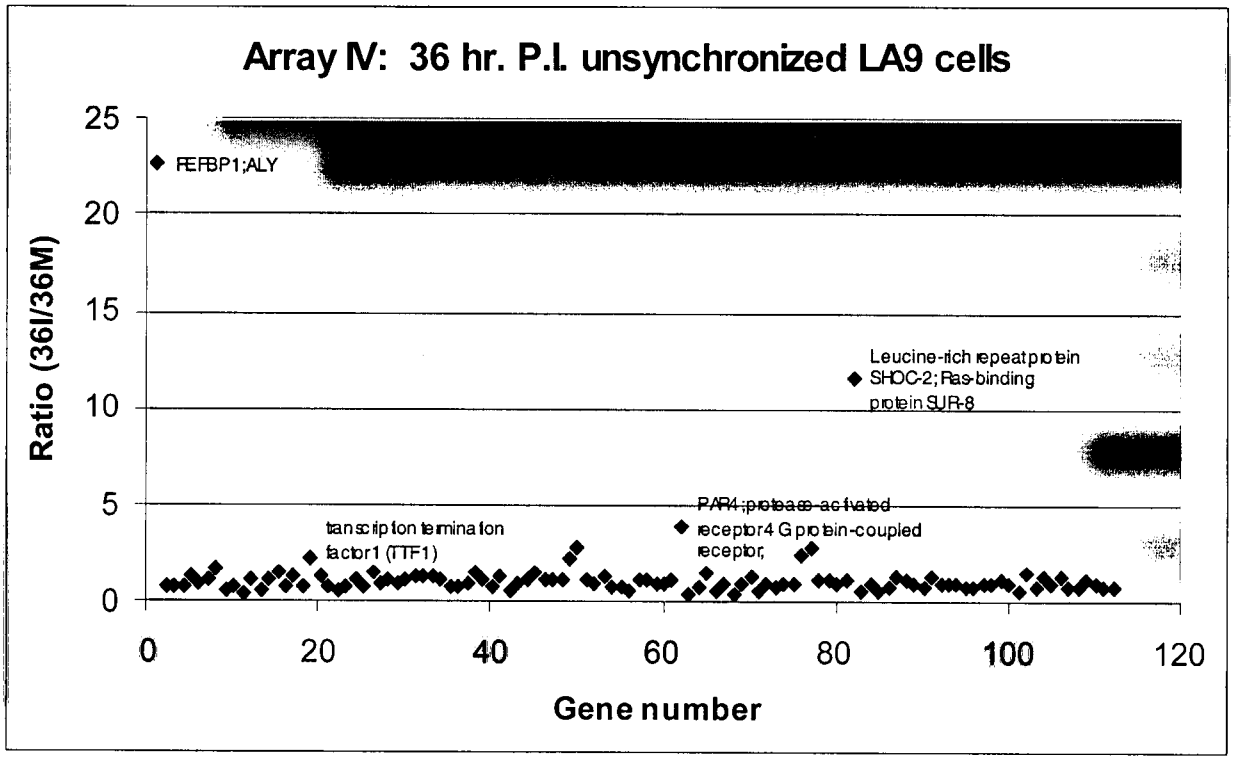

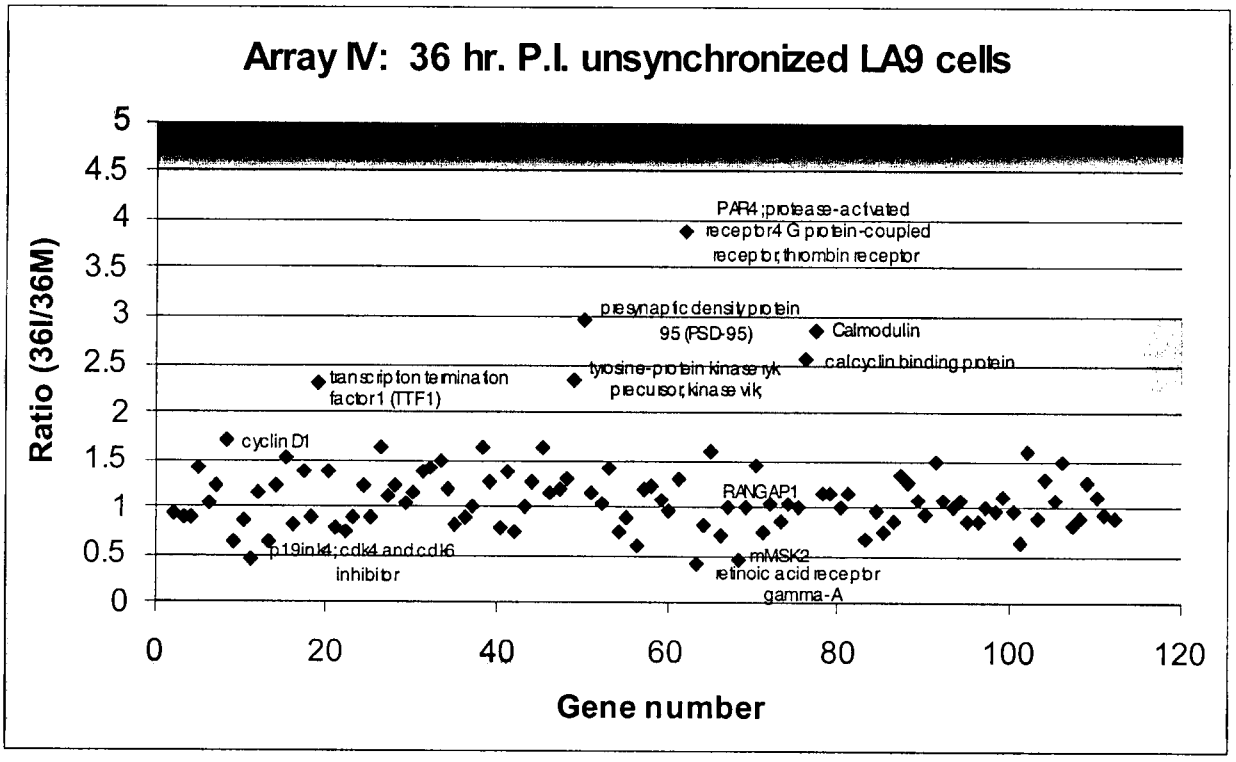

Figure 22: Gene ratios (36I/36M) with a signal >500 counts from unsynchronized LA9 cells 36 hours post infection. No normalization was needed. Ratios with a value >1 indicate an increase in abundance in the infected cells, ratios with a value <1 indicate a decrease in abundance. Both graphs plot the same data, but at different scales. mMSK: Mitogen & Stress-activated Kinase 2; RANGAP: Ran GTPase Activating Protein 1; REFBP1: RNA and Export Factor interacting protein 1.

Array III Synch. 12l/12M	Array I Sync. 24l/24M	Array II Sync. 24l/24M	Array IV Unsync 36l/36M	Gene Identity
1.30	2.43	1.61	22.68	transcriptional coactivator of AML-1 & LEF-1 (ALY)
LS	0.50	0.59	LS	HOMEOBOX PROTEIN HOX-C10 (HOX-3.6)
LS	LS	0.55	LS	early growth response protein 1 (EGR1)
LS	0.61	0.43	LS	transcription factor C 1
LS	0.17	0.57	LS	G2/M-specific cyclin B2 (CCNB2; CYCB2)
1.41	0.26	0.61	1.72	G1/S-specific cyclin D1 (CCND1; CYL-1)
LS	0.49	0.37	LS	G1/S-specific cyclin D3 (CCND3; CYL3)
2.10	0.49	0.85	0.87	Cyclin-dependent kinases regulatory subunit 2 (CKS-2)
LS	0.82	0.76	0.49	p19ink4; cdk4 and cdk6 inhibitor
0.80	2.76	2.88	2.31	transcription termination factor 1 (TTF1)
1.07	5.41	HB	HB	ERp72 endoplasmic reticulum stress protein
1.62	2.08	HB	HB	major prion protein precursor (PRP)
2.08	1.13	1.72	1.28	defender against cell death 1 (DAD1)
2.13	LS	HB	LS	clusterin precursor (CLU); clustrin
2.06	0.76	1.33	2.34	tyrosine-protein kinase ryk precursor; kinase vik; nyk-R
LS	LS	3.34	LS	transforming growth factor beta receptor 1
LS	LS	LS	2.97	presynaptic density protein 95 (PSD-95)
LS	HB	0.25	LS	wingless-related MMTV integration site 10b protein precursor
LS	0.00	LS	LS	suppressor of cytokines signaling protein 5 (SOCS5)
LS	LS	LS	3.92	PAR4; protease-activated receptor 4 G protein-coupled receptor; thrombin receptor
LS	LS	0.31	0.43	retinoic acid receptor gamma-A (RAR-gamma-A; RARG)
0.87	0.50	0.73	0.86	retinoid X receptor alpha (RXR-alpha; RXRA)
1.28	0.48	0.61	0.49	mitogen- & stress-activated protein kinase 2 (mMSK2)
LS	LS	0.28	LS	Rac1 murine homolog
LS	LS	LS	2.56	calcyclin binding protein
LS	LS	LS	2.87	Calmodulin
LS	LS	LS	11.80	Leucine-rich repeat protein SHOC-2; Ras-binding protein SUR-
LS	0.23	LS	LS	mast cell protease (MMCP) - 4

Table 3: Genes altered in at least one array set. HB: High Background; LS: Low Signal.

significantly altered in expression. This was based on the manufacturer's recommendations and my own observations. Table 3 lists all the ratios for genes that were altered in at least one array set. It should be pointed out that in arrays II and IV, there was an area of high background on the extreme right of the arrays. Because of this, many genes in this region of the array could not be analyzed. To examine reproducibility, genes with signals greater than 1000 are plotted for array I & II (24 hours synchronized) as shown in Figure 23. There is significant overlap between the two arrays suggesting that they are fairly reproducible.

Several basic observations can be made from the data. First, the signal strength was lower than expected. Approximately one hundred of the over one thousand genes on the array had signals above the threshold. Furthermore, many of these genes' signals were on the lower end, making data interpretation difficult. Second, during the first 12 hours after release from the block, expression levels of few genes changed even though the cells were infected 24 hours previously. This is not necessarily surprising as the cells are still in G1 and MVM requires cells to be in S/G2. In contrast with the 24 hour post block sample (36 h after infection) where the cells are now in S/G2, a number of host cell genes now appear to be altered in expression. Finally, there are both similarities and differences between synchronized and unsynchronized infected LA9 cells. Several genes were altered in both synchronized and unsynchronized cells, including the SINEs, REFBP1 (RNA exchange factor binding protein one), and components of the retinoic acid receptor. However, other proteins like cyclin D1 and cdk4/cdk6 inhibitor show different expression patterns. There is yet another sub-group of genes that shows altered

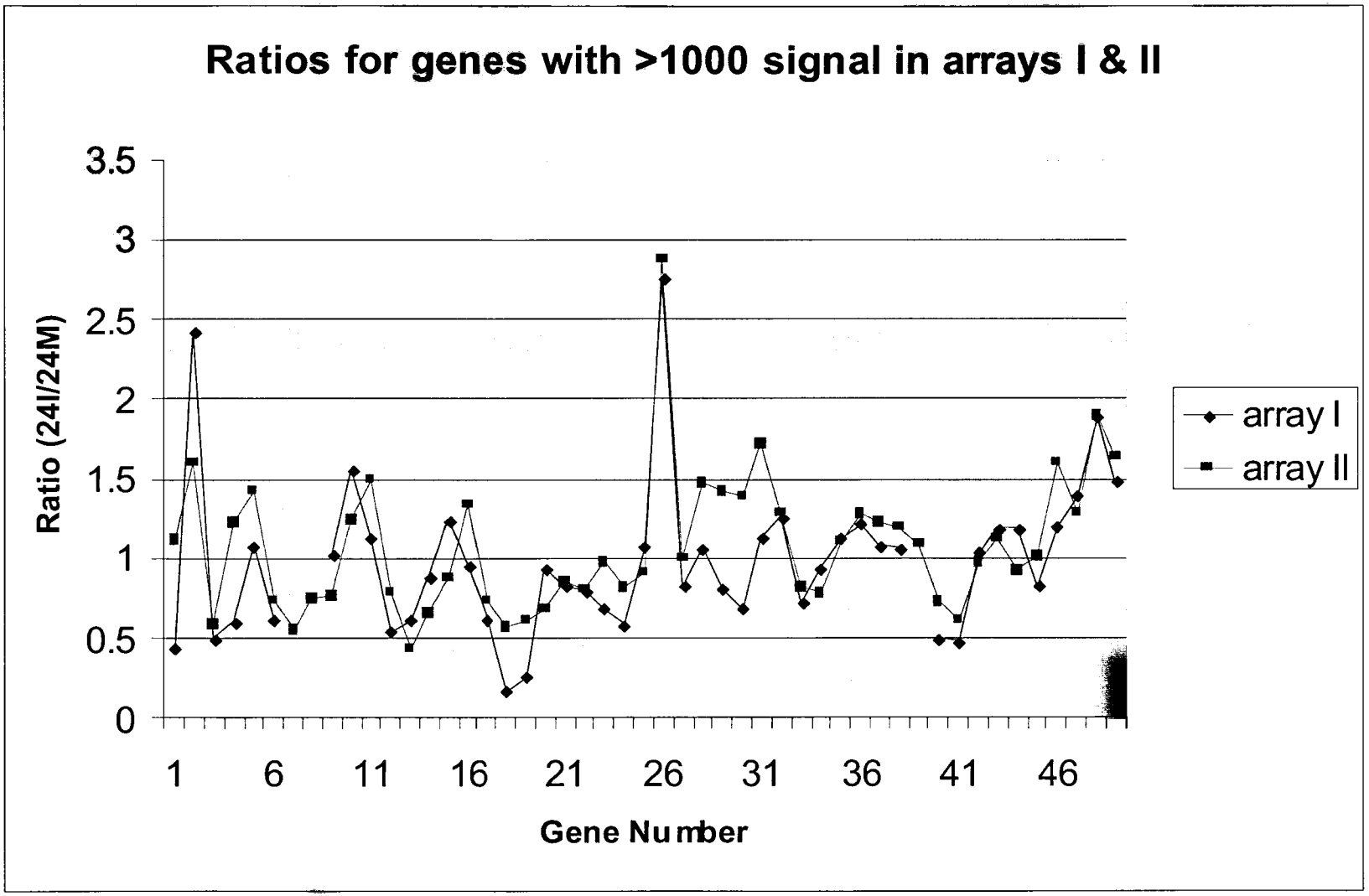

Figure 23: Comparing gene ratios (24I/24M) from arrays I and II (synchronized LA9 cells 24 hours post block). Genes with a signal >1000 from array II were chosen. Discontinuities in the array I data results due to signals below the threshold.

expression in unsynchronized cells whose signals were too low to be analyzed in the synchronized cell arrays.

To confirm gene expression levels, I conducted northern blot analysis on two genes, RANGAP (RAN GTPase Activating Protein 1) and TTF1 (Transcription Termination Factor 1). RANGAP gave a consistently strong signal with a ratio of approximately one in the arrays analyzed. A fragment of the RANGAP cDNA (nt 283 to 2263) containing the majority of the open reading frame and the 3' untranslated region (supplied by Dr. James Degregori, University of Colorado) was used to probe a northern blot of synchronized LA9 cell total RNA (Figure 24a). A band of the expected size, 3kb, was detected and the expression level did not appear to change at 12 or 24 hours post block, agreeing with the array results. In contrast, TTF1 was up-regulated in response to virus infection in both the synchronized and unsynchronized later time point arrays. I therefore probed an unsynchronized total LA9 cell RNA northern blot with a full-length TTF cDNA probe (supplied by Dr. I. Grummt, German Cancer Research Centre) with the results shown in Figure 24b. However, instead of detecting the expected 4 kb transcript for the TTF mRNA, a much smaller band, <250 nt, was found that significantly increased as the infection progressed. This looked very similar to the B2 SINE northern blots (see Figure 15). Sequence analysis of the TTF cDNA confirmed the presence of a murine B2 SINE in the 3' untranslated region of the transcript. Discussions with the array manufacturer eventually confirmed that the TTF1 spot also contained B2 SINE sequence, thus, the TTF1 spot detects both TTF1 and the murine B2 SINE. Since the TTF1 transcript could not be detected by northern blot analysis, I concluded that signal coming

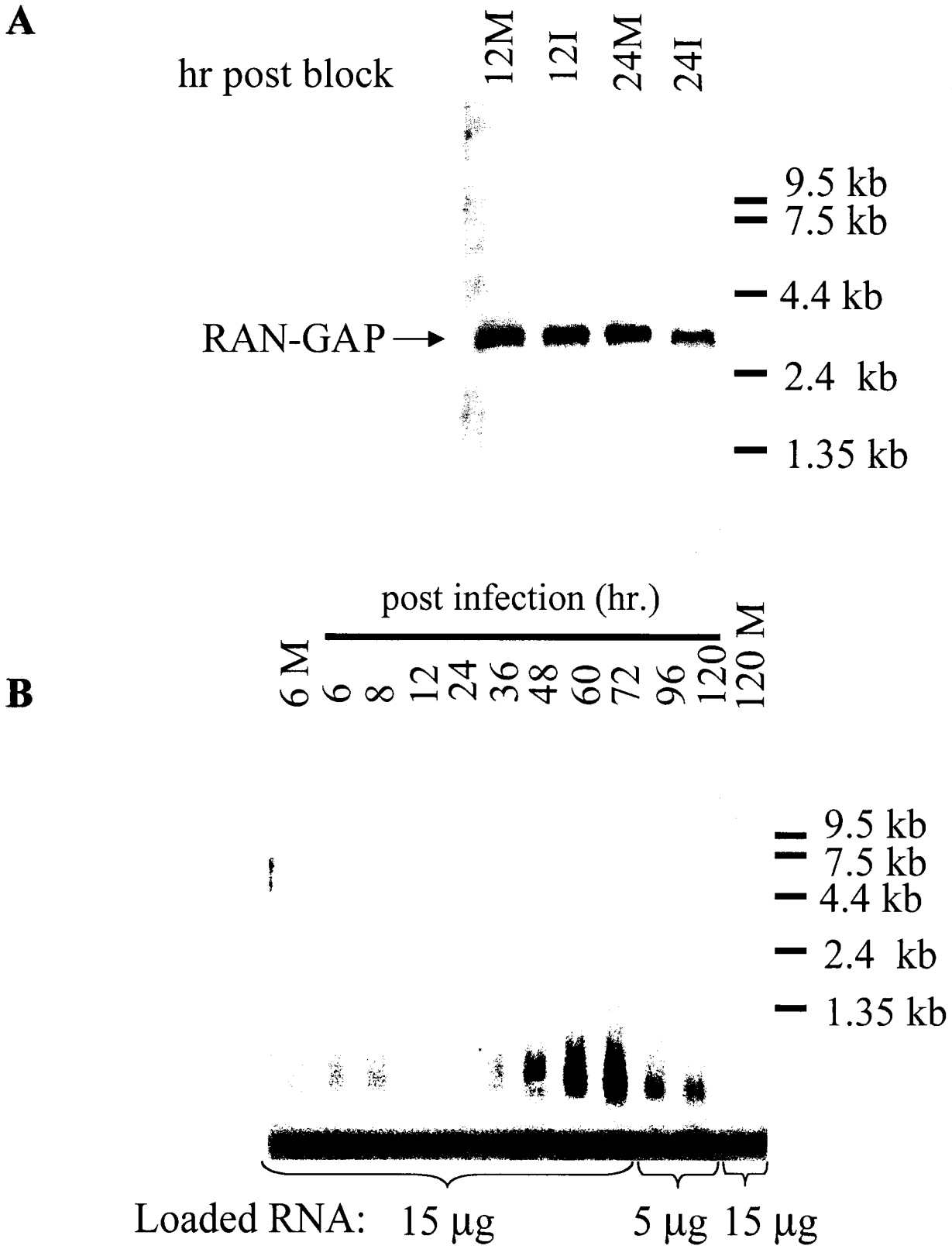

Figure 24: Northern blot hybrization to confirm array results. **A:** Synchronized LA9 cell total RNA blot (15 µg/lane) probed with a 413 nt fragment of RANGAP (cDNA nt. 1230 to 1640). M: mock infected cells, I: MVM infected cells. **B:** Unsynchronized LA9 cell total RNA blot probed with full length TTF cDNA. M: Mock infected cells. Actin was used as a loading control for both gels. See Materials and Methods section 14.

from this spot was solely from increased B2 SINE expression which confirmed the results seen in the differential display experiments seen earlier.

3. Affymetrix Microarrays

Late into the writing of this thesis an opportunity developed to study gene expression using Affymetrix's mouse U74 Av2 microarray. This is a quartz wafer coated in silane on which 25 nucleotide oligomers (known as probes) are synthesized. The technology allows close packing of the different probes, resulting in the ability to screen some 12,000 different genes. These arrays are far superior in design compared to the Clontech cDNA arrays not only in increased number of detectable genes, but also in sensitivity, redundancy and accuracy. Unlike the Clontech arrays, which contain one spot per gene, the Affymetrix system contains between 14 to 20 separate oligomer spots, known as perfect match probes (Figure 25a), allowing for multiple independent measurements of each gene. These spots are scattered around the chip such that should one region contain a high background (a problem I encountered with the Clontech arrays), it can be safely ignored. Furthermore, for each oligonucleotide spot, a second oligonucleotide spot containing a single nucleotide mutation exists (Figure 25a), known as a mismatch probe. This serves as a specificity control, allowing a measure of non-specific binding for each oligomer sequence. The array system also contains both internal (the so called house keeping genes) and external controls spiked into the RNA sample at known concentrations. These external controls allow a measure of the sensitivity of the array, with the criterion that a transcript of 1.5 pM is detected 50% of the time. Finally, the Affymetrix array system comes with extremely powerful software, Affymetrix

A

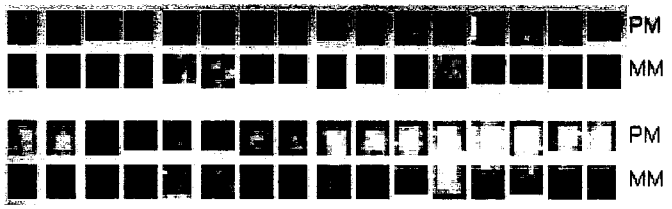

36 mock

36 infected

GRO Oncogene

B

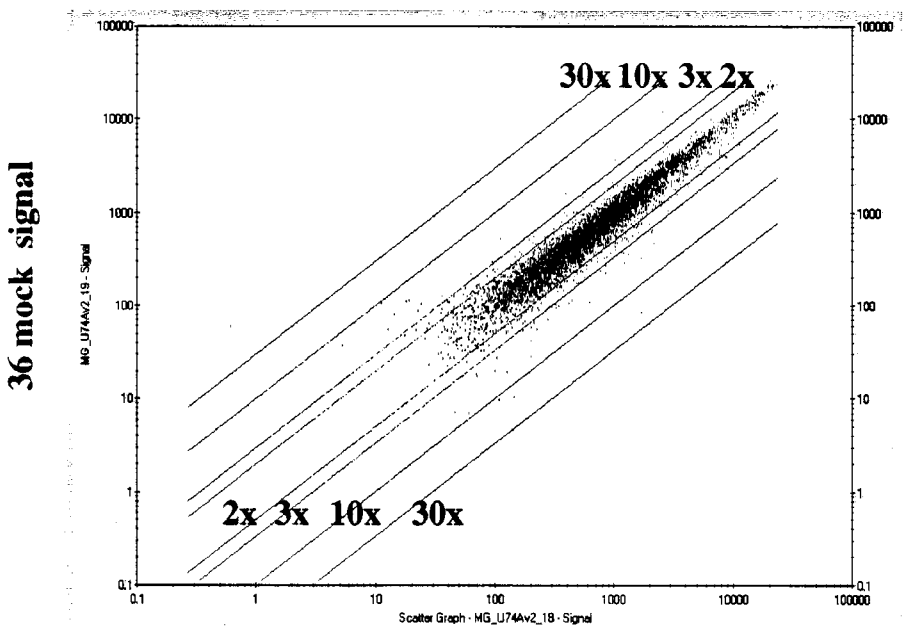

36 mock signal

36 infected signal

Red: Signal present both arrays

Blue: Signal present in one array and absent in the other or signal present in one array and marginal in the other

..arginal in one array

..ier

Figure 25: Legend on next page

Figure 25: **A:** Probe sets for GRO oncogene. PP: Perfect match oligomer; MM: Mismatch oligomer. The brighter the pixel, the higher the signal. The GRO oncogene transcript was expressed in MVM infected cells four fold higher than uninfected cells. **B:** Scatter plot of the signal data for the two arrays. Each dot represents one transcript (one probe pair set). The light blue line represents 2, 3, 10, and 30 fold changes as either an increase in infected cells (top) or as a decrease (bottom). 36 mock: mock infected unsynchronized LA9 fibroblasts at 36 hours post treatment. 36 infected: MVMp infected unsynchronized LA9 cells at 36 hours post infection.

Microarray Suite 5.0. Taking all the data discussed above, it determines the probability of the gene being present or absent and in the case of comparing two arrays, the probability that the gene is altered in one array as compared to the other.

Given the strengths of the Affymetrix microarray, the reader may wonder why these arrays were not used in the first place. As mentioned earlier, the mouse microarrays were not available at the beginning of these experiments. When they initially came on the market, they were extremely expensive and the equipment to process them was not present at UBC. Only recently has this technology become available for my use. In addition, the costs have decreased considerably.

To further examine changes in gene expression in mouse fibroblast cells by infection with MVMp, total RNA from either mock-infected or MVMp-infected unsynchronized LA9 cells at 36 hours post infection was hybridized to the Affymetrix arrays. The resulting data analysis and results are discussed below. Two caveats need to be taken into account when examining these data. First, these data are the result of one set of arrays—to make these data more significant at least two or three biological replicates as well as technical repeats need to be done. Second, because the Affymetrix experiment was performed late in the writing of this thesis, only a preliminary analysis has been accomplished. A more thorough examination is left for the future.

Data analysis was done using Affymetrix microarray suite 5.0 and is described in detail in the Affymetrix manual entitled "GeneChip Expression Analysis: Data Analysis Fundamentals" which is available on the Affymetrix website (www.affymetrix.com). This is a complex process and will only be discussed superficially here. The software first determines if a transcript is present or absent by an algorithm that uses the signal

data from each of the perfect match probes and mismatch probes (together known as a probe pair) for that particular transcript (known as a probe set). The signal intensity is then calculated, using the same probe pair data above, by a weighted mean method involving the entire probe set. When the two arrays (mock vs infected) are compared, the software compares each probe pair for both arrays and generates for each probe set a change *p*-value and a quantitative measure of the change. To compare the two arrays, the global scaling method was used. Figure 25b shows an infected signal versus mock signal scatter plot for all the probe sets on the array. Most transcripts ranked present in both arrays (red) clustered around one, indicating no change, as expected. Transcripts that were ranked absent in both arrays (yellow) had a much wider scatter and were not examined further. Of the 12,473 probe sets, 5347 were considered present (43%); 6869 were considered absent (55%), and 257 were considered marginal (2%).

Transcripts that changed expression during MVM infection were determined as per Affymetrix's instructions. In order for a transcript to have increased expression as a result of infection, it had to be present in the MVMp infected array, to have increased (as detected by the change call algorithm), and have a fold change of 2 or greater. In order for a transcript to have decreased expression as a result of infection, it to be present in the mock array, to have decreased (as detected by the change call algorithm), and have a fold change of –2 or greater. Using this method, 23 transcripts were found to have increased expression in MVM-infected cells, with 6 being unknown ESTs. A further 50 transcripts were found to have decreased expression in MVMiinfected cells, with 18 being unknown ESTs. This yields a total of 74 altered transcripts, 23 which are unknown ESTs. These are listed in Table 4.

ID	Fold Change
epiregulin	13.9 U
Lymphocyte antigen 84, Interleukin 1 receptor-like 1, T1, ST2	6.1 U
GRO1 oncogene	4 U
Mouse glucocortoid-regulated inflammatory prostaglandin G/H synthase (griPGHS)	3 U
calcium-activated potassium channel	2.8 U
CD44 antigen	2.8 U
TEA domain family member 4	2.6 U
Small inducible cytokine A2	2.6 U
Autosomal Zinc finger protein group	2.5 U
Interleukin-4 receptor alpha	2.5 U
Transferrin Receptor group	2.3 U
Latent TGF beta binding protein #1	2.3 U
Myeloblastosis oncogene-like 1, A-myb	2.3 U
second largest subunit of RNA polymerase I (RPA2)	2.1 U
Small inducible cytokine A7	2.1 U
Nerve Growth Factor beta	2.1 U
RalBP1-associated EH domain protein Reps1 (reps1)	2 U
Cyclin G2	5 D
Enhancer Trap locus 1	5 D
Bcl-2	3.3 D
Nuclear Protein 1, p8	3.3 D
D site albumin promoter binding protein	3.3 D
Lipin	3.3 D
ATP binding cassette sub-family A (ABC1) member 1	3.3 D
Plasma membrane associated protein S3-12 (carbohydrate kinase)	2.5 D
Semaphorin A	2.5 D
ganglioside-induced differentiation associated protein 10	2.5 D
CCAAT/enhancer binding protein (C/EBP) beta	2.5 D
Solute carrier family 2 (facilitated glucose transporter), member 1	2.5 D
Max-interacting transcriptional repressor (Mad4)	2.5 D
PPAR gamma coactivator (PGC-1)	2.5 D
Mevalonate (diphospho) decarboxylase	2.5 D
Transforming growth factor, beta induced, 68 kDa	2.5 D
E1B 19K/Bcl-2-binding protein homolog (Nip3)	2.5 D
TDD5, Ndr1 protein (N-myc downstream regulated like)	2.5 D
basic-helix-loop-helix protein class B2	2.5 D
Alpha-L-iduronidase	2.5 D
Chromobox homolog 4 (Drosophila Pc class)	2.5 D

Table 4: Affymetrix microarray altered transcripts. All work was done in unsynchronized mouse fibroblast LA9 cells. U: Transcript is up-regulated in response to MVMp; D: Transcript is down-regulated in response to MVMp. Table continues on next page.

ID	Fold Change
Transcription factor GIF	2 D
Bone morphogenetic receptor for Bmp2 and Bmp4	2 D
Interferon activated gene 202	2 D
Vascular endothelial growth factor	2 D
Lamin B1	2 D
Farnesyl diphosphate sythetase	2 D
Zn-transcription factor 292, Zn-15 TF	2 D
Ets-2	2 D
Stearoyl-coenzyme A desaturase 2	2 D
Tob 1	2 D
c-Cbl associated protein, CAP	2 D
unknown EST (GB: AV170591)	9.2 U
unknown EST (GB: AV235001)	9.2 U
unknown EST (GB: AV335799)	3.7 U
unknown EST (GB: AI152789)	2.8 U
unknown EST (GB: AI837905)	2.6 U
unknown EST (GB: AV250694)	2.1 U
unknown EST (GB: AA770736)	3.3 D
unknown EST (GB: AI849939)	3.3 D
unknown EST (GB: AA691628)	2.5 D
unknown EST (GB: AW120767)	2.5 D
unknown EST (GB: AA798624)	2.5 D
unknown EST (GB: AV228594)	2.5 D
unknown EST (GB: AW120614)	2.5 D
unknown EST (GB: AW120868)	2.5 D
unknown EST (GB: AI837497)	2.5 D
unknown EST (GB: AI317205)	2 D
unknown EST (GB: AI849035)	2 D
unknown EST (GB: AI447783)	2 D
unknown EST (GB: C80410)	2 D
unknown EST (GB: AW123157)	2 D
unknown EST (GB: AW125508)	2 D
unknown EST (GB: AA212964)	2 D
unknown EST (GB: AW122114)	2 D
unknown EST (GB: AW047223)	2 D

Table 4 continued: Affymetrix microarray altered transcripts. All work was done in unsynchronized mouse fibroblast LA9 cells. U: Transcript is up-regulated in response to MVMp; D: Transcript is down-regulated in response to MVMp.

4. SINE Experiments

Both the differential display and Clontech array experiments detected the up-regulation of B2 SINEs expression in mouse LA9 fibroblasts in response to MVM infection. Hence, it was decided to begin characterization of this SINE response with the goal of understanding how it related to the virus/host response.

B2 SINE transcripts range from 200-600 nt

The size of the B2 SINE transcripts seen in previous northern blot analysis was investigated. Northern blots were conducted on LA9 RNA separated through a 5% acrylamide gels (Figure 26a). A band at approximately 190 nt was resolved along with a larger smear that ran from ~200 to 600 nt. As mentioned in the introduction, RNA polymerase III transcripts do not have a specific termination sequence; rather termination occurs when the polymerase encounters a run of Ts [140]. This will result in a pool of transcripts of varying lengths, possibly the smear observed in the northern blot. These results resemble those seen in SV-40 transformed mouse fibroblasts (3T3 cells [141]). The distinct band at approximately 190 nt is presumably due to a processed B2 SINE transcript as it is similar in size to the B2 SINE consensus sequence of 209 nt.

B2 SINE transcripts are RNA and not DNA

Because of the high abundance of SINEs in the murine genome, it was possible, although unlikely, that the signal seen in the previous northern blots was the result of DNA contamination. To eliminate this possibility I compared RNA samples treated with

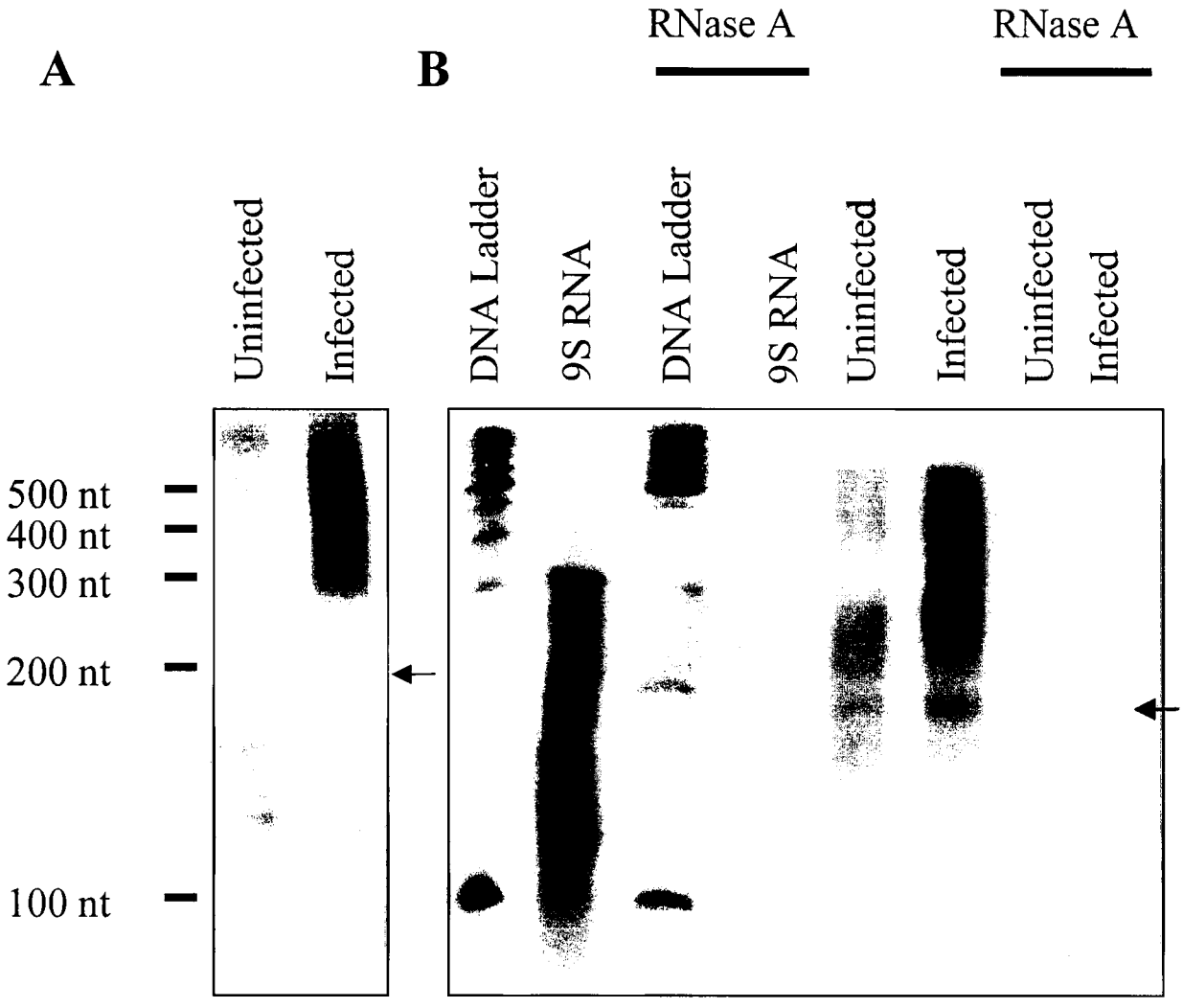

Figure 26: **A:** Resolving the size of the B2 SINE transcripts. Northern blots containing 5μg uninfected or MVM-infected total LA9 cell RNA per lane were probed with B2 SINE (differential display fragment 2A1 amplified and radiolabelled by PCR). **B:** Sensitivity ofSINE transcripts to RNase. 5 μg of uninfected or MVM infected total LA9 cell RNA were treated or mock treated with RNase A (10 μg/ml, 30' at 37°C), separated on a 5% acrylamide gel, blotted and probed with B2 SINE. As controls, a radiolabeled DNA ladder and bacterial 9S RNA (~ 246 nt) were included. The arrow marks the 190 nt SINE band. See Materials and Methods, section 14.

RNase A against untreated samples. As Figure 26b demonstrates, treatment of RNA with RNase A, results in elimination of signal when the blot is hybridized with a B2 SINE probe. A DNA control (5' end-labeled DNA ladder) and RNA control (radiolabeled 9S bacterial RNA) were included to demonstrate that only RNA was degraded.

B2 and B1 SINEs levels are up-regulated throughout infection

Primer extension, using primers against the B1and B2 SINEs (see Figure 27 for primers and expected product sizes), was conducted on MVM-infected LA9 cell total RNA. Figures 28 and 29 show the resulting products from the primer extension reactions separated on 5% acrylamide gels. In both cases the abundance of SINE transcripts appeared to increase by 24 hours post infection and continued to increase throughout the duration of the experiment in a more or less linear fashion. This was in contrast to an uninfected time course, where both SINEs showed no significant increase in expression until extremely late time points, presumably due to the cells becoming overgrown (data not shown). Not surprisingly, there appeared to be significantly more B2 SINE transcript than the B1 SINE transcript. This could be because B2 SINEs are more abundant in the genome than B1 SINEs. Other possibilities are that the viral infection could be stimulating B2 SINE expression more than the B1 SINE expression, or that the B2 SINE genes are less repressed than the B1 SINE genes. Finally, this difference could be due to a difference in primer preference. Further work is needed to distinguish among these possibilities.

A. Polymerase III transcripts

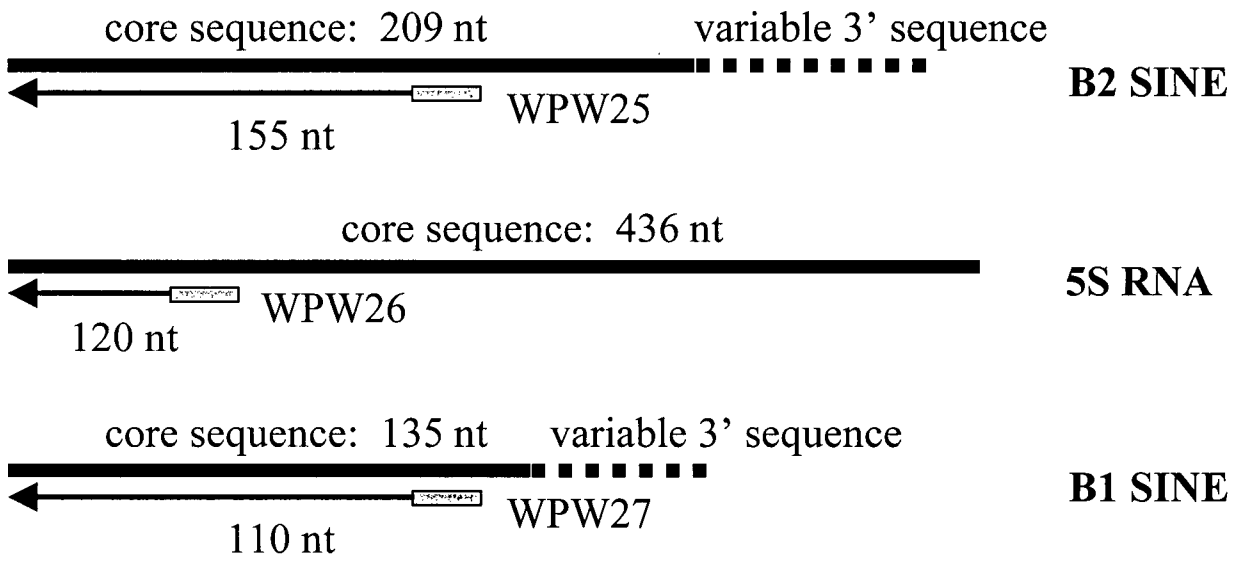

B. Polymerase II transcripts

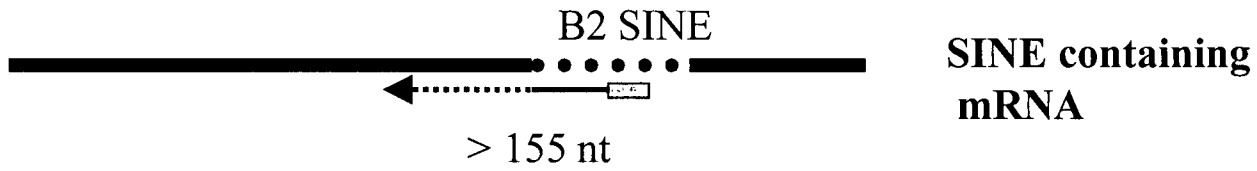

Figure 27: Reverse transcription of SINEs in polymerase III and II transcripts. **A:** Polymerase III transcripts: Primer WPW25 primes a 155 nt B2 SINE cDNA. Primer WPW27 primes a 110 nt B1 SINE cDNA. In both cases, reverse transcription is terminated at the 5' end of SINE transcript. Primer WPW26 primes a 120 nt 5S RNA cDNA which is used as a loading control. **B:** Polymerase II transcripts: Primer 25 primes a B2 SINE cDNA larger than 155 nt as termination continues past the 5' end of the SINE. Primer sequences were based on data from Liu et al., 1995 [161].

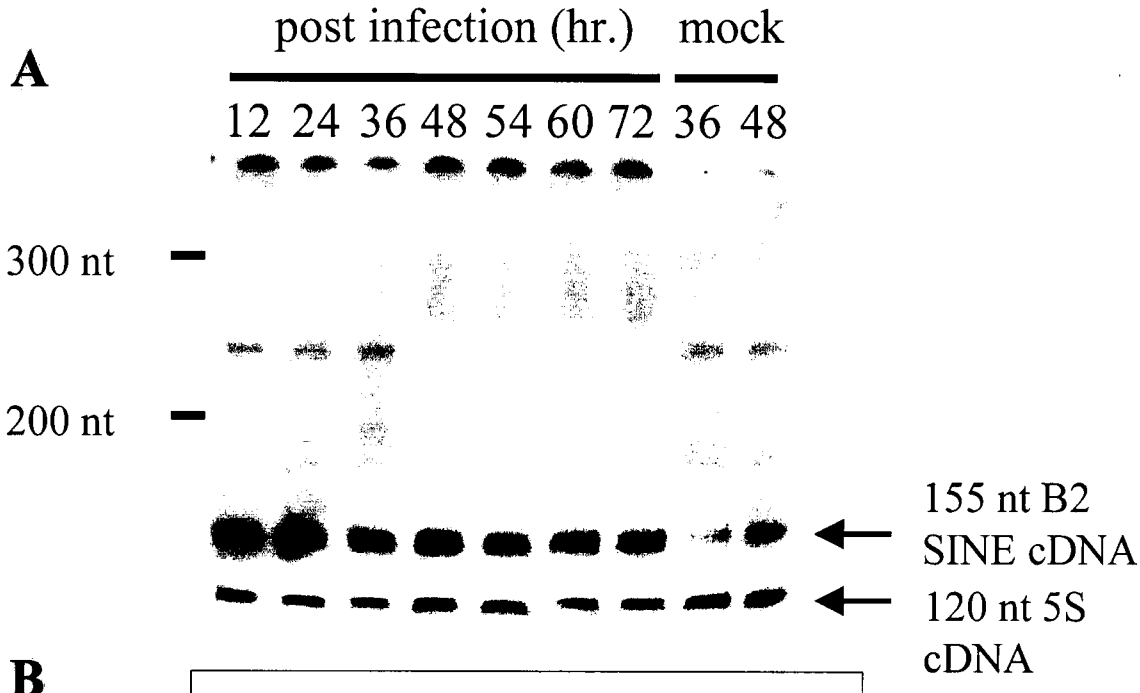

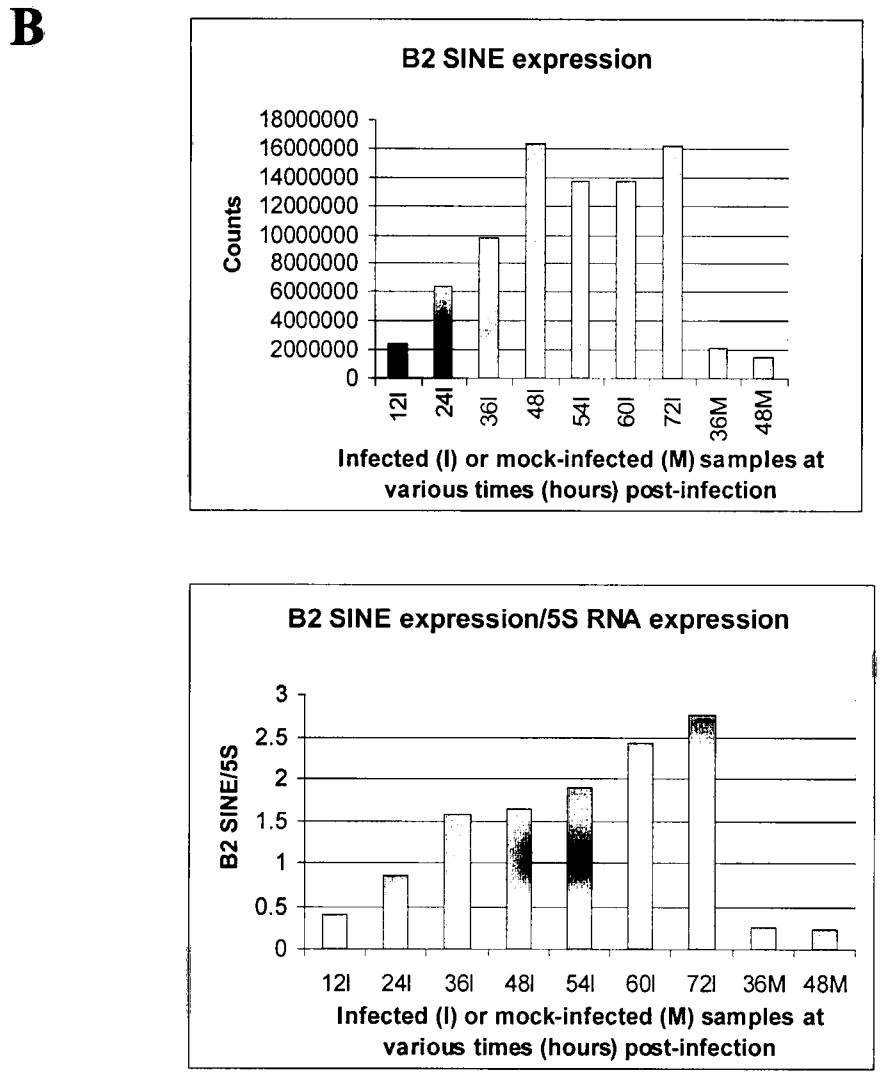

Figure 28: Legend on next page

Figure 28: Expression of B2 SINE transcripts during MVM infection. **A:** 5% acrylamide gel showing the products of primer extension with a B2 SINE (WPW25) and 5S RNA (WPW 26) specific primers. The B2 SINE product (155 nt) and 5S product (120 nt) are indicated by the bold arrows. **B:** Radiometric quantification of the B2 SINE band in **A** both directly, top panel, and as a ratio, bottom panel, (B2 SINE counts/5S RNA counts) to adjust for loading. M: Mock-infected unsynchronized LA9 cells. I: MVM-Infected unsynchronized LA9 cells.

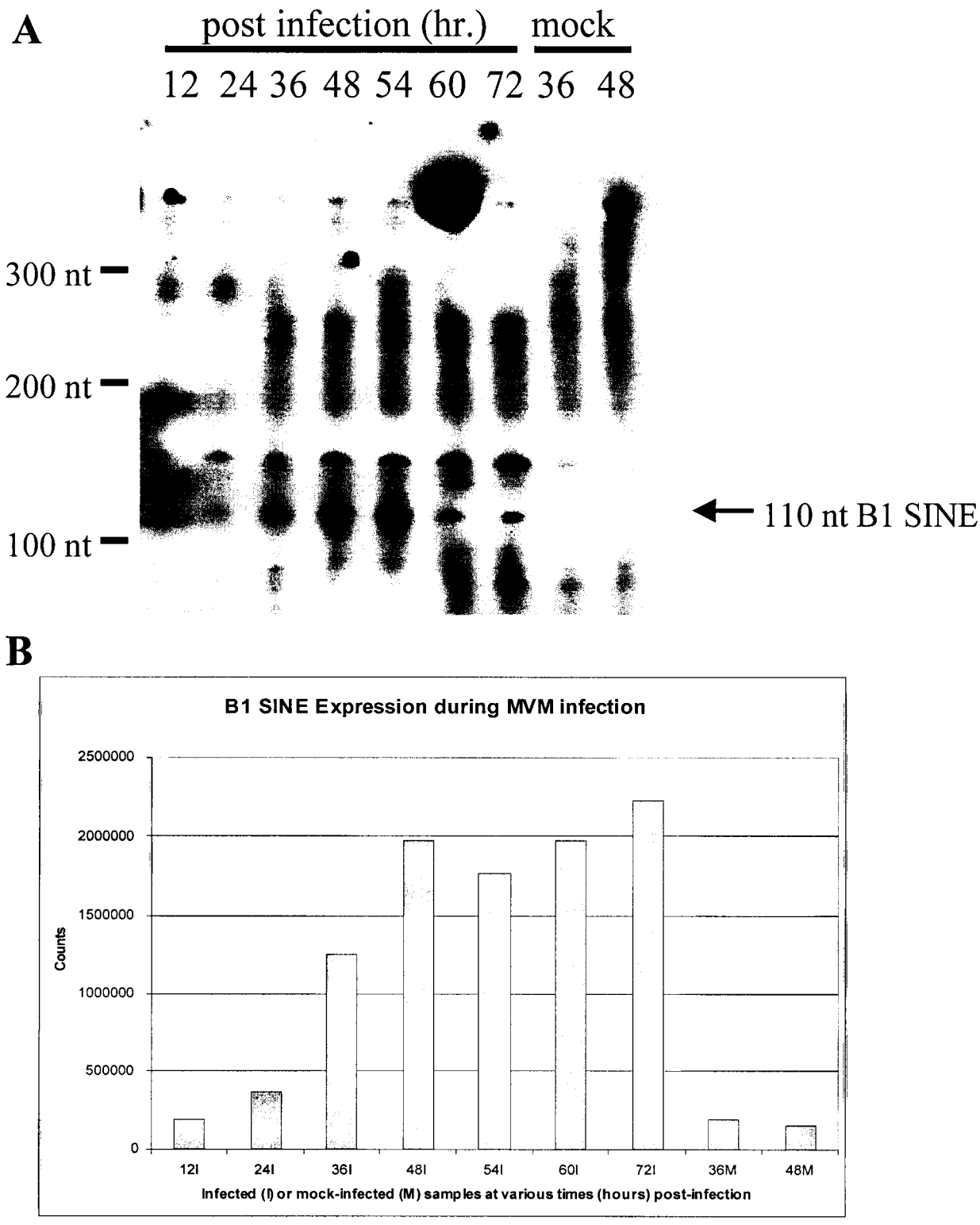

Figure 29: Expression of B1 SINE transcripts during MVM infection. **A:** 5% acrylamide gel showing the products of primer extension with a B1 SINE specific primer (WPW 27). The B1 SINE product (110 nt) is indicated by the bold arrow. **B:** Radiometric analysis of the B1 SINE band (arrow) in **A**. M: Mock infected unsynchronized LA9 cells. I: MVM Infected unsynchronized LA9 cells. 5S RNA primer extension was not done simultaneously as the 120 nt 5S RNA band overlaps the 110 nt B1 SINE band.

B2 and B1 SINE transcripts are transcribed predominantly by RNA polymerase III

To confirm the size of the major B1 and B2 SINE amplified products (Figure 28 and 29) primer extension products were separated on sequencing gels (not shown). In both cases, the major band was of the size of the expected RNA polymerase III transcript. This further suggested that the majority of SINE transcripts were of RNA polymerase III origin, rather than another possibility in which the SINE is embedded in a Polymerase II transcript. In the latter case, products larger than either the 110 nt (for B1 SINEs) or 155 nt (for B2 SINEs) band would be expected (Figure 27). Interestingly, in the B1 SINE primer extension (Figure 29), a second band of 144 nt was also seen to be up-regulated. Presumably this is due to a B1 SINE sequence embedded in another altered transcript.

The major nonstructural protein of MVM, NS1, induces increased B2 and B1 SINE levels

It was suspected that the major nonstructural protein of MVM, NS1, was responsible for increased B2 and B1 SINE levels. To test this hypothesis, LA9 cells were transfected with plasmids expressing either NS1/NS2 (pCMVNS1), NS1 only (pCMV1989, a gift from Dr. David Pintel, University of Missouri), or as a control β-galactosidase (pCMVβ-gal) and RNA was harvested at various times post-transfection. The pCMV1989 plasmid contains NS-1 coding sequence with a point mutation (A to C) that alters a splice acceptor site, preventing splicing of the NS1 (R1) transcript into the NS2 (R2) transcript [81]. Primer extension analysis was used to quantify B2 SINE RNA expression (Figure 30). At 12 hours post-transfection, there was no significant difference in B2 SINE levels in the cells transfected with the NS1-expressing plasmids as compared to the pCMVβ-gal control.

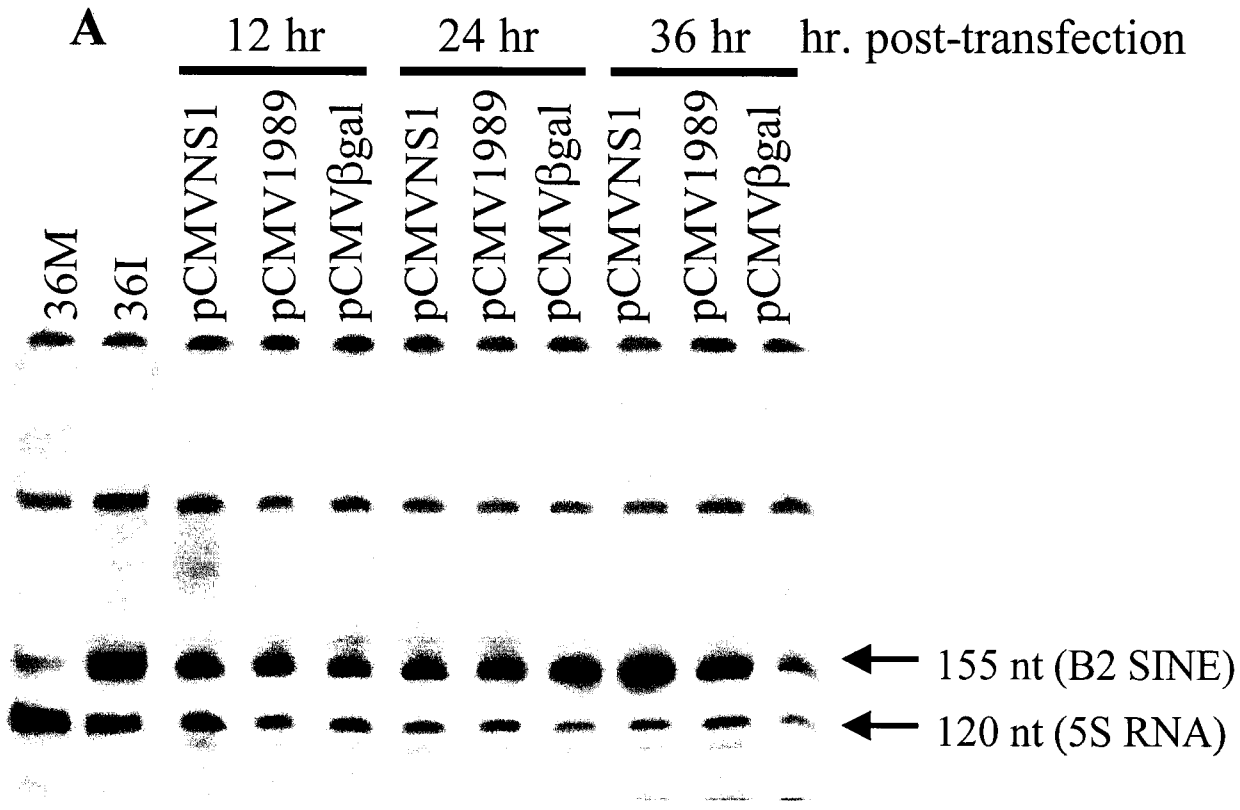

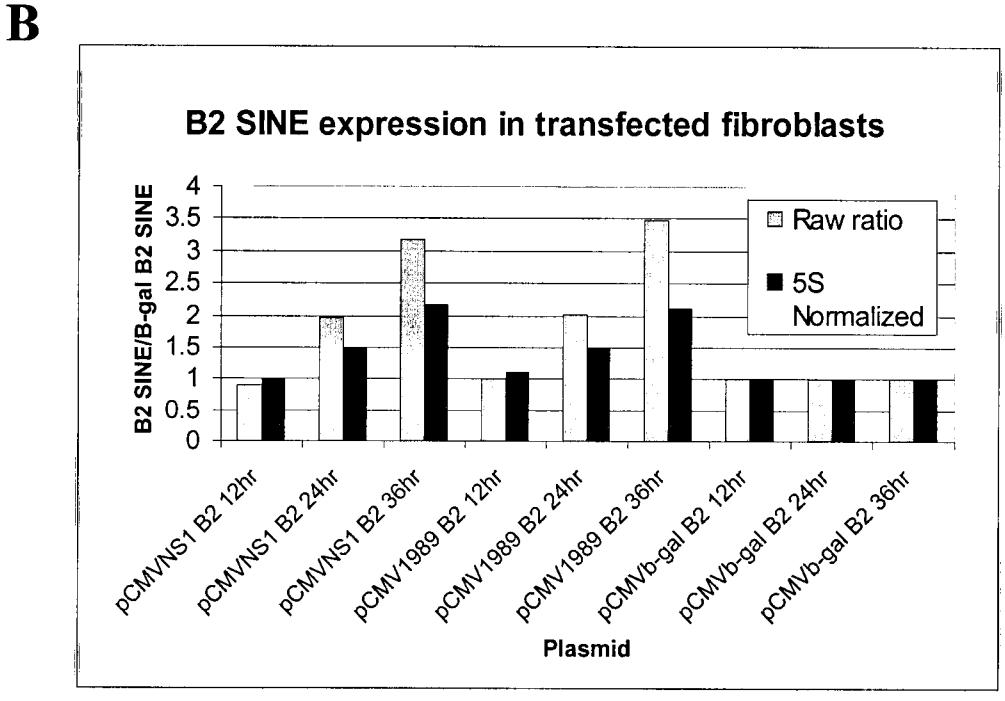

Figure 30: Legend on next page

Plasmid	Expresses
pCMVNS1:	NS-1 & NS-2
pCMV1989:	NS-1
pCMVβgal:	β-galactasidase

Figure 30: MVM NS1 induces increased B2 SINE expression. **A:** 5% acrylamide gel containing the products of B2 SINE primer extension from LA9 cells transfected with plasmids expressing NS1, NS1/NS2 or β-galactasidase at various times post-transfection. 36M: Mock-infected unsynchronized LA9 cells 36 hours. 36I: MVM-infected unsynchronized cells 36 hours post infection. **B:** Radiometric analysis of the 155 nt band in **A**. Data are expressed as fold change compared to the β-galactasidase control. 5S Normalized: Data normalized relative to the 5S RNA signal (B2 SINE/5 S) to correct for variable loading.

However, at 24 hours post transfection, B2 SINE levels increased in cells transfected with either pCMVNS1 or pCMV1989. This trend continued at the 36-hour time point, where an approximate 3-fold increase in B2 SINE levels was seen for both pCMVNS1 and pCMV1989 as compared to the pCMVβ-gal control. Interestingly, there appeared to be no difference between cells expressing NS1/NS2 or just NS1 alone. A similar trend was seen when B1 SINE levels were examined (Figure 31), with an approximate 2-fold change seen by 36 hours. It should be noted that the changes in B2 and B1 SINE levels were observed in spite of the fact that transfection efficiency was only 15-20% (by X-gal staining). From these data, it was concluded that expression of the NS1 protein alone could increase both B2 and B1 SINE levels.

Altering SINE levels

Theoretically, SINE levels may be increased in several different ways (Figure 32). SINE transcription can be up regulated by either altering promoter accessibility (and thus removing SINE transcriptional repression) or by increasing the amount of basal RNA polymerase III transcription factors. Alternatively, transcription levels could remain unchanged, but the rate of SINE RNA degradation could be reduced. This would also lead to an increase in concentration of SINEs within the cell.

TFIIIC220 and TFIIIC110 protein levels do not increase during MVM infection

As mentioned above, one way to increase SINE transcription is by increasing the amounts of the various basal RNA polymerase III transcription factors. It has been reported that murine fibroblasts (3T3 cells) transformed with SV-40 expressed higher

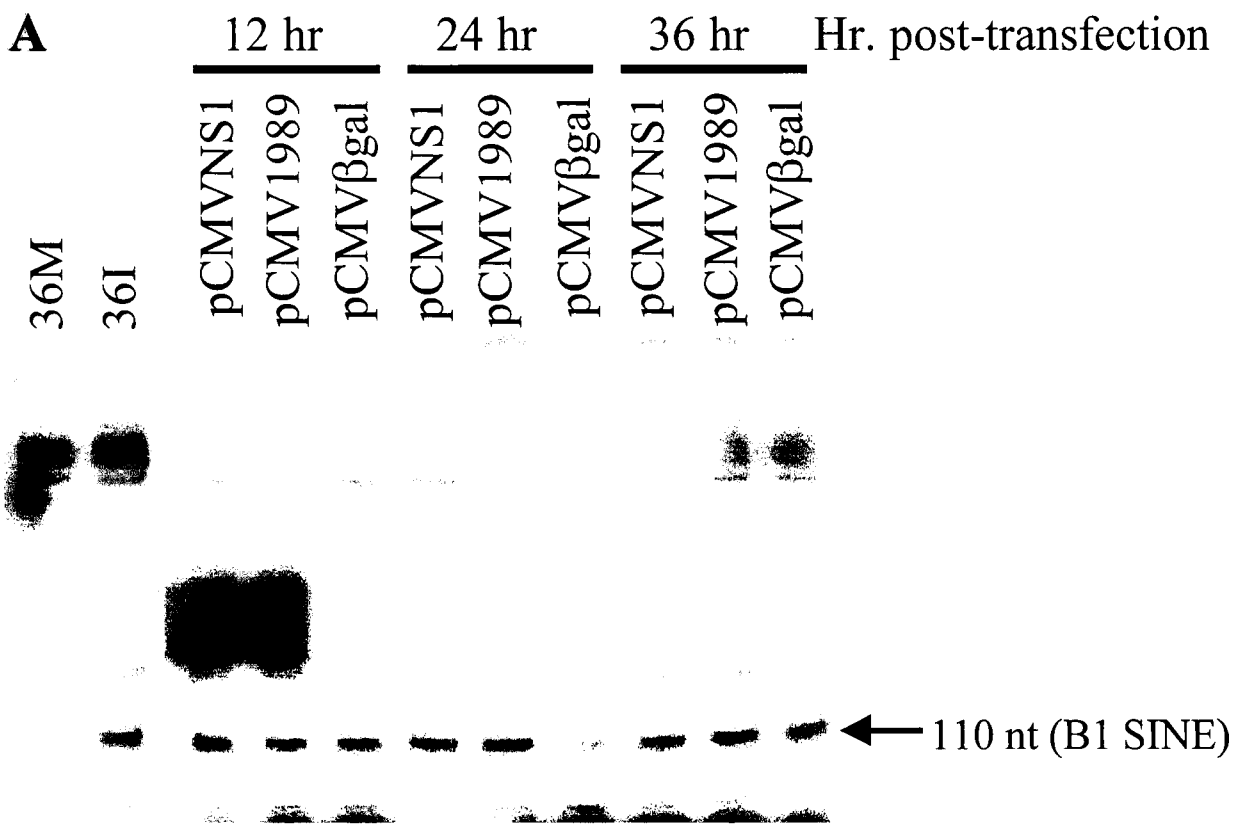

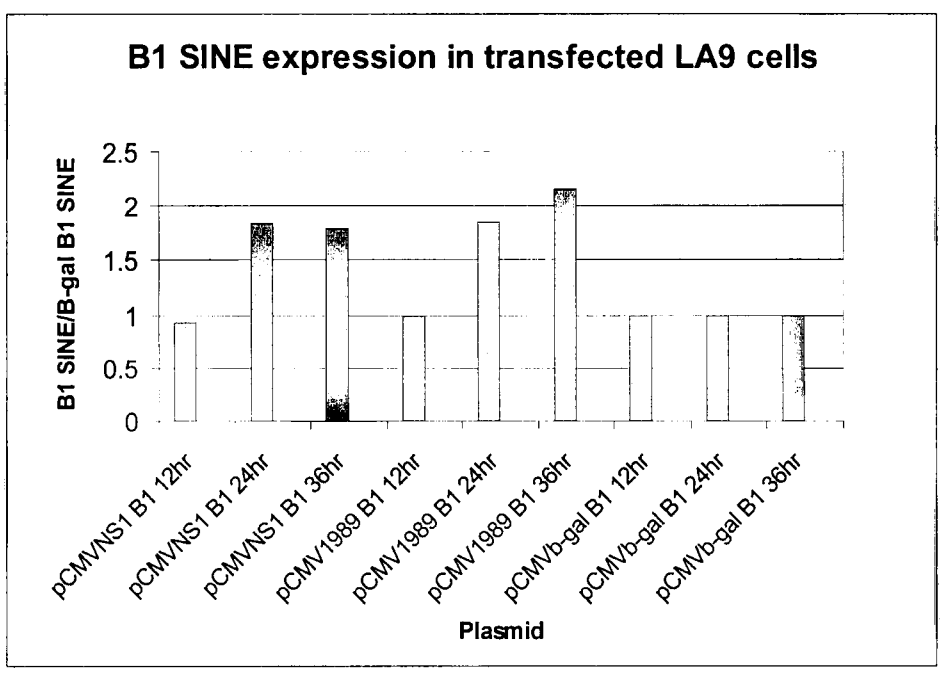

Figure 31: Legend on next page

Plasmid	Expresses
pCMVNS1:	NS-1 & NS-2
pCMV1989:	NS-1
pCMVβgal:	β-galactasidase

Figure 31: Effect of MVM NS1 on B1 SINE expression. **A:** 5% acrylamide gel containing the products of B1 SINE primer extension from LA9 cells transfected with plasmids expressing NS1, NS1/NS2 or β-galactasidase at various times post-transfection. 36M: Mock-infected unsynchronized LA9 cells 36 hours. 36I: MVM-infected unsynchronized cells 36 hours post infection. **B:** Radiometric analysis of the 110 nt band in **A**. Data are expressed as fold change compared to the β-galactasidase control.

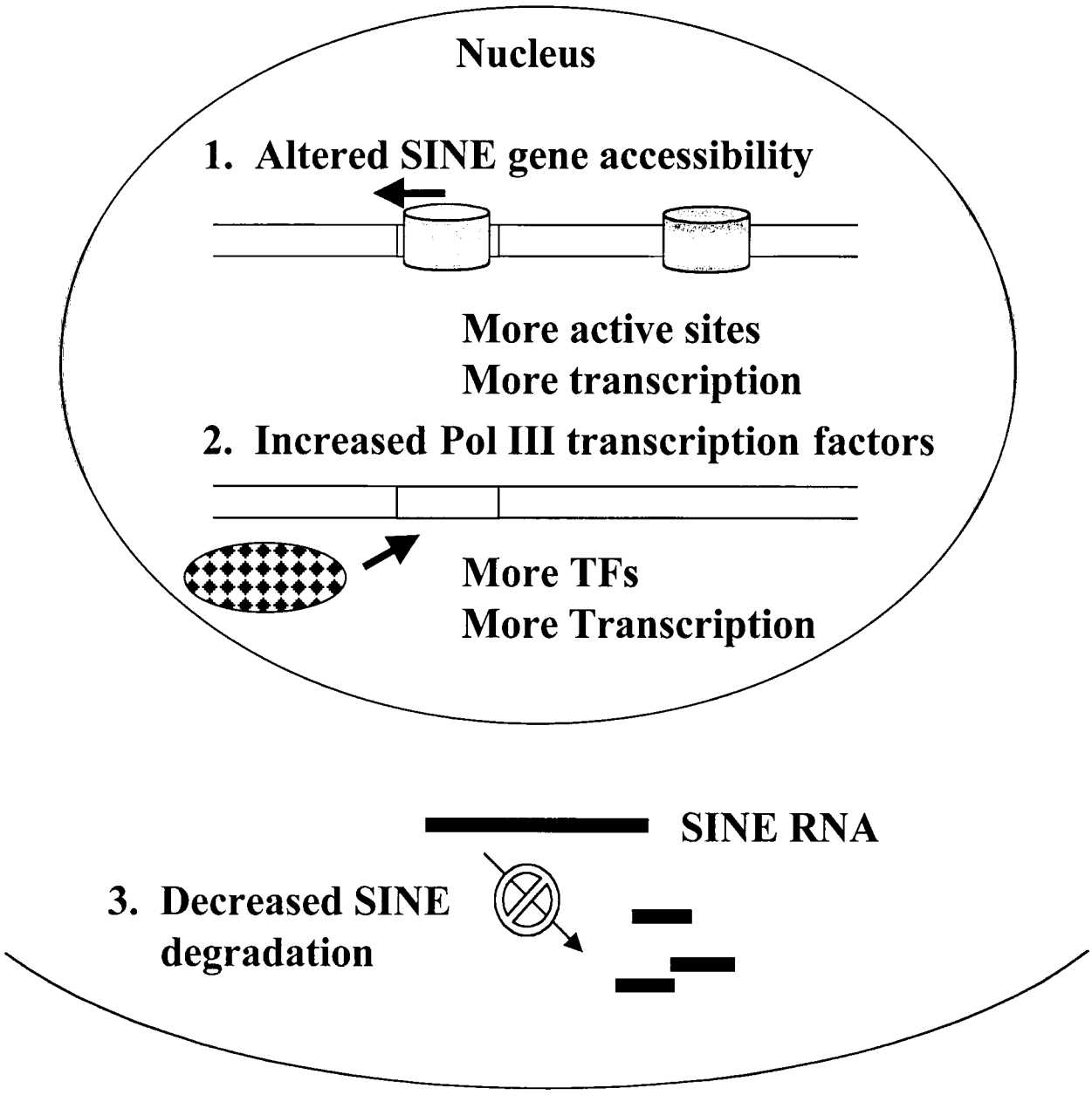

Figure 32: Methods of increasing SINE abundance: A: Increasing transcription by either altering the SINE genes so transcription can take place or by increasing the abundance of the polymerase III transcription factors. B: Decreasing degradation of the SINE transcripts.

levels of TFIIIC220 and TFIIIC110 [142]. Adenovirus infection has also been shown to cause up-regulation of TFIIIC110 in HeLa cells [143]. To determine if this could explain the increase in abundance of the SINE transcripts in MVM infected LA9 fibroblast cells, expression of TFIIIC220 and TFIIIC110 proteins (see introduction for review of these proteins) was examined. Western blots of both mock-infected and infected unsynchronized protein time courses were probed with Ab 2/anti TFIIICα (anti-TFIIIC220, a gift from Dr. Arnold Berk; [144]) and 4286-4 (anti-TFIIIC110, a gift from Dr. Robert White), as shown in Figures 33 and 34. TFIIIC220 appeared to decrease but only at late time points post-infection. This may be due to general protein degradation occurring at these time points. TFIIIC110 did not appear to change during infection (the apparent decrease in TFIIIC110 expression at 30 and 36 hours is due to loading variation). The interesting band at 66 kDa (Figure 34) that appears to increase as infection progresses is unknown, although its size is close to the major viral coat protein of MVM, VP2.

These results suggest that SINE up-regulation is likely not due to an increase in the basal RNA polymerase III transcription factors TFIIIC220 or TFIIIC110. However, I cannot rule out up-regulation of other polymerase III transcription factors. The literature suggests that TFIIIC110 and TFIIIC220 play crucial roles in transcription and are up-regulated by several viruses and as a result of cell transformation [142-147].

Transcriptional up-regulation of B1 and B2 SINEs remains unresolved

To determine if the increase in SINE levels in MVMp-infected mouse fibroblasts was due to increased transcription, nuclear run-on experiments were undertaken. This

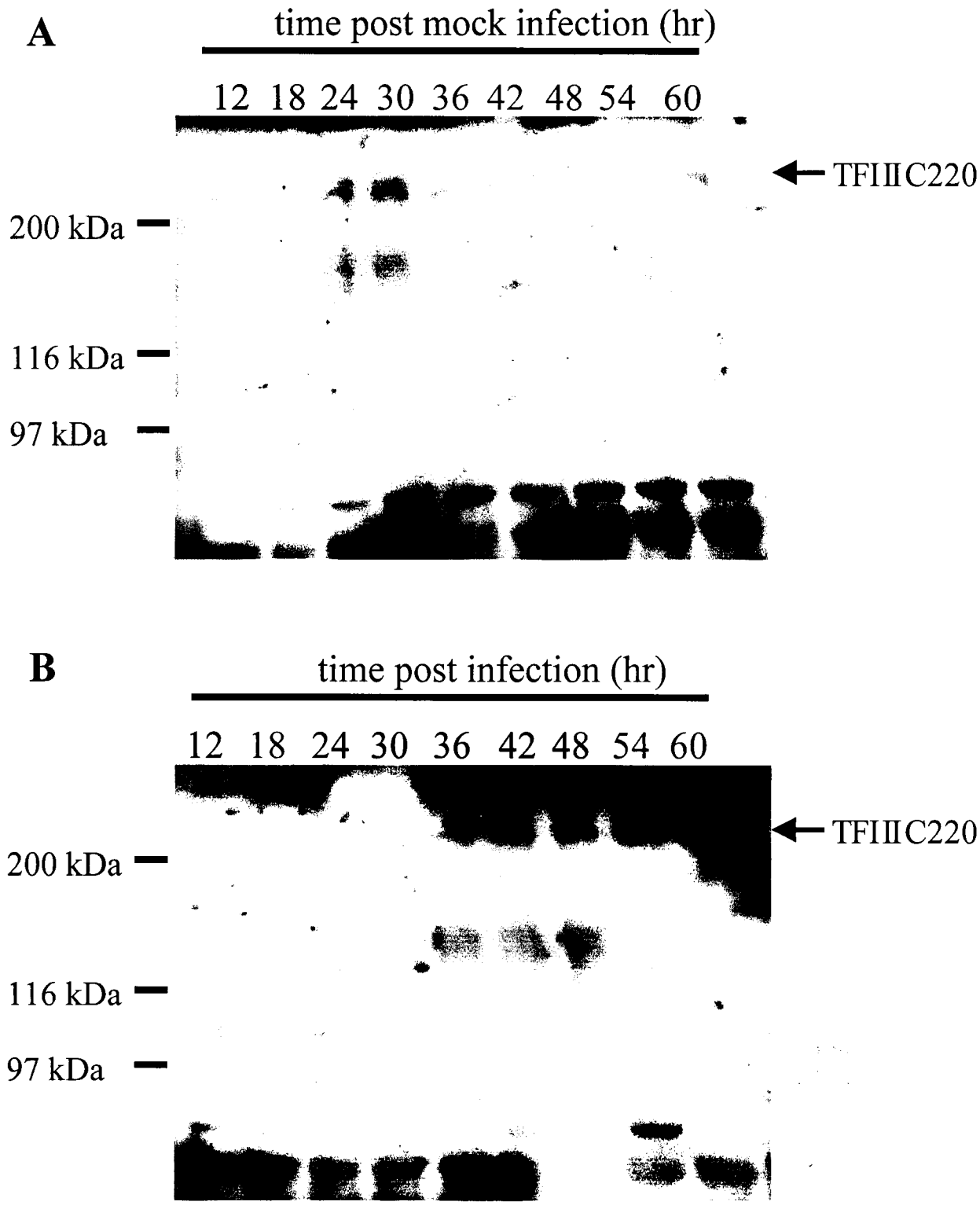

Figure 33: Levels of TFIIIC220 protein during MVM infection. **A:** Western blot of total protein from unsynchronized uninfected LA9 cells harvested at increasing times after a mock infection probed with anti-TFIIIC220 (Ab2/anti TFIIICα, REF). **B:** Western blot of total protein from unsynchronized MVM-infected LA9 cells at increasing times after MVMp infection probed with anti-TFIIIC220. Protein concentration was determined by BCA assay. See Materials and Methods section 17.

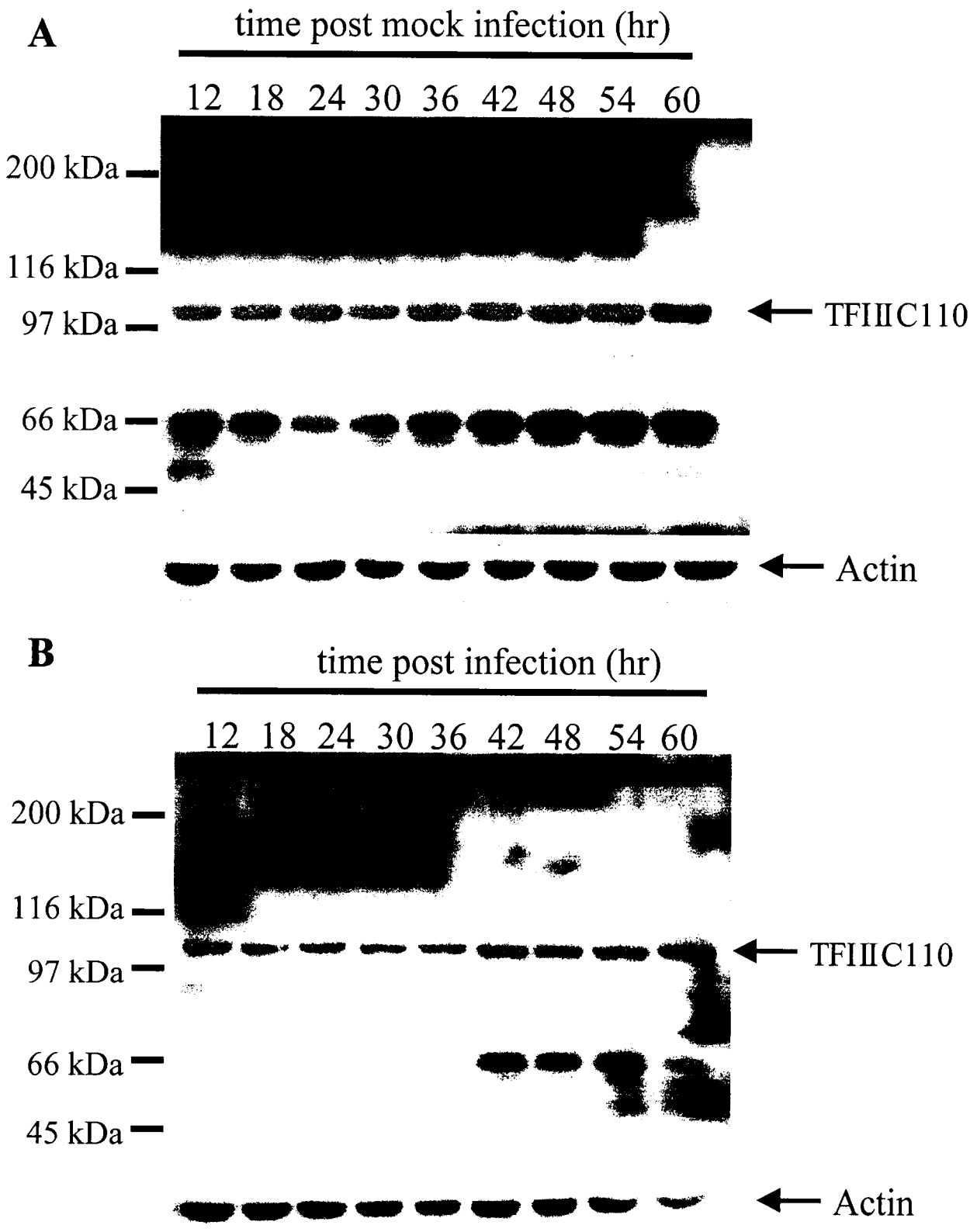

Figure 34: Levels of TFIIIC110 protein during MVM infection. **A:** Western blot of total protein from unsynchronized uninfected LA9 cells harvested at increasing times after a mock-infection probed with anti-TFIIIC110 (4286-4, REF). **B:** Western blot of total protein from unsynchronized MVM-infected LA9 cells at increasing times after MVMp infection probed with anti-TFIIIC110. Actin is provided as a loading control. Protein concentration was determined by BCA assay. See Materials and Methods section 17.

involves isolating nuclei, incubating them with radiolabelled α-^{32}P UTP at 30°C for 30 minutes, isolating the radiolabelled RNA and using this RNA to probe a dot blot containing the target sequences of interest. During the 30-minute incubation, only actively synthesized RNA will incorporate the radiolabel, resulting in a radioactive probe of only newly synthesized RNA.

Nuclei from mock or MVMp-infected mouse fibroblast cells at 36 hours post-infection were isolated via a detergent lysis method and stored in liquid nitrogen until needed. The nuclear run-on incubation was described as above, and the resulting RNA was used to probe dot blots on which were spotted plasmids containing B1 & B2 SINE, MVM NS1, 5S, tRNA, or actin DNA. Although the nuclear run-on experiments and subsequent dot blots were shown to give sufficient signal for quantitation (Figure 35), RNA polymerase II transcription was not blocked by addition of α-amanitin (during the 30 minute incubation) at various concentrations (data not shown) as determined by the presence of RNA polymerase II transcribed MVMp NS1 mRNA. As RNA polymerase II transcripts can contain embedded B1 and B2 SINEs, this creates a large background that prevents accurate quantification of the RNA polymerase III-derived SINE transcripts. Because I was unable to block in RNA polymerase II transcription, no conclusions regarding upregulation of B1 and B2 SINE transcription can be drawn. This is examined further in the discussion.

5. Kinase expression Analysis

As a side project related to beginning to understand the host cell response to MVM infections, I also investigated the protein levels of a series of different cellular kinases

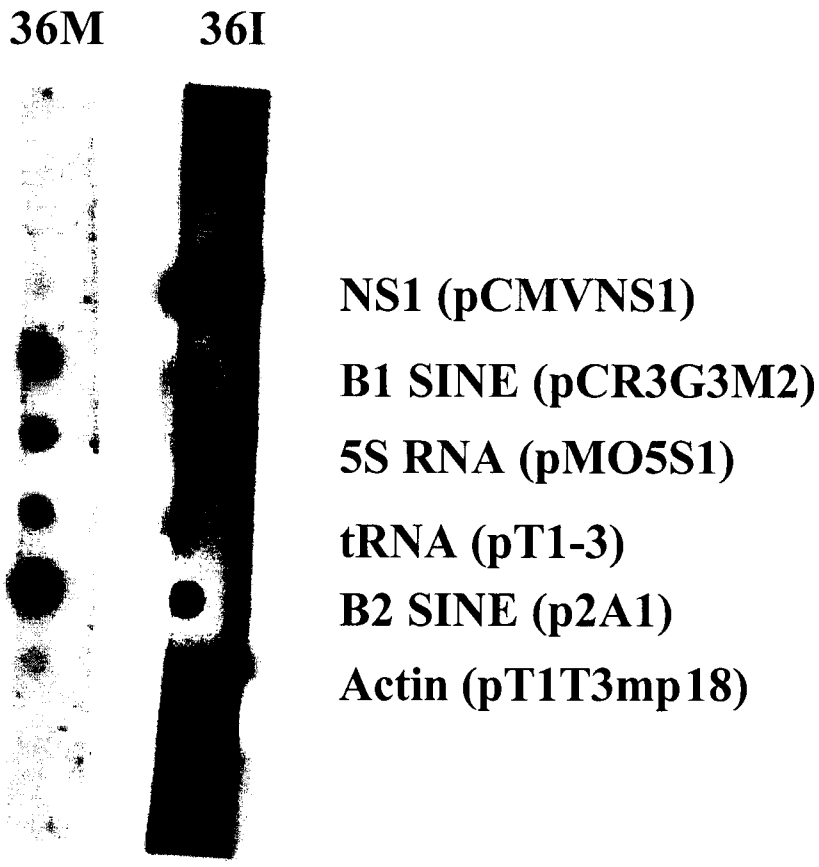

Figure 35: Assay of B1/B2 SINE expression by nuclear run-on. Dot blots were probed with radiolabelled RNA isolated from nuclei incubated with α ^{32}P UTP but without α-amanitin. 36M: Mock-infected unsynchronized LA9 cells 36 hours post treatment; 36I: MVMp-infected unsynchronized LA9 cells 36 hours post-infection. See Materials and Methods section 22

using a protein kinase screening method available from Kinexus. This is a fee-based service that takes a protein sample and conducts a series of western blots using antibodies to 75 protein kinases (see Appendix 4 for a full list of kinases examined). These results are then visualized with a digital camera.

As described in Materials and Methods, protein samples were prepared from synchronized mock and infected LA9 cells at 24 hours post-block and submitted to Kinexus for analysis. Figure 36 shows the resulting western blots, where each lane represents a protein sample probed with two to three different antibodies. By comparing the mock and infected blots, changes in kinase expression can be ascertained. Seven bands that showed altered expression were identified.

Quantification data for each band were obtained and analyzed as described. First, a global background was calculated and subtracted from each signal. Next, the infected signals were normalized to the mock-infected signals. A normalization factor of 1.6 was determined based on the top ten highest signals in both the blots as shown below:

$$\Sigma(\text{Top 10 mock infected signals})/\Sigma(\text{Same 10 infected signals})$$

Infected signals were normalized to the mock-infected signals by multiplying by this value. Finally, the infected/mock-infected ratio was calculated, and is shown in Figure 36 for each of the bands indicated. Candidate bands and their identification were determined in consultation with Dr. Steven Pelech. Kinexus considers a 2-fold change as being significant.

To confirm the results seen in Figure 36, I repeated the western blots on all seven of the altered kinases using the protein samples that were submitted to Kinexus (see

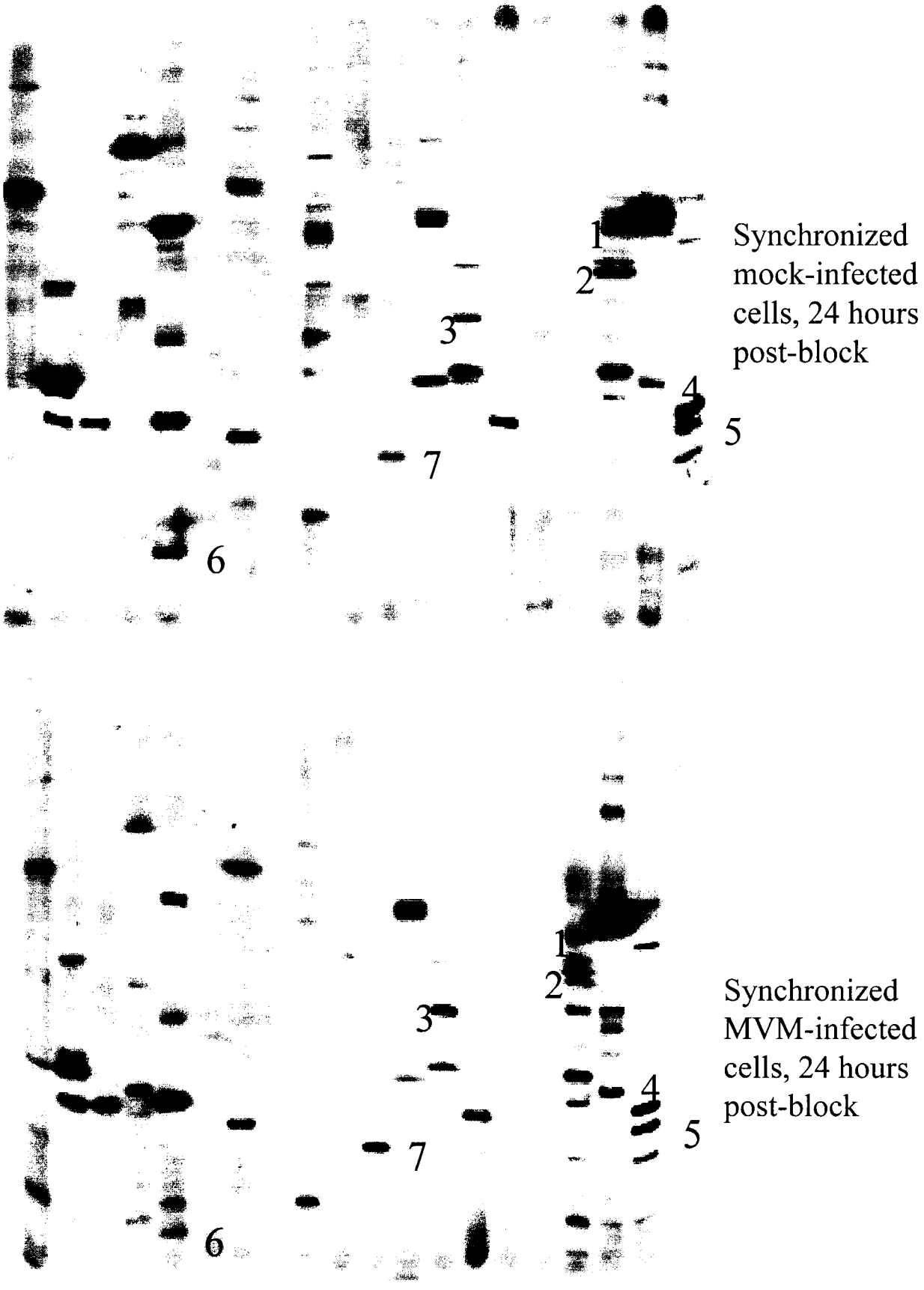

Figure 36: Legend on next page

1. p90 S6K (2.2x U)
2. S6K p70 (1.7x D)
3. Unclassified (2.3x U)
4. Unclassified (2.8x U)
5. CKII α' (1.9x U)
6. Cdk5 (2.3x D)
7. Mos (1.8x U)

Figure 36: Kinexus's protein kinase screen for mock and MVM-infected synchronized LA9 cells 24 hours post-block. Numbers indicate bands that showed altered expression upon MVM infection. Values represent the fold change (infected/mock) as a result of infection. U: Up-regulated. D: Down-regulated. The unclassified band three was recognized by PAK-α antibody and unclassified band four was recognized by Rsk1 antibody. Infected values were multiplied by 1.6 to normalize to infected values.

appendix 3 for antibodies and expected protein sizes). The resulting western blots are shown in Figure 37. Four of the proteins analyzed were confirmed to display altered expression during infection. These were Ribsosomal protein S6 kinase p70 (S6Kp70) and p90 (S6Kp90), unclassified band #3, and unclassified band #4. Of the remaining three proteins, one (cyclin-dependent kinase 5) could not be detected by the western blot and two, Casein kinase II α' and MOS kinase, did not appear to change upon infection.

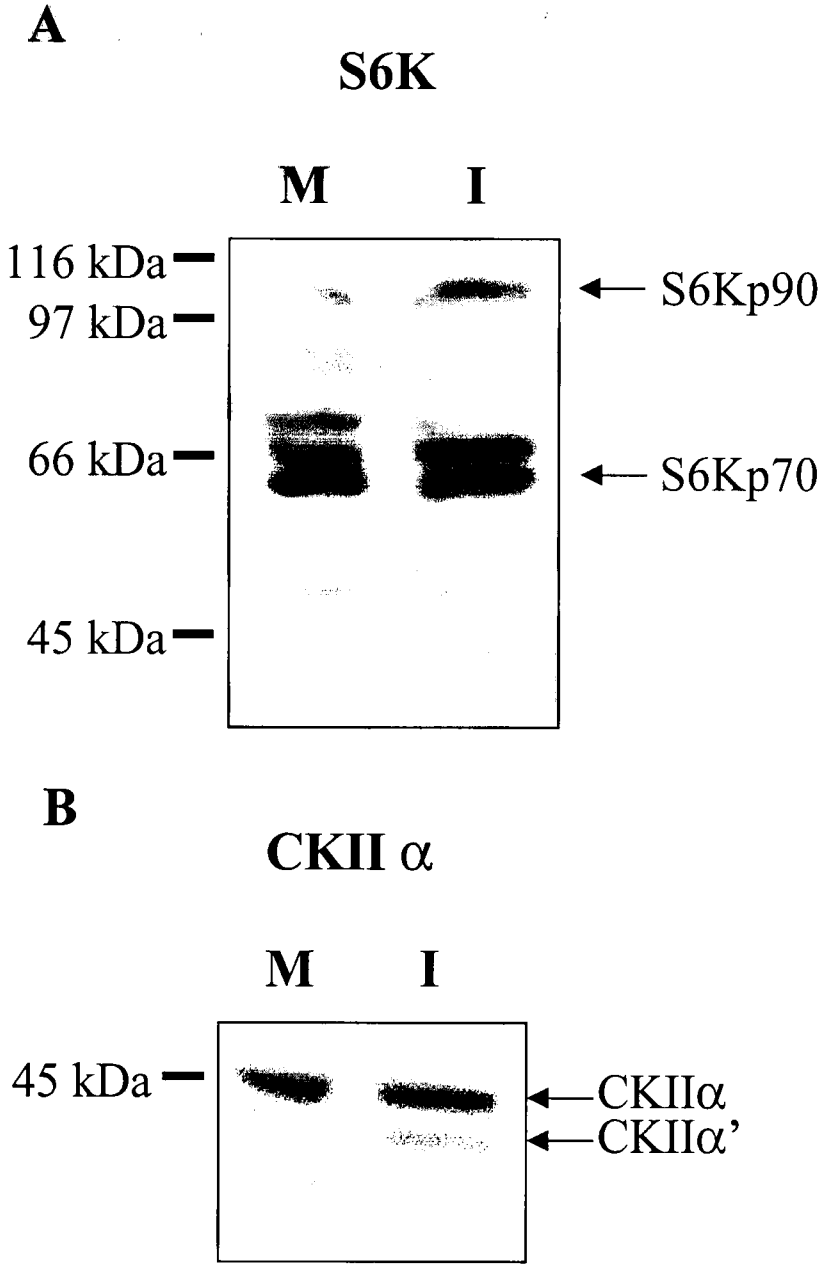

Figure 37: Confirming Kinexus's protein kinase screen. Western blots of the same protein samples used in Figure 25 probed with: **A.** Anti-S6K (Santa Cruz) which detects S6Kp70 (triplet of bands around 70 kDa) and S6Kp90 (90 kDa). **B.** Anti-CKII (Gift from Dr. Steve Pelech) which detects CKIIα and α'. M: Mock-infected synchronized LA9 cells, 24 hours post-block; I: MVM-infected LA9 cells, 24 hours post-block.

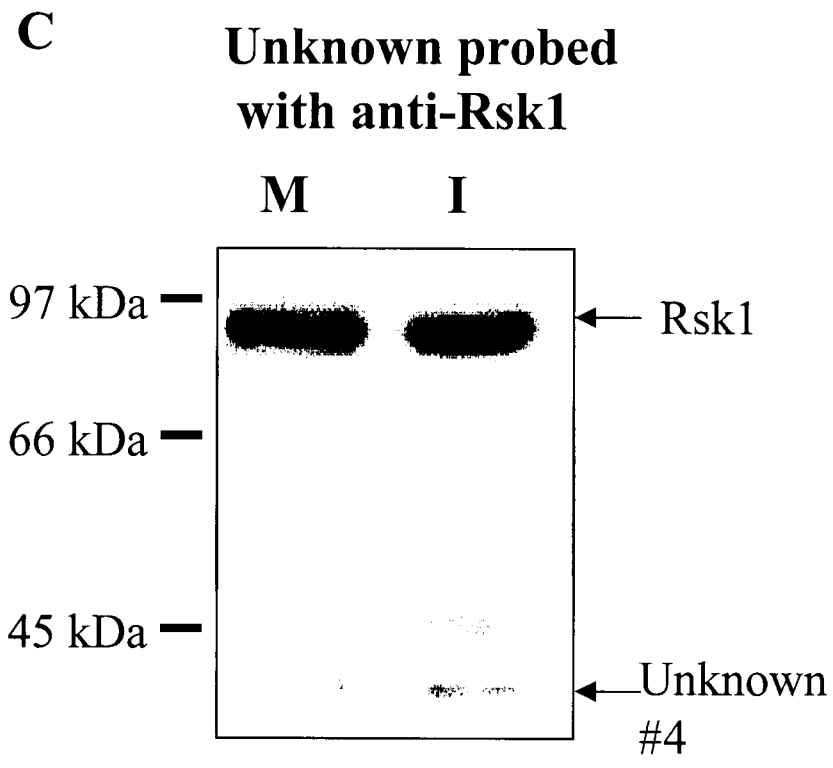

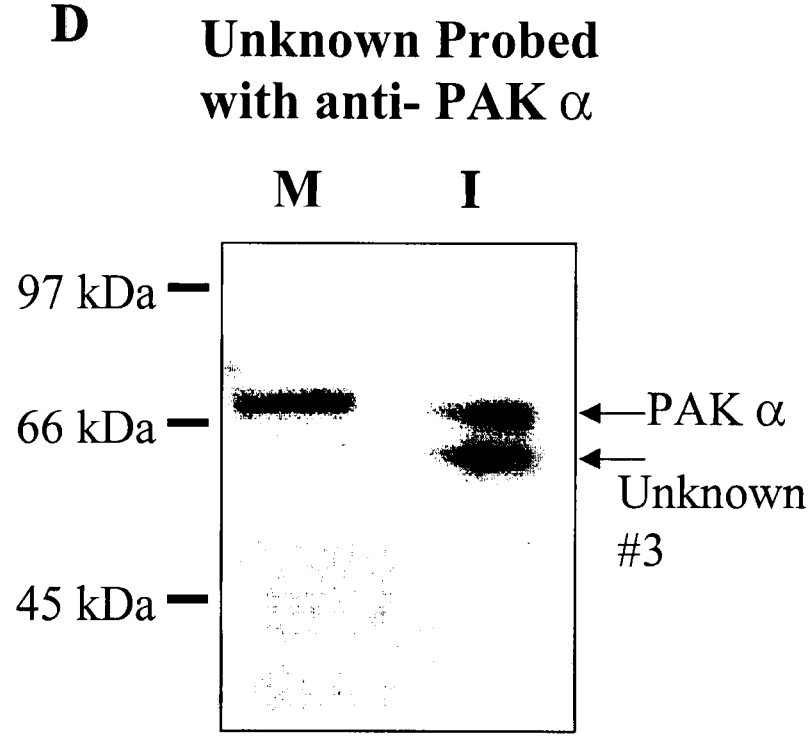

Figure 37 continued: **C.** Anti-Rsk1 (Santa Cruz) which detects Rsk1 (90 kDa) and the unknown band #4 in Figure 25. **D.** Anti-PAK which detects PAK (70 kDa) and the unknown band #3 in figure 25. M: Mock-infected synchronized LA9 cells, 24 hours post-block; I: MVM-infected LA9 cells, 24 hours post-block.

Discussion:

The goal of this project was to further characterize viral/host interactions by examining changes in gene expression in the mouse fibroblast cell line LA9 infected with MVMp. MVMp is cytotoxic to LA9 cells, resulting in cell death three days after infection (Figure 5). It is hoped that these initial studies would aid in the understanding on how MVM, and possibly other parvoviruses, causes cytopathic effects in cells.

Differential Display

At the beginning of these studies, the differential display technique (see Results page 49 for an explanation of the technique), one of the standard methods for identifying genes that changed expression [148-151], had been used to study expression changes in cells infected with human papillomaviruses [152], cytomegalovirus [153], herpes simplex virus 1 [154], and human immunodeficiency virus [155] [156]. In most cases, viral infection led to alteration in expression levels of large numbers of host cell genes and it was expected that MVMp infection of mouse fibroblast LA9 cells would do the same, however, the MVM genome is much smaller than most other viral genomes.

Before starting a large-scale screen examining MVM infection of mouse fibroblasts, I first tested the differential display technique. Human embryo kidney 293 cells were infected with adenovirus and screened by differential display RT/PCR using as an arbitrary primer that could recognize an adenovirus transcript. One strongly altered band was detected (data not shown) and confirmed to correspond to the adenovirus type 5 fibre protein gene. A second test was conducted on MVM-infected LA9 mouse fibroblasts, with the RT/PCR screen using an arbitrary primer specific to MVM NS1

(data not shown). Again the screen successfully detected the NS1 transcript as an altered RNA during infection. Together, these two tests confirmed that the differential display technique in my hands could be used to identify altered transcript abundance during viral infection.

The main differential display screen examined unsynchronized mouse fibroblast cells (LA9) infected with MVMp at 12, 24, and 36 hours post-infection compared with uninfected mouse fibroblast cells. These time points were chosen to examine changes in transcription early in infection before the virus was actively replicating in most cells (12 h time point) and during the initial stages of replication occurring as the cells reach and arrest in S phase (24 and 36 hour time points). A total of 24 primer pairs was used, representing approximately 15% of the actively transcribed RNA within the cell [137]. Table 2 shows the results of this screen, summarizing the various altered bands that were detected. All of the confirmed altered bands were found to be up regulated in response to infection, although some care should be taken in interpreting this statement, as these bands were comprised of retroposons and viral transcripts.

Three key observations can be made from these results. First, few (if any normal) genes were found to be altered as a result of MVMp infection. Second, the MVM NS1 transcript was detected multiple times, again confirming that the technique could detect transcripts of altered abundance. Finally, the majority of confirmed altered transcripts contained repetitive elements, including the B1 & B2 SINEs and the L1 LINE.

Although the low number of altered bands and confirmed altered genes is not unprecedented since a similar screen with Coxsackievirus-infected mouse heart tissue identified 5 altered genes [157], it was surprising given the pathogenic nature of MVM

towards these cells. The low number of detected altered genes could be due to the high stringency in selecting bands to be studied, difficulties with reproducibility, false positives and downstream cloning, or it could be that MVM infection simply does not cause large changes in host gene expression. This last possibility should be viewed with caution. Only a small portion of the transcriptome was analyzed and only early times post-infection were examined.

The repeated detection of the NS1 mRNA further confirmed that the screen was indeed detecting altered levels of transcripts. It was interesting that in both cases, PCR amplification did not occur at the 3' end of the transcript, but rather towards the 5' end at polyA rich sequences. These internal amplifications during differential display are an added benefit as they further increase the number of transcripts screened. However it does emphasize the unreliability of the technique as the 3' end of the transcript was not detected.

The majority of altered transcripts detected in the differential display screen were transposable elements comprising the B1 and B2 SINEs and the L1 LINE. Fragments of SINEs and LINEs can be found in the 3' untranslated region of some mRNAs, so the sequences detected in the screen could be of this origin. It is clear, however, that both B1 and B2 SINEs and the L1 LINE transcripts increase upon infection (Figures 15, 28, & 29). This is not the first differential display screen to detect repetitive elements. Differential display has detected L1 LINEs [158], Alus [159], and endogenous retroviral-like elements [160]. Furthermore, other viruses, discussed in more detail below, up-regulate SINEs, specifically the Alu element.

Changes in gene expression in response to MVMp infection as detected by Clontech cDNA arrays:

The inherent difficulties in screening altered transcripts (in MVMp infected mouse fibroblast cells) through differential display resulted in the decision to use arrays for further screening experiments. At the time of these experiments, there were few mouse arrays available and most were very expensive. Based on limited choices, Clontech's cDNA macroarrays were chosen. These contain approximately 1000 genes in single spot orientation. To further increase my chances of detecting altered patterns of expression, the mouse fibroblast cells being screened were synchronized, so that all MVM-infected cells would enter S phase and begin viral replication at the same time. Three different conditions were examined: Mock and MVM-infected synchronized mouse fibroblast cells at 12 or 24 hours post-block, or mock and MVM-infected unsynchronized mouse fibroblast cells at 36 hours post-infection (to compare with the synchronized cells).

Overall, there were two weaknesses with these arrays: First, the signal strength was low, with only approximately 100 spots per array above the signal threshold cut off and many of these were on the low end. Second, the arrays were prone to high background, both in the form of small random background dots, making spot identification difficult, and in some cases, much larger sploches, covering larger sections of the membrane. The latter was due to the two ends of the array overlapping each other during hybridization in the hybridization oven, resulting in the loss of data from the overlapped areas. This was corrected in later experiments.

Infected synchronized cells at 12 hours post-block showed very few changes in gene expression with most of the detectable genes clustering around an infected/mock ratio of one (Figure 21). Only three mRNA were observed to change in abundance (all increased) and none of these changes were sustained at the 24 hour time point. The low number of altered transcripts at this point is not surprising, as virus is not actively replicating at this point.

Infected synchronized cells at 24 hours post-block, by contrast, showed more changes in transcription. Of the approximately 90 detectable transcripts, 7 appeared to change reproducibly in the two replicates done. Another 7 transcripts were detected as altered in one array set but were not in the other (Table 3). These included genes involved in cell cycle, and transcription. The two replicates were fairly reproducible for transcripts with signals above 1000 (Figure 23).

Interestingly, infected unsynchronized cells at 36 hours post-infection, also showed altered transcription, but in a different pattern. Many of the cell cycle genes altered in synchronized cells were not altered in unsynchronized cells or demonstrated different expression patterns (for example cyclin D1, which was down-regulated in synchronized cells but up-regulated in unsynchronized cells). This was not too surprising as synchronized cells are all in the same stage of the cell cycle, whereas unsynchronized cells are not. Transcripts from three genes (ALY/RFBP1, Transcription termination factor/TTF, and mitogen & stress activated protein kinase 2) appeared to change in abundance in both synchronized and unsynchronized cells. Northern blot analysis was done with either transcription termination factor or RAN-GAP (a transcript that did not change in expression in any of the arrays) probes, as both had high signals in both the

mock and infected arrays. In both cases, the Northern blot data confirmed the changes (or lack of changes) identified in the array; however, the transcript band detected in the northern blot for TTF was much smaller than expected, and was due to the TTF transcript containing a B2 SINE. Subsequent communication with Clontech confirmed that the TTF transcript did indeed contain B2 SINE sequence (confirming nicely the results seen in differential display). The B2 SINE transcripts was probably what was altered during transfection, as I was unable to detect the correct sized TTF transcript (Figure 24b).

In conclusion, the data obtained with the Clontech array indicated that very few transcripts change in abundance early in infection, although more transcripts change as infection progresses. Problems with low signals and background made detection and confirmation difficult. These arrays also confirmed that B2 SINE transcripts increased during MVM infection.

SINE expression during MVM infection

The increase in SINE transcription, as detected by two different screening techniques, led me to focus my investigations on transcription of SINEs and their role in MVM infection. Initial experiments confirmed that the apparent increase in the number of SINE transcripts was due to RNA polymerase III transcription and not due to contaminating DNA or fragmented SINE-containing RNA polymerase II transcripts.

SINE transcripts are up regulated in a variety of conditions, usually associated with cell stress. These include heat shock (Alu, B1 & B2 SINES) [161, 162], ethanol treatment (B1 & B2 SINES) [162], cyclohexamide treatment (Alu SINE) [161], DNA damaging agents such as cisplatin, etoposide, and γ-irradiation (Alu SINE) [159], as a result of cell transformation by SV-40 virus (B2 SINE) [141] and by viral infection

including adenovirus infection (Alu SINE) [163], herpes simplex virus (HSV) infection (Alu SINE) [164], and HIV infection [146]. To my knowledge, the increased B1 and B2 SINE expression during MVMp infection is the first example of viral infection altering murine SINEs. It would be interesting to know whether MVMi infected lymphocytes or other parvovirus-mediated infections, such as B19, AAV, or CPV, can also cause an increase in SINE expression.

Theoretically, SINE transcript levels can be increased in one of two ways (Figure 32): Either SINE transcription is increased (options one and two) or SINE transcript degradation is decreased (option 3). In all of the viruses studied thus far, SINE induction has always been due to increased transcription [146, 147, 163]. To determine if the increase in B1 and B2 SINE transcripts was due to increased transcription, nuclear run-on (NRO) studies were undertaken to measure the amount of newly synthesized RNA in MVM infected cells. Although this technique was shown to work, RNA polymerase II transcription could not be blocked by addition of α-amanitin at concentrations ranging from 5 to 25 μg/ml. As RNA polymerase II transcripts can contain embedded B1 and B2 SINEs, this creates a large background that prevents accurate quantification of the RNA polymerase III derived SINE transcripts. It is currently unclear why α-amanitin was unable to block RNA polymerase II transcription, as the drug was present at the right concentration (concentration was checked spectrally and increasing the concentration of the drug to 25 μg/ml had no effect. One hypothesis is that the drug failed to enter the nuclei. This may be due to debris surrounding the nucleus, preventing uptake. Isolating nuclei for these experiments is not trivial, as the nuclei should be free from debris and yet not be damaged such that the contents can leak out. Alternatives methods of isolating

nuclei (like dounce homogenization/sucrose gradient separation) could be attempted to get around this issue.

It seems unlikely that the increase in SINEs in response to MVM infection is due to decreased degradation. Due to the unique location of each integrated SINE and the lack of a RNA polymerase III termination signal, each SINE transcript has a unique 3' end, which will influence RNA stability. Any method of affecting SINE degradation would have to affect each individual SINE transcript. Furthermore, the decrease in degradation would have to affect B1 SINEs, B2 SINEs, and L1 LINEs equally and yet not global RNA levels (total cellular RNA does not increase with infection, W. Williams, unpublished observations, data not shown). However, without data indicating an increase in transcription, decreased RNA degradation cannot be ruled out.

One potential method of increasing polymerase III transcription is to increase the basal RNA polymerase III transcription factors. This occurs during HSV infection [164], HIV infection [146], and adenovirus infection [143] (although increasing RNA transcription factors only during adenovirus infection is not sufficient for SINE up-regulation [165] and in cells transformed with large T antigen [142]. Specifically, transcription factor TFIIIC activity was increased and in some cases this was due to increased expression of TFIIIC110 and TFIIIC220 component proteins. These proteins are essential for RNA polymerase III type II promoter activation (see introduction for more details). I used antibodies obtained from Dr Robert White and Dr. Arnold Berk to measure expression levels of the TFIIIC110 and TFIIIC220 proteins. Levels of neither protein were altered as a result of MVMp infection (Figure 33 & 34), suggesting that increasing RNA polymerase transcription factors may not play a role in MVM altered

SINE expression. However, this does not rule out the possibility of altered expression of other TFIIIC or TFIIIB proteins.

Chromatin rearrangement can also mediate increased SINE expression presumably by exposing new SINE promoter sites for transcription and thus releasing SINE transcriptional repression. Increased chromatin accessibility on Alu SINE, alpha satellite DNA, and L1 LINE has recently been demonstrated in heat-shocked HeLa cells [166]. Increased SINE expression in adenovirus-infected HeLa cells is also thought to occur by increased chromatin re-arrangement [165]. MVM infection causes DNA damage, which would be expected to cause changes in the chromatin structure. It is tempting to suggest that this could be the reason for increased SINE numbers during MVM infection. A chromatin re-arrangement assay (nuclease digestion of SINE containing chromatin) would be informative.

MVMp nonstructural protein NS1 alone can up-regulate B1 and B2 SINE (Figure 31). As NS1 is responsible for introducing DNA nicks in both the host and viral genome [91], it is tempting to speculate that this function could be responsible for SINE induction (as suggested above). Repeating mouse fibroblast transfection/primer extension experiments with an NS-1 nickase deficient mutant would be informative. It would also be interesting to determine if MVM structural protein VP1, which contains a phospholipase domain [90], also can induce increased SINE expression. The phospholipase domain could stimulate an inflammatory response which in turn could stimulate SINE expression.

The role(s) of SINEs within the cell is not fully understood. It is clear that SINE retroposition is a powerful mutational force. SINE integration can interrupt exons, alter

splicing, alter promoter activity, alter or add poly adenylation sites, and can cause sequence duplications and deletions through unequal homologous recombination [112, 167, 168]. Alu SINE integration can cause genetic disorders and cancer in humans with examples including hemophilia, B-cell lymphoma, Tay-Sachs disease, thalassemia, and Lesch-Nyhan syndrome [112]. What is not clear, however, is whether SINEs are selfish parasites or if they convey a benefit to the host (for example in a mechanism similar to adenovirus VAI RNA). Supporters of a beneficial role for SINEs argue that SINEs are up-regulated in a manner similar to the heat shock genes following hyperthermic shock [162], that the Alu SINE RNA can bind and antagonize PKR activation [169], and that the Alu, B1 and B2 SINEs can transiently stimulate translation of reporter constructs in a PKR-independent manner [170]. Furthermore, SINEs are found in G/C rich (gene rich) DNA whereas LINEs are found in A/T rich (gene poor) DNA [115, 116]. As SINEs and LINEs are believed to share the same integration mechanism, this suggests that there might be some sort of selective pressure on SINEs to remain in G/C rich DNA that is absent on the LINEs.

Likewise, the role of SINEs in MVMp infection is also unclear. The increase in B1 and B2 SINEs may simply be a consequence of viral perturbations to the host cell. As such, they could act as indicators of problems within the cell, for example chromatin re-arrangements or changes in RNA degradation. Alternatively, SINEs could be playing a protective function within the cell. SINEs could be maintaining protein synthesis by inactivating PKR. However, there have been no reports that MVM infection leads to activation of PKR or of host cell protein synthesis shutdown. SINEs could also potentially bind the major MVM nonstructural protein, NS1, sequestering it away from

the viral replication machinery. NS1 may not need to bind directly with SINE RNA as NS1 has been shown to bind cellular proteins that have RNA binding motifs [78]. Further understanding of the roles SINEs play within the host cell will be helpful in understanding their role in MVM infection.

Kinase Expression Analysis

The protein expression levels of some 75 protein kinases were examined in synchronized mock or MVMp-infected mouse fibroblast cells at 24 hours post block. Surprisingly, expression of only seven bands changed at least-two fold out of the over 70 kinases screened. Of these seven candidates, levels of only four were observed to change in a standard western blots using the same proteins samples as used in the initial screen. Two of the candidates were unknown proteins. The remaining two proteins were variants of S6 kinase. S6 kinase is known to phosphorylate ribosomal protein S6 amongst others. This promotes selective translation of certain mRNAs needed for cell replication from G1 to S. Down-regulation of S6 kinase, would suggest a block in cell proliferation in G1 whereas most of the microarray data suggest an increase in proliferation. These kinase experiments were undertaken to give an overview of the extent of perturbation of cellular protein kinases expression during MVM infection. While a few changes are seen, I decided not to pursue the kinase expression changes at this time, but rather focus on changes at the RNA expression level.

Changes in gene expression in response to MVM infection as detected by Affymetrix oligonucleotide microarrays:

Late into the writing of this thesis, an opportunity developed to study changes in mouse fibroblast gene expression in response to MVMp infection with Affymetrix's

oligonucleotide array. These results yielded a plethora of information and, although still preliminary, have begun to greatly enhance our understanding of MVM/host cell interactions. This section will focus on some of the preliminary findings of these results but should in no way considered to be exhaustive. The groupings seen below were made based on information gathered from the Affymetrix website, Genespring 6.0, and various review articles. More work will be needed to confirm these initial findings and to characterize them further (e.g., biological and technical replicates as well as RT-PCR confirmation). Not all of the altered genes are discussed below.

Mouse fibroblasts seem to induce a strong overall growth signal in response to MVMp infection (Table 5a). Multiple transcripts that are involved in promoting cell proliferation are up-regulated. These include transcripts encoding growth factors (epiregulin, nerve growth factor beta, and the chemokine oncogene GRO), a transcription factor (oncogene A-myb), and a protein involved in EGF signaling (Reps1). Epiregulin, an epidermal growth factor (EGF) like growth factor that can bind and activate the EGF receptor, showed a 14-fold increase as a result of MVMp infection. In contrast, transcripts that encode proteins that suppress cell proliferation are generally down-regulated. These include transcription factors (Mad, Nup1 p8), an interferon-induced protein (Interferon activated gene 202A, p202), and a protein without a known molecular function (Tob).

MVMp infection also appears to induce immune and inflammation responses in mouse fibroblast cells. Several cytokines and chemokines are up-regulated in response to infection (Table 5b). The immune response modulator transforming growth factor β cytokine (TGFβ) (the so called anti-cytokine) is down-regulated in response to infection.

A

Cell growth/anti growth	
Growth	
epiregulin	13.9 U
GRO1 oncogene	4 U
Myeloblastosis oncogene-like 1, A-myb	2.3 U
Nerve Growth Factor beta	2.1 U
RalBP1-associated EH domain protein Reps1	2 U
Vascular endothelial growth factor	2 D
Anti-growth	
Nuclear Protein 1, p8	3.3 D
Max-interacting transcriptional repressor (Mad4)	2.5 D
Transforming growth factor, beta induced, 68 kDa	2.5 D
Bone morphogenetic receptor for Bmp2 and Bmp4	2 D
Interferon activated gene 202	2 D
Tob family	2 D

B

Immune/Imflammatory	
Lymphocyte antigen 84, Interleukin 1 receptor-like 1	6.1 U
glucocortoid-regulated inflammatory prostaglandin G/H synthase	3 U
GRO1 oncogene	4 U
CD44 antigen (also involved in cell adhesion induced signalling)	2.8 U
Interleukin-4 receptor alpha	2.5 U
Small inducible cytokine A2	2.6 U
Small inducible cytokine A7	2.1 U
Transforming growth factor, beta induced, 68 kDa	2.5 D
Bone morphogenetic receptor for Bmp2 and Bmp4	2 D
Transcription factor GIF	2 D
Latent TGF beta binding protein	2.3 U

C

Transforming growth Factor	
Transforming growth factor, beta induced, 68 kDa	2.5 D
Bone morphogenetic receptor for Bmp2 and Bmp4	2 D
Transcription factor GIF	2 D
Latent TGF beta binding protein	2.3 U

Table 5: Grouping of altered genes detected by Affymetrix microarrays based on similar function or pathways. Table continues next page. U: Transcript is up-regulated in response to MVMp; D: Transcript is down-regulated in response to MVMp.

D

Transcription factors	
TEA domain family member 4	2.6 U
Autosomal Zinc finger protein group	2.5 U
Myeloblastosis oncogene-like 1	2.3 U
Enhancer Trap locus 1	5 D
D site albumin promoter binding protein (Dbp)	3.3 D
Nuclear Protein 1, p8 (probable TF)	3.3 D
CCAAT/enhancer binding protein (C/EBP)	2.5 D
Max-interacting transcriptional repressor (Mad4)	2.5 D
PPAR gamma coactivator (PGC-1)	2.5 D
basic-helix-loop-helix protein class B2	2.5 D
Chromobox homolog 4 (Drosophila Pc class)	2.5 D
Transcription factor GIF	2 D
Zn-15 transcription factor (zfp 292)	2 D
Ets-2	2 D

E

C/EBP & Dbp TFs	
CCAAT/enhancer binding protein (C/EBP)	2.5 D
D site albumin promoter binding protein (Dbp)	3.3 D
Nuclear Protein 1, p8	3.3 D
c-Cbl associated protein CAP	2 D
Stearoyl-coenzyme A desaturase 2	2 D

F

Cholesterol	
Farnesyl diphosphate sythetase	2 D
Mevalonate (diphospho) decarboxylase	2.5 D
ATP binding cassette sub-family A (ABC1) member 1	3.3 D

Table 5 continued. U: Transcript is up-regulated in response to MVMp; D: Transcript is down-regulated in response to MVMp.

Furthermore, its receptor (bone morphogenetic receptor for Bmp2 and Bmp4) and a transcription factor (GIF) that is activated by and enhances the effects of TGFβ are also down-regulated. In contrast, a protein (latent TGF beta binding protein) that binds the latent form of TGFβ and down-regulates its activity is up-regulated. Together, these results suggest a multi-pronged approach to down-regulate TGFβ activity (Table 5c). TGFβ is also involved in suppressing cell proliferation, so down-regulation of TGFβ agrees with the observations made in the previous paragraph.

Expression of many transcription factors is altered during MVM infection of mouse fibroblasts (Table 5d). The majority of the transcription factors appear to be down regulated. In the case of the down-regulated transcription factor C/EBP β, and the related transcription factor Dbl, three genes (Nuclear protein 1 p8, c-cbl associated protein CAP, and Stearoyl-coenzyme A desaturase 2) under the control of these factors were also down regulated (table 5e). C/EBP β and Dbl are involved in cell differentiation, cell proliferation, inflammation, and metabolism specifically in hepatocytes, adipocytes and haematopoietic cells [171].

Interestingly, MVM infection also seemed to alter genes involved in both cholesterol synthesis and transport (ATP binding cassette sub-family A member 1) as listed in Table 5f. What potential role cholesterol synthesis and transport plays in infection remains unclear.

Finally, there are 24 EST sequences that remain to be identified and characterized (Table 4) with respect to MVM infection.

Future work would also focus on both confirming altered gene expression by northern blot analysis, semi-quantitative PCR and primer extension analysis. The arrays

must be repeated, possibly with flanking time points (perhaps 24 and 48 hours post MVM infection). It would also be interesting to repeat the array studies with MVMi in a lymphocytic cell line to try and determine key transcription alterations. Array studies on cells fibroblast cells expressing just MVM's non-structural protein NS1 or just the capsid protein VP1 (to determine what role the phospholipase active site has on inflammation) would also be informative.

Comparing the two types of arrays

Table 6 lists the gene that were altered by MVM infection in unsynchronized LA9 cells at 36 hr P.I. as detected by Clontech macroarray. Also listed are the values found for the same genes in the Affymetrix oligonucleotide array. Interestingly, there is not perfect agreement between the two. Genes that did not show altered expression in response to MVM infection in the macroarray generally demonstrated the same trend in the oligonucleotide microarray (for example cyclin-depndent kinase regulatory subunit 2). Genes that were altered in the cDNA macroarray, however, often were not predicted to be altered in the oligonucleotide array (for example calmodulin and RNA exchange factor binding protein one). The possible reasons for these discrepancies may lie in the different nature of the two arrays. The Clontech macroarray has each gene represented by one cDNA spot whereas the Affymetrix oligonucleotide array has each gene represented by at least 16 different oligonucleotides scattered throughout the chip. Therefore the oligonucleotide array system allows a better averaging of the signal from any one specific gene. Furthermore the oligonucleotide arrays also has a mis-match oligonucleotide for every perfect oligonucleotide, allowing a measurement of the specific background to each sequence. The macroarray system lacks mis-match probes and as

Macrorray IV Unsync 36I/36M	Microarray Unsync 36I/36M	Gene Identity
22.68	1.31	transcriptional coactivator of AML-1 & LEF-1 (ALY)
LS	1.00	G2/M-specific cyclin B2 (CCNB2; CYCB2)
1.72	1.52	G1/S-specific cyclin D1 (CCND1; CYL-1)
LS	1.15	G1/S-specific cyclin D3 (CCND3; CYL3)
0.87	0.93	Cyclin-dependent kinases regulatory subunit 2 (CKS-2)
0.49	0.54	p19ink4; cdk4 and cdk6 inhibitor
1.28	1.00	defender against cell death 1 (DAD1)
2.34	1.00	tyrosine-protein kinase ryk precursor; kinase vik; nyk-R
2.97	LS	presynaptic density protein 95 (PSD-95)
3.92	LS	PAR4; protease-activated receptor 4 G protein-coupled receptor; thrombin receptor
0.43	LS	retinoic acid receptor gamma-A (RAR-gamma-A; RARG)
0.86	1.15	retinoid X receptor alpha (RXR-alpha; RXRA)
0.49	1.23	mitogen- & stress-activated protein kinase 2 (mMSK2)
2.56	1.23	calcyclin binding protein
2.87	1.41	Calmodulin
11.80	1.00 (?)	Leucine-rich repeat protein SHOC-2; Ras-binding protein SUR-8

Table 6: Comparing macro- and microarrays for unsynchronized MVM infected LA9 cells at 36 hr P.I. LS: Low signal

such, certain spots may have higher background. Alternatively, the signal cut-off values in the macroarrays could have been set too low, resulting in slightly skewed ratios. Northern blot confirmations and repeating the microarray experiments to confirm these results will resolve these discrepancies.

Conclusions

Through the use of differential displays and arrays, altered gene expression in MVMp infected mouse fibroblasts was investigated. Overall, MVMp infection seemed to alter transcription in a small number of genes. This was true for each experimental approach: differential display, Clontech macroarrays (approximately 10 changes out of 1200 genes assessed), and Affymetrix microarrays (74 changes out of 12,000 genes assessed). However, from these altered expression profiles several interesting results were seen: One, that MVMp infection appears to promote cell proliferation through the up-regulation of several growth factors and the down-regulation of suppressors of cell proliferation. Two, infection also appears to stimulate an inflammatory and immune response, by activating cytokines and by specifically targeting transforming growth factor β. Three, a small number of different transcription factors are altered during infection suggesting that transcription would further change as the infection progressed. Finally, cholesterol metabolism and transport may be altered as a result of infection.

Differential display and macroarray analysis also indicate that the retroposons B1 & B2 SINEs and the L1 LINE are also up-regulated as a result of MVMp infection. This was confirmed by northern blots and primer extension assays. Furthermore, expression of just MVMp's major non-structural protein NS1 could cause up-regulation of B1 and B2 SINE, suggesting that this multi-functional protein may play a major role in SINE up

regulation. Two critical basal RNA polymerase III transcription factors (TFIIIC220 and 110) were not altered during MVMp infection, suggesting that altered SINE expression many not be due to increased levels of RNA polymerase III transcription factors. Whether the increase in SINE transcription is due to increased transcription or decreased degradation remains to be determined.

Appendix One: Plasmid Constructs

Plasmid	Contains
p1B6-1	RAN-GAP cDNA fragment (nt 283 to 2263). A gift fromDr. James Degregori.
p2A1	DD fragment of B2 SINE (nt 32-174) in Topo-pCR2.1
p7A1U	DD fragment of NS1 (nt 439-687) in Topo-pCR2.1
pCMV1989p	Expressible NS1 containing a A to C point mutation at nt 1989. This alters a splice acceptor site and prevents splicing to the NS2 transcript. A gift from Dr. David Pintel.
pCMVNS1	Expressible NS1/NS2
pCR3G3M2	DD fragment of B1 SINE (nt 1-131) in Topo-pCR2.1
pMO5S1	Murine 5S cDNA. A gift from Dr. G. Frederiksen.
pRSETmTTF	Murine transcription termination factor cDNA (TTF). A gift from Dr. I. Grummt.
pT1-3	Rat tRNA cluster. A gift from Dr. T. Sekiya.
pT1T3mp18	Expressible Chicken β-Actin.

Appendix Two: Oligonucleotides

Primer	Sequence	Function
H-AP1	5'-AAGCTTGATTGCC-3'	Arbitrary differential display primer
H-AP2	5'-AATCTTCGACTGT-3'	Arbitrary differential display primer
H-AP3	5'-AATCTTTGGTCAG-3'	Arbitrary differential display primer
H-AP4	5'-AATCTTCTCAACG-3'	Arbitrary differential display primer
H-AP5	5'-AATCTTAGTAGGC-3'	Arbitrary differential display primer
H-AP6	5'-AATCTTGCACCAT-3'	Arbitrary differential display primer
H-AP7	5'-AATCTTAACGAGG-3'	Arbitrary differential display primer
H-AP8	5'-AATCTTTTACCGC-3'	Arbitrary differential display primer
H-T_{11}A	5'-AACGTTTTTTTTTTA-3'	Anchored differential display primer
H-T_{11}C	5'-AACGTTTTTTTTTTC-3'	Anchored differential display primer
H-T_{11}G	5'-AACGTTTTTTTTTTG-3'	Anchored differential display primer
M13R-24:	5'-AACAGCTATGACCATG-3'	M13 reverse sequencing primer
M13F-20	5'-GTAAAACGACGGCCAGT-3'	M13 forward sequencing primer
NS1-265	5'-GCGGATCCCAGTAACCACTGCG-3'	MVM NS1 amplification
NS1-415	5'-GTGGATCCTGCTTGTGCTATGGC-3'	MVM NS1 amplification
PW10	5'-GCCTGGGTACATGGTGGT-3'	β-Actin amplification
PW11	5'-CAACACCCCAGCCATGTA-3'	β-Actin amplification
WPW25	5'-TACACTGTAGCTGTCTTCAGACA-3'	B2 SINE primer extension (Liu et al., 1995)
WPW26	5'-AAAGCCTACAGCACCCGGTATT-3'	5S RNA primer extension (Liu et al., 1995)
WPW27	5'-CTGGCTGTCCTGGAACTCACTG-3'	B1 SINE primer extension (Liu et al., 1995)

Appendix Three: Antibodies

Antibody	Recognizes
Anti-Actin, Sigma	skeletal actin, 42 kDa
Casein kinase II, Dr. Steven Pelech	CKIIα, 45 kDa
	CKIIα', 41 kDa
sc-750, Santa Cruz	Cdk5, 33 kDa. Did not detect
Mos kinase, Dr. Steven Pelech	Mos kinase, 43 kDa
Goat anti mouse-peroxidase conjugated, Jackson	Mouse IgG (mouse secondary)
CE-10, in lab	NS-1 (MVM), 83 kDa
sc-881, Santa Cruz	PAK-α, 68 kDa
	Unknown band (#3), ~ 60 kDa
Donkey anti rabbit-peroxidase conjugated, Jackson	Rabbit IgG (rabbit secondary)
sc-231, Santa Cruz	Rsk1, 83 kDa
	Unknown band (#4), ~40 kDa
sc-230, Santa Cruz	S6Kp70, 56 kDa (AMW 70 kDa)
	S6Kp90, 85 kDa (AMW 90 kDa)
Ab-2/anti TFIIICα, Dr. Arnold Berk	TFIIIC220, ~ 220 kDa
4286-4, Dr Robert White	TFIIIC110, ~ 110 kDa

AMW: Apparent Molecular Weight

Appendix Four: Kinexus Kinetworks Protein Kinase Screen

Kinases screened in Kinexus Kinetworks protein kinase screen

Bmx	Mek6
Btk	Mek7
Calmodulin-dep. kinase kinase	Mnk2
Calmodulin-dep. kinase 1	Mos
Calmodulin-dep. kinase 4	Mst1
Cyclin-dep. kinase 1 (Cdc2)	Nek2
Cyclin-dep. kinase 2	p38 Hog MAPK
Cyclin-dep. kinase 4	PAK α (PAK1)
Cyclin-dep. kinase 5	PAK β (PAK3)
Cyclin-dep. kinase 6	PDK1 (PKB kinase)
Cyclin-dep. kinase 7	Pim1
Cyclin-dep. kinase 9	PKA (cAMP-dep. protein kinase)
Casein kinase 1 δ	PKB α (Akt1)
Casein kinase 1 ε	PKG1 (cGMP-dep. protein kinase)
Casein kinase 2 α/α'/α"	PKR
Cot (Tpl2)	Protein kinase C α
Csk	Protein kinase C β1
DAPK	Protein kinase C γ
DNAPK	Protein kinase C δ
Extracellular regulated kinase 1	Protein kinase C λ
Extracellular regulated kinase 2	Protein kinase C ε
Extracellular regulated kinase 3	Protein kinase C ζ
Extracellular regulated kinase 6	Protein kinase C θ
Focal adhesion kinase	Protein kinase C μ
Fyn	Pyk2
GCK	Raf1
GRK2	RafB
GSK3 α/β	ROK α
Hpk1	Rsk1
Inhibitor NF κB kinase α	Rsk2
JAK1	S6K p70
JAK2	SAPK β (JNK2)
Ksr1	Src
Lck	Syk
Lyn	Yes
Mek1	Zap70 kinase
Mek2	ZIP kinase
Mek4	

References

1. Bergoin, M. and P. Tijssen, *Molecular biology of the densovirinae*, in *Parvoviruses: from molecular biology to pathology and therapuetic uses*, S. Faisst and J. Rommelaere, Editors. 2000, Kager: Basel. p. 12-32.

2. Faisst, S. and J. Rommelaere, eds. *Parvoviruses: from molecular biology to pathology and therapeutic uses*. Contributions to microbiology, ed. A. Schmidt. Vol. 4. 2000, Karger: Basel.

3. Heegaard, E.D. and K.E. Brown, *Human parvovirus B19.* Clin. Microbiol. Rev., 2002. **15**: 485-505.

4. Thurn, J., *Human parvovirus B19: Historical and clinical review.* Rev. Infect. Dis., 1988. **10**: 1005-1011.

5. Truyen, U. and C.R. Parrish, *Epidemiology and pathology of autonomous parvoviruses*, in *Parvoviruses: from molecular biology to pathology and therapeutic uses*, S. Faisst and J. Rommelaere, Editors. 2000, Karger: Basel. p. 149-159.

6. Parrish, C.R., *Pathogenesis of feline panleukopenia virus and canine parvovirus.* Baillieres Clin. Haematol., 1995. **8**: 57-71.

7. Bloom, M.E., et al., *Aleutian mink disease: puzzles and paradigms.* Infect. Agents Dis., 1994. **3**: 279-301.

8. Seki, H., *Mode of inheritance of the resistance to the infection with densonucleosis virus (Yamanashi isolate) in the silk worm Bombyx mori.* Journal of Sericulture Science Japan, 1984. **53**: 472-475.

9. Watanabe, H. and T. Shimizu, *Epizootiological studies on the occurrence of densonucleosis in the silk worm, Bombyx mori, reared at sericultural farms.* Journal of Sericulture Science Japan, 1980. **49**: 485-492.

10. Rabinowitz, J.E. and J.R. Samulski, *Building a better vector: The manipulation of AAV Virions.* Virology, 2000. **278**: 301-308.

11. Friedman, T., ed. *The development of Human Gene Therapy.* 1999, Cold Spring Harbour: San Diego. 729.

12. Wagner, J.A., et al., *A phase II, double-blind, randomized, placebo-controlled clinical trial of tgAAVCF using maxillary sinus delivery in patients with cystic fibrosis with antrostomies.* Hum. Gene Ther., 2002. **13**: 1349-1359.

13. Manno, C.S., et al., *AAV-mediated factor IX gene transfer to skeletal muscle in patients with severe hemophilia B.* Blood, 2002. **Blood First Edition Paper, prepublished online December 19, 2002.**

14. Weigel-kelly, K.A. and A. Srivastava, *Recombinant human parvovirus B19 vectors.* Pathol. Biol. (Paris), 2002. **50**: 295-306.

15. Maxwell, I.H., K.L. Terrell, and F. Maxwell, *Autonomoous parvovirus vectors.* Methods, 2002. **28**: 168-181.

16. Afanasiev, B. and J. Carlson, *Densovirinae as gene transfer vehicles*, in *Parvoviruses: from molecular biology to pathology and therapeutic uses.*, S. Faisst and J. Rommelaere, Editors. 2000, Karger: Base. p. 33-58.

17. Genty, P. and D. Mariau, *Utilisation d'un germe entomopathogene dans la lutte contre Sibine fusca (Limacodidae).* Oleagineux, 1975. **30**: 349-354.

18. Fediere, G., et al., *A denosovirus of Casphalia extranea (Lepidoptera: Limacodidae): Characterization and use fpr biological control*, in *Fundemental and applied aspects of invertebrate pathology*, R.A. Samson, J.M. Vlak, and D. Peters, Editors. 1986, Foundation IVth Int Colloq Invertebr pathol: Wageningen. p. 705.

19. Buchatsky, L.P., et al., *Field trials of viral preparation Viroden on preimaginal stages of blood-sucking mosquitoes.* Med. Parazitol. (Mosk), 1987. **4**.

20. Lebedinets, N.N. and A.G. Kononko, *Experimental study of the pathway of densovirus infection transmission in a population of blood-sucking mosquitoes.* Med. Parazitol. (Mosk)., 1989. **2**: 79-83.

21. Moffatt, S., et al., *Human parvovirus B19 non-structural protein induces apoptosis in erythriod lineage cells.* J. Virol., 1998. **72**: 3018-3028.

22. Sol, N., et al., *Possible interactions between the NS1 protein and tumor necrosis factor alpha pathways in erythroid cell apoptosis induced by human parvovirus B19.* J. Virol., 1999. **73**: 8762-8770.

23. Ohshima, T., et al., *Induction of apoptosis in vitro and in vivo by H1 parvovirus infection.* J. Gen. Virol., 1998. **79**: 3067-3071.

24. Rommelaere, J. and J.J. Cornelis, *Antineoplastic activity of parvoviruses.* J. Virol. Meth., 1991. **33**: 233-251.

25. Op De Beeck, A., et al., *NS1 and minute virus of mice-induced cell cycle arrest: involvement of p53 and $p21^{cip1}$.* J. Virol., 2001. **75**: 11071-11078.

26. Morita, E., et al., *Human parvovirus B19 induces cell cycle arrest at G(2) phase with accumulation of mitotic cyclins.* J. Virol. Meth., 2001. **75**: 7555-7563.

27. Hirt, B., *Molecular biology of autonomous parvoviruses*, in *Parvoviruses: from molecular biology to pathology and therapeutic uses*, S. Faisst and J. Rommelaere, Editors. 2000, Karger: Basel. p. 163-177.

28. Cotmore, S.F. and P. Tattersall, *Parvovirus DNA replicaton*, in *DNA replication in Eukaryotic cells*, M.L. DePamphilils, Editor. 1996, Cold spring harbour press: Woodbury. p. 799-813.

29. Astell, C.R., et al., *The complete sequence of minute virus of mice, an autonomous parvovirus.* Nucl. Acids Res., 1983. **11**: 999-1018.

30. Clemens, K.E., et al., *Cloning of minute virus of mice cDNAs and preliminary analysis of individual viral proteins expressed in murine cells.* J. Virol., 1990. **64**: 3967-3973.

31. Cotmore, S.F. and P. Tattersall, *Organization of nonstructural genes of the autonomous parvovirus minute virus of mice.* J. Virol., 1986. **58**: 724-732.

32. Pintel, D., et al., *The genome of minute virus of mice, an autonomous parvovirus, encoding two overlapping transcription units.* Nucl. Acids Res., 1983. **11**: 1019-1038.

33. Tattersall, P., et al., *Three structural polypetides coded for by Minute Virus of Mice, a parvovirus.* J. Virol., 1976. **20**: 273-289.

34. Christensen, J. and P. Tattersall, *Parvovirus initiator protein NS1 and RPA coordinate replication fork progression in a reconstituted DNA replication system.* J. Virol., 2002. **76**: 6518-6537.

35. Hernando, E., et al., *Biochemical and physical characterization of parvovirus minute virus of mice virus-like particles.* Virology, 2000. **267**: 299-309.

36. Merchlinsky, M.J., et al., *Construction of an infectious molecular clone of the automous parvovirus minute virus of mice.* J. Virol., 1983. **47**: 227-232.

37. Toolan, H.W., *The rodent parvoviruses*, in *Hanbook of parvoviruses*, P. Tijssen, Editor. 1990, CRC press: Boca Raton. p. 159-176.

38. Segovia, J.C., et al., *Severe leukopenia and dysregulated erythropiesis in SCID mice persistently infected with the parvovirus minute virus of mice.* J. Virol., 1999. **73**: 1774-1784.

39. Brownstein, D.G., et al., *Pathogenesis of infection with a virulent allotropic variant of minute virus of mice and regulation by host genotype.* Lab. Invest., 1991. **65**: 357-364.

40. Bonnard, D.G., et al., *Immunosupressive actvity of a subline of the mouse EL-4 lymphoma. Evidence for minute virus of mice causing the inhibition.* J. Exp. Med., 1976. **143**: 187-205.

41. McMaster, G.K., et al., *Characterization of an immunosupressive parvovirus related to minute virus of mice.* J. Virol., 1981. **38**: 317-326.

42. Agbandje-McKenna, M., et al., *Functional implications of the structure of the murine parvovirus, minute virus of mice.* Structure, 1998. **6**: 1369-1381.

43. Tam, P. and C.R. Astell, *Replication of Minute Virus of Mice minigenomes: Novel replication Elements required for MVM replication.* Virology, 1993. **193**: 812-824.

44. Cotmore, S.F. and P. Tattersall, *The NS-1 polypeptide of minute virus of mice is covalently attached to the 5' termini of duplex replicative-form DNA and progeny single strands.* J. Virol., 1988. **62**: 851-860.

45. Cotmore, S.F. and P. Tattersall, *A genome-linked copy of the NS-1 polypeptide is located on the outside of infectious parvovirus particles.* J. Virol., 1989. **63**: 3902-3911.

46. Palmer, G.A. and P. Tattersall, *Autonomous parvovrisuses as gene transfer vehicles*, in *Parvoviruses: from molecular biology to pathology and therapeutic uses.*, S. Faisst and J. Rommelaere, Editors. 2000, karger: Basel. p. 178-202.

47. Bashir, T., et al., *Cyclin A activates the DNA polymerase δ-dependent elongation machinary in vitro: A parvovirus DNA replication model.* Proc. Natl. Acad. Sci. USA, 2000. **97**: 5522-5527.

48. Christensen, J., S.F. Cotmore, and P. Tattersall, *Parvovirus initiation factor PIF: a novel human DNA-binding factor which coordinately recognizes two ACGT motifs.* J. Virol., 1997. **71**: 5733-5741.

49. Cotmore, S.F. and P. Tattersall, *High-mobility group 1/2 proteins are essential for initiating rolling-circle-type DNA replication at a parvovirus hairpin origin.* J. Virol., 1998. **72**: 8477-8484.

50. Wolter, S., R. Richards, and R.W. Armentrout, *Cell cycle-dependent replication of the DNA of minute virus of mice, a parvovirus.* Biochim. Biophys. Acta, 1980. **607**: 420-431.

51. Astell, C.R., M.B. Chow, and D.C. Ward, *Sequence analysis of the termini of virion and replicative forms of minute virus of mice suggests a modified rolling hairpin model for automonous parvovirus DNA replication.* J. Virol., 1985. **54**: 171-177.

52. Bashir, T., J. Rommelaere, and C. Cziepluch, *In vivo accumulation of cyclin A and cellular replication factors in autonomous parvovirus minute virus of mice-associated replication bodies.* J. Virol., 2001. **75**: 4394-4398.

53. Clemens, K.E. and D. Pintel, *Minute virus of mice (MVM) mRNAs predominately polyadenylate at a single site.* Virology, 1987. **160**: 511-514.

54. Cotmore, S.F., L.J. Sturzenbecker, and P. Tattersall, *The autonomous parvovirus MVM encodes two nonstructural proteins in addition to its capsid proteins.* Virology, 1983. **129**: 333-343.

55. Jongeneel, C.V., et al., *A precise map of splice junctions in the mRNAs of minute virus of mice, an autonomous parvovirus.* J. Virol., 1986. **59**: 564-573.

56. Morgan, W.R. and D.C. Ward, *Three splicing patterns are used to excise the small intron common to all minute virus of mice RNAs.* J. Virol., 1986. **60**: 1170.

57. Cotmore, S.F. and P. Tattersall, *Alternate splicing in a parvoviral nonstructural gene links a common amino-terminal sequence to downstream domains which confer radically different localization and turnover characteristics.* Virology, 1990. **177**: 477-487.

58. Labieniec-pintel, L. and D. Pintel, *The minute virus of mice (MVM) P39 transcription unit can encode both capsid proteins.* J. Virol., 1986. **57**: 1163.

59. Hanson, N.D. and S.L. Rhode, *Parvovirus NS1 stimulates P4 expression by interaction with the terminal repeats and through DNA amplification.* J. Virol., 1991. **65**: 4325-4333.

60. Doerig, C., et al., *Minute virus of mice non-structural protein is necessary and sufficient for trans-activation of the viral P39 promoter.* J. Gen. Virol., 1988. **69**: 2563-2573.

61. Deleu, L., et al., *Opposite transcriptional effects of cyclic AMP-reponsive elements in confluent or p27KIP-overexpressing cells versus serum-starved or growing cells.* Mol. Cell. Biol., 1998. **18**: 409-419.

62. Deleu, L., et al., *Activation of promoter P4 of the autonomous parvovirus minute virus of mice at early S phase is required for productive infection.* J. Virol., 1999. **73**: 3877-3885.

63. Lorson, C.L., et al., *A SP1-binding site and TATA element are sufficient to support full transactivation by proximally bound NS1 protein of minute virus of mice.* Virology, 1998. **240**.

64. Ohshima, T., et al., *Effects of interaction between parvovirus minute virus of mice NS1 and coactivator CBP on NS1- and p53-transactivation.* Int. J. Mol. Med., 2001. **7**: 49-54.

65. Nuesch, J.P.F., et al., *Replicative functions of minute virus of mice NS1 protein are regulated in vitro by phosphorylation through protein kinase C.* J. Virol., 1998. **72**: 9966-9977.

66. Dettwiler, S., J. Rommelaere, and J.P.F. Nuesch, *DNA unwinding functions of minute virus of mice NS1 protein are modulated specifically by the lambda isoform of protein kinase C.* J. Virol., 1999. **73**: 7410-7420.

67. Corbau, R., et al., *Phosphorylation of the viral nonstructural protein NS1 during MVMp infection of A9 cells.* Virology, 1999. **259**.

68. Corbau, R., et al., *Regulation of MVM NS-1 by protein kinase C: Impact of mutagenesis at consensus phosphorylation sites on replicative functions and cytopathic effects.* Virology, 2000. **278**: 151-167.

69. Nuesch, J.P.F. and P. Tattersall, *Nuclear targetting of the parvoviral replicator molecule NS1: Evidence for self-association prior to nuclear transport.* Virology, 1993. **196**: 637-651.

70. Nuesch, J.P.F., S.F. Cotmore, and P. Tattersall, *Sequence motifs in the replicator protein of parvovirus MVM essential for nicking and covalent attachment to the viral origin: Identification of the linking tyrosine.* Virology, 1995. **209**: 122-135.

71. Wilson, G.M., et al., *Expression of minute virus of mice major nonstructural protein in insect cells: Purification and identification of ATPase and helicase activities.* Virology, 1991. **185**: 90-98.

72. Mouw, M. and D. Pintel, *Amino acids 16-275 of minute virus of mice NS1 include a domain that specifically binds $(ACCA)_{2-3}$-containing DNA.* Virology, 1998. **251**: 123-131.

73. Astell, C.R., C.D. Mol, and W.F. Anderson, *Structural and functional homology of parvovirus and papovavirus polypeptides.* J. Gen. Virol., 1987. **68**: 885-893.

74. Legendre, D. and J. Rommelaere, *Terminal regions of the NS-1 proteins of parvovirus minute virus of mice are involved in cytotoxicity and promoter trans inhibition.* J. Virol., 1992. **66**: 5705-5713.

75. Pujol, A., et al., *Inhibition of parvovirus minute virus of mice replication by a peptide involved in the oligomerization of nonstructural protein NS1.* J. Virol., 1997. **71**: 7393-7403.

76. Christensen, J., S.F. Cotmore, and P. Tattersall, *Minute virus of mice initiator protein NS1 and a host KDWK family transcription factor must form a precise ternary complex with origin DNA for nicking to occur.* J. Virol., 2001. **75**: 7009-7017.

77. Young, P.J., et al., *Minute virus of mice NS1 interacts with the SMN protein, and they colocalize in novel nuclear bodies induced by parvovirus infection.* J. Virol., 2002. **76**: 3892-3904.

78. Harris, C.E., R.A. Boden, and C.R. Astell, *A novel hetrogeneous nuclear ribonucleoprotein-like protein interacts with NS1 of the minute virus of mice.* J. Virol., 1999. **73**: 72-80.

79. Bodendorf, U., et al., *Nuclear export factor CRM1 interacts with nonstructural proteins NS2 from parvovirus minute virus of mice.* J. Virol., 1999. **73**: 7769-7779.

80. Cater, J. and D. Pintel, *The small non-strucutral protein NS2 of the autonomous parvovirus minute virus of mice is required for virus growth in murine cells.* J. Gen. Virol., 1992. **73**: 1839-1843.

81. Naeger, L.K., J. Cater, and D. Pintel, *The small nonstructural protein (NS2) of parvovirus minute virus of mice is required for efficient DNA replication and infectious virus production in a cell-type-specific manner.* J. Virol., 1990. **64**: 6166-6175.

82. Naeger, L.K., N. Salome, and D. Pintel, *NS2 is required for efficient translation of viral mRNA in minute virus of mice infected murine cells.* J. Virol., 1993. **67**: 1034-1043.

83. Cotmore, S.F., et al., *The NS2 polypeptide of parvovirus MVM is required for capsid assembly in murine cells.* Virology, 1997. **231**: 267-280.

84. Ohshima, T., et al., *CRM1 mediates nuclear export of nonstructural protein 2 from parvovirus minute virus of mice.* Biochem. Biophys. Res. Commun., 1999. **264**: 144-150.

85. Eichwald, V., et al., *The NS2 proteins of parvovirus minute virus of mice are required for efficient nuclear egress of progeny virions in mouse cells.* J. Virol., 2002. **76**: 10307-10319.

86. Miller, C.L. and D. Pintel, *Interaction between parvovirus NS2 protein and nuclear export factor Crm1 is important for viral egress from the nucleus of murine cells.* J. Virol., 2002. **76**: 3257-3266.

87. Young, P.J., et al., *Minute virus of mice small nonstructural protein NS2 interacts and colocalizes with the SMN protein.* J. Virol., 2002. **76**: 6364-6369.

88. Brockahus, K., et al., *Nonstructural proteins NS2 of minute virus of mice associate in vivo with 14-3-3 protein family members.* J. Virol., 1996. **70**: 7527-7534.

89. Tattersall, P., A.J. Shatkin, and D.C. Ward, *Sequence homology between the structural polypeptides of minute virus of mice.* J. Mol. Biol., 1977. **111**: 375-394.

90. Zadori, Z., et al., *A viral phospholipase A2 is required for parvovirus infectivity.* Dev. Cell, 2001. **1**: 291-302.

91. Op De Beeck, A. and P. Caillet-fauquet, *The NS-1 protein of autonomous parvovirus minute virus of mice blocks cellular replication: A consequence of lesions to the chromatin?* J. Virol., 1997. **71**: 5323-5329.

92. Kerr, D.A., et al., *Survival of motor neuron protein modulates neuron-specific apoptosis.* Proc. Natl. Acad. Sci. USA, 2000. **97**: 13312-13317.

93. Krauskopf, A., E. Ben-Asher, and Y. Aloni, *Minute virus of mice infection modifies cellular transcription elongation.* J. Virol., 1994. **68**: 2741-2745.

94. Deleu, L., et al., *Inhibition of transcription-regulating properties of nonstructural protein 1 (NS1) of parvovirus minute virus of mice by a dominant-negative mutant form of NS1.* J. Gen. Virol., 2001. **82**: 1929-1934.

95. Legendre, D. and J. Rommelaere, *Targeting of promoters for trans-activation by carboxy-terminal domain of the NS-1 protein of the parvovirus minute virus of mice.* J. Virol., 1994. **68**: 7974-7985.

96. Vanacker, J., et al., *Interconnection between thyroid hormone signalling pathways and parvovirus cytotoxic functions.* J. Virol., 1993. **67**: 7668-7672.

97. Vanacker, J., et al., *Transactivation of a cellular promoter by the NS1 protein of the parvovirus minute virus of mice through a putative hormone-response element.* J. Virol., 1996. **70**: 2369-2377.

98. Thormeyer, D. and A. Baniahmad, *The v-erbA oncogene.* Int. J. Mol. Med., 1999. **4**: 351-358.

99. Beug, H., E.W. Mullner, and M.J. Hayman, *Insights into erythroid differentiation obtained from studies on avian erythroblastosis virus.* Curr. Opin. Cell Biol., 1994. **6**: 816-824.

100. Mourelatos, Z., et al., *SMN interacts with a novel family of hnRNP and spliceosomal proteins.* EMBO J., 2001. **20**: 5443-5452.

101. Fischer, U., et al., *Rev activation domain is a nuclear export signal that accesses a export pathway used by specific cellular RNAs.* Cell, 1995. **82**: 475-483.

102. Dobbelstein, M., et al., *Nuclear export of the E1B 55-kDa and E4 34-kDa adenoviral oncoproteins mediated by a rev-like signal sequence.* EMBO J., 1997. **16**: 4276-4284.

103. Waite, M., *The phospholipases*. Handbook of lipid research, ed. D.J. Hanahan. Vol. 5. 1987, New York: Plenum press.

104. Kini, R.M., *Venom phospholipase A_2 enzymes*. 1997, Toronto: John wiliey and sons.

105. Muslin, A.J. and H. Xing, *14-3-3 proteins: regulation of subcellular localization by molecular interference.* Cell. Signal., 2000. **12**: 703-709.

106. Cornelis, J.J., et al., *Susceptibility of human cells to killing by parvoviruses H-1 and minute virus of mice correlates with viral transcription.* J. Virol., 1990. **64**: 2537-2544.

107. Rommelaere, J. and P. Tattersall, *Oncosupression by parvoviruses*, in *Handbook of parvoviruses*, P. Tijssen, Editor. 1990, CRC press: Boca Ranton. p. 41-57.

108. Mousset, S., et al., *The cytotoxicity of the autonomous parvovirus minute virus of mice non-structural proteins in FR3T3 rat cells depends on oncogene expression.* J. Virol., 1994. **68**: 6446-6453.

109. Caillet-fauquet, P., et al., *Programmed cell killing of human cells by means of an inducible clone of parvoviral genes encoding the nonstructural proteins.* EMBO J., 1990. **9**.

110. Legrand, C., J. Rommelaere, and P. Caillet-fauquet, *MVMp NS-2 protein expression is required with NS-1 for maximal cytotoxicty in human transformed cells.* Virology, 1993. **195**: 149-155.

111. Anouja, F., et al., *The cytotoxicity of the parvovirus minute virus of mice nonstructural protein NS1 is related to changes in the synthesis and phosphorylation of cell proteins.* J. Virol., 1997. **71**: 4671-4678.

112. Labuda, D., E. Zietkiewicz, and G.A. Mitchell, *Alu elements as a source of genomic variation: Deleterious effects and evolutionary novelties*, in *The impact of short interspersed elements (SINEs) on the host genome*, R.J. Maraia, Editor. 1995, R. G. Landes: Austin.

113. Gilbert, N., et al., *Plant S1 SINEs as a model to study retroposition.* Genetica, 1997. **100**: 155-160.

114. Gilbert, N. and N. Labuda, *CORE-SINEs: Eukaryotic short interspersed retroposing elements with common sequence motifs.* Proc. Natl. Acad. Sci. USA, 1999. **96**: 2869-2874.

115. International human genome sequencing consortium, *Initial sequencing and analysis of the human genome.* Science, 2001 860-921.

116. Mouse genome sequencing consortium, *Initial sequencing and comparative analysis of the mouse genome.* Nature, 2002. **420**: 520-562.

117. Weiner, A.W., *SINEs and LINEs: The art of biting the hand that feeds you.* Curr. Opin. Cell Biol., 2002. **14**: 343-350.

118. Daniels, G.R. and P.L. Deininger, *Repeat sequence families derived from mammalian tRNA genes.* Nature, 1985. **317**: 819-822.

119. Ohshima, K., et al., *The 3' ends of tRNA-derived short interspersed repetitive elements are derived from the 3' ends of long interspersed repetitive elements.* Mol. Cell. Biol., 1996. **16**: 3756-3764.

120. Mayorov, V.I., et al., *B2 elements present in the human genome.* Mamm. Genome, 2000. **11**: 177-179.

121. Jurka, J., *Sequence patterns indicate an enzymatic involvement in integration of mammalian retroposons.* Proc. Natl. Acad. Sci. USA, 1997. **94**: 1872-1877.

122. Schramm, L. and N. Hernandez, *Recruitment of RNA polymerse III to its target promoters.* Genes Dev., 2002. **16**: 2593-2620.

123. Huang, Y. and R.J. Maraia, *Comparison of the RNA polymerase III transcription machinery in schizosaccharomyces pombe, saccharomyces cerevisiae and human.* Nucl. Acids Res., 2001. **29**: 2675-2690.

124. Paule, M.R. and R.J. White, *Transcription by RNA polymerases I and III.* Nucl. Acids Res., 2000. **28**: 1283-1298.

125. Arnaud, P., et al., *SINE retroposons can be used in vivo as nucleation centers for de novo methylation.* Mol. Cell. Biol., 2000. **20**: 3434-3441.

126. Schmid, C.W., *Does SINE evolution prclude Alu function?* Nucl. Acids Res., 1998. **26**: 4541-4550.

127. Rubin, C.M., et al., *Alu repeated DNAs are differentially methylated in primate germ cells.* Nucl. Acids Res., 1994. **22**: 5121-5127.

128. Yu, F., et al., *Methyl-CpG-binding protein 2 represses LINE-1 expression and retrotransposition but not Alu transcription.* Nucl. Acids Res., 2001. **29**: 4493-4501.

129. Jensen, S., M. Gassama, and T. Heidmann, *Taming of transposable elements by homology dependent gene silencing.* Nat. Genet., 1999. **21**: 209-212.

130. Littlefield, J.W., *Three degrees of guanylic acid - inosinic acid pyrophosphorylase deficeinecy in mouse fibroblasts.* Nature, 1964. **203**: 1142-1144.

131. Tattersall, P., *Replication of the parvovirus MVM. I. Dependence of virus multiplication and plaque formation on cell growth.* J. Virol., 1972. **10**: 586-590.

132. Altschul, S.F., et al., *Basic local alignment search tool.* J. Mol. Biol., 1990. **215**: 403-410.

133. Sambrook, J., E.F. Fritsch, and T. Maniatis, eds. *Molecular cloning: a labratory manual.* 2 ed. Vol. 1. 1989, Cild spring harbor laboratory press: Cold spring harbor.

134. Golub, E.L., *One minute" transformation of competent E. Coli by plasmid DNA.* Nucl. Acids Res., 1988. **16**: 1641.

135. Greenberg, M.E. and T.P. Bender, *Identification of newly transcribed RNA (Unit 4.10, supplement 26)*, in *Current protocols in molecular biology*, F.M. Ausubel, et al., Editors. 1997, John Wiley and Sons. p. 4.10.01-4.10.11.

136. Liang, P. and A.B. Pardee, *Differential display of eukaryoitc messenger RNA by means of poylmerase chain reaction.* Science, 1992. **257**: 967-971.

137. Liang, P. and A.B. Pardee, *Method of differential display*, in *methods in molecular genetics*. 1994, academic press. p. 3-16.

138. Zhu, H., et al., *Cellular gene expression altered by human cytomegalovirus: Global monitoring with oligonucleotide arrays.* Proc. Natl. Acad. Sci. USA, 1998. **95**: 14470-14475.

139. Geiss, G.K., et al., *Large-scale monitoring of host cell gene expression during HIV-1 infection using cDNA microarrays.* Virology, 2000. **266**: 8-16.

140. Bogenhagen, D.F. and D.D. Brown, *Nucleotide sequences in Xenopus 5s DNA required for transcription termination.* Cell, 1981. **24**: 261-270.

141. Singh, K., et al., *Expression of enhanced levels of small RNA polymerase III transcripts encoded by the B2 repeats in simian virus 40-transformed cells.* Nature, 1985. **314**: 553-556.

142. Larminie, C.G.C., et al., *Activation of RNA polymerase III transcription in cells transformed by simian virus 40.* Mol. Cell. Biol., 1999. **19**: 4927-4934.

143. Sinn, E., et al., *Cloning and characterization of a TFIIIC2 subunit (TFIIIβ) whose presence correlates with activation of RNA polymerase III-mediated transcription by adenovirus E1A expression and serum factors.* Genes Dev., 1995. **9**: 675-685.

144. Shen, Y., et al., *DNA binding domain and subunit interactions of transcription factor IIIC revealed by dissection with poliovirus 3C protease.* Mol. Cell. Biol., 1996. **16**: 4163-41-71.

145. Winter, A.G., et al., *RNA polymerase III transcription factor TFIIIC2 is overexpressed in ovarian tumors.* Proc. Natl. Acad. Sci. USA, 2000. **97**: 12619-12624.

146. Jang, K.L., M.K. Collins, and D.S. Latchman, *The human immunodeficiency virus tat protein increases the transcription of human Alu repeated sequences by increasing the activity of the cellular transcription factor TFIIIC.* J. Acquir. Immune Defic. Syndr., 1992. **5**: 1142-1147.

147. Jang, K.L. and D.S. Latchman, *The herpes simplex virus immediate-early protein ICP27 stimulates the transcription of cellular Alu repeated sequences by increasing the activity of transcription factor TFIIIC.* Biochem. J., 1992. **284**: 667-673.

148. Vietor, I. and L.A. Huber, *In search of differentially expressed genes and proteins.* Biochim. Biophys. Acta, 1997. **1359**: 187-99.

149. Rothchild, C.B., C.S. Brewer, and D.W. Offden, *DD/AP-PCR: Combination of differential display and arbitrarily primed PCR of oligo(dt) cDNA.* Anal. Biochem., 1997. **245**: 48-54.

150. Wan, J.S., et al., *Cloning differentially expressed mRNAs.* Nat. Biotechnol., 1996. **14**: 1685-1691.

151. Ito, T. and Y. Sakaki, *Towards genome-wide scanning of gene expression: A functional aspect of the genome project.* Essays Bioc., 1996. **31**: 11-21.

152. Nees, M., et al., *Identification of novel molecular markers which correlate with HPV-induced tumor progression.* Oncogene, 1998. **16**: 2447-2458.

153. Zhu, H., J.P. Cong, and T. Shenk, *Use of differential display analysis to assess the effect of human cytomegalovirus infection on the accumulation of cellular RNAs: Induction of interferon-responsive RNAs.* Proc. Natl. Acad. Sci. USA, 1997. **94**: 13985-13990.

154. Tal-Singer, R., et al., *Use of differential display reverse transcription-PCR to reveal cellular changes during stimuli that result in herpes simplex virus type 1 reactivation from latency: Upregulation of immediate-early cellular response genes TIS7, interferon, and interferon regulatory factor-1.* J. Virol., 1998. **72**: 1252-1261.

155. Madarelli, F., et al., *The expression of the essential nuclear splicing factor SC35 is altered by human immunodeficiency virus infection.* Virus Res., 1998. **53**: 39-51.

156. Scheuring, U.J., et al., *Early modification of host cell gene expression induced by HIV-1.* AIDS, 1998. **12**: 563-570.

157. Yang, D., et al., *Viral myocarditis: Identification of five differentially expressed genes in coxsackievirus B3-infected mouse heart.* Circ. Res., 1999. **84**: 704-712.

158. Nangia-makker, P., et al., *Galectin-3 and L1 retrotransposons in human breast carcinomas.* Breast Cancer Res. Treat., 1998. **49**: 171-183.

159. Rudin, C.M. and C.B. Thompson, *Transcriptional activation of short interspersed elements by DNA-damaging agents.* Genes Chromosomes Cancer, 2001. **30**: 64-71.

160. Pogue-Geule, K.K. and J.S. Greenberger, *Effect of the irradiated microenvironment on the expression and retrotransposition of intracisternal type A particles in hematopoietic cells.* Exp. Hematol., 2000. **28**: 680-689.

161. Liu, W., et al., *Cell stress and translational inhibitors transiently increase the abundance of mammalian SINE transcripts.* Nucl. Acids Res., 1995. **23**: 1758-1765.

162. Li, T., et al., *Physiological stresses increase mouse short interspersed element (SINE) RNA expression in vivo.* Gene, 1999. **239**: 367-372.

163. Panning, B. and J.R. Smiley, *Activation of RNA polymerse III transcription of human Alu repetitive elementes by adenovirus type 5: Requirement for the E1b 58 kilodalton protein and the products of the E4 open reading frames 3 and 6.* Mol. Cell. Biol., 1993. **13**: 3231-3244.

164. Jang, K.L. and D.S. Latchman, *HSV infection induces increased transcription of Alu repeated sequences by RNA polymerase III.* FEBS Lett., 1989. **258**: 255-258.

165. Panning, B. and J.R. Smiley, *Activation of RNA polymerase III transcription of human Alu elements by adenovirus type 5 and herpes simplex virus type 1*, in *The impact of short interspersed elements (SINEs) on the host genome*, R.J. Maraia, Editor. 1995, R. G. landes: Austin. p. 143-161.

166. Kim, C., C.M. Rubin, and C.W. Schmid, *Genome-wide chromatin remodeling modulates the Alu heat shock response.* Gene, 2001. **276**: 127-133.

167. Brosius, J., *RNAs from all categories generate retrosequences that may be exapted as novel genes or regulatory elements.* Gene, 1999. **238**: 115-134.

168. Ferrigno, O., et al., *Transposable B2 SINE elements can provide mobile RNA polymerase II promoters.* Nat. Genet., 2001. **28**: 77-81.

169. Chu, W., et al., *Potential alu function: Regulation of the activity of double-stranded RNA-activated kinase PKR.* Mol. Cell. Biol., 1998. **18**: 58-68.

170. Rubin, C.M., R.H. Kimura, and C.W. Schmid, *Selective stimulation of translational expression by Alu RNA.* Nucl. Acids Res., 2002. **30**: 3253-3261.

171. Ramji, D.P. and P. Foka, *CCAAT/enhancer-binding proteins: structure, function and regulation.* Biochem. J., 2002. **365**: 561-575.